Marine geology of the East London continental shelf

By

Nontuthuzo Dlamini

Submitted in fulfilment of the academic

requirements for the degree of

Master of Science in the

School of School of Agricultural,

Earth and Environmental Sciences,

University of KwaZulu-Natal

Durban

December 2017

ABSTRACT

This dissertation examines the marine geology of the continental shelf offshore East London, on the east coast of South Africa. High-resolution seismic, multibeam bathymetric and backscatter tools are employed to reveal the stratigraphic, geomorphic and oceanographic controls on the shelf development. Eight seismic units (A-H) are revealed and comprise Campanian-age limestones of the Igoda Formation at their base, with an overlying transgressive stratigraphic package associated with the last deglaciation. A subaerial unconformity transects the shelf and is infilled by Late-Pleistocene to Holocene-age material of Unit C. Overlying the subaerial unconformity in other places are isolated shoreface deposits of Unit B. Unit D comprises a series of aeolianites and beachrocks which form palaeo-shorelines at -100 and -60 m. They are mantled to landward by the back-barrier deposits of Unit E, and to seaward by the disaggregated barrier deposits of Unit F. Unit G comprises shoreface deposits and is interfingered with Unit H, a series of rhodoliths that mantle the modern day seafloor.

Multibeam data reveal extraordinarily preserved palaeo-shorelines which are the outcrop expression of Unit B. The most seaward of these form barrier islands and associated back-barrier segmented coastal waterbodies that evolved to planform equilibria before being overstepped. These are bordered by large, well-preserved parabolic dunefields that signify planform equilibrium with high-rates of sediment supply. These shorelines formed during the Bølling-Allerod stillstand and were overstepped by Melt Water Pulse (MWP) 1-A.

A -60 m shoreline is preserved as an isolated drumstick barrier, and a series of cuspate spits that are welded onto palaeo-embayments in Gondwana-aged bedrock. These formed during the Younger Dryas slowstand and were overstepped by MWP-1B. Underfilled incised valleys are still exposed at the seafloor along these palaeo-embayments and formed due to rapid transgression and limited marine sediment supply during the conditions associated with MWP-1B. They are currently being filled by the submerged prodeltas of the contemporary drainage systems.

Backscatter data reveal eight acoustic facies (A-H). These units all show marked current sweeping of the shelf, with dredge samples revealing gravels that fill in erosional furrows, or

form streamers and ribbons. The AMS C^{14} dating of the rhodolith fields of Unit H indicates that the vigorous Agulhas Current has continuously swept the shelf since ~7400 years BP, post MWP 1-B. This has caused the sediment starvation of most of the shelf, and has transported much of the available sediment to the deep sea via the shelf-indenting canyon systems of the area.

PREFACE

The work in this dissertation was carried out at the University of KwaZulu-Natal, under the supervision of Prof. Andrew Green, Dr. Errol Wiles and Miss Nonkululeko Dladla.

The project was funded by the National Research Foundation and the African Coelacanth Ecosystem Program, with additional assistance from Prof. Andrew Green.

As the candidate's supervisor I have/have not approved this dissertation for submission.

Signed: _____ Name: _____ Date: _____

As the candidate's co-supervisor I have approved this thesis for submission and examination.

Signed: _____ Name: _____ Date: _____

Signed: _____ Name: _____ Date: _____

DECLARATION – PLAGIARISM

I, Nontuthuzo Dlamini, declare that

1. The research reported in this thesis, except where otherwise indicated, is my original research.
2. This thesis has not been submitted for any degree or examination at any other university.
3. This thesis does not contain other persons' data, pictures, graphs or other information, unless specifically acknowledged as being sourced from other persons.
4. This thesis does not contain other persons' writing, unless specifically acknowledged as being sourced from other researchers. Where other written sources have been quoted, then:
    a. Their words have been re-written but the general information attributed to them has been referenced
    b. Where their exact words have been used, then their writing has been placed in italics and inside quotation marks, and referenced.
5. This thesis does not contain text, graphics or tables copied and pasted from the Internet, unless specifically acknowledged, and the source being detailed in the thesis and in the References sections.

Signed_____

ACKNOWLEDGEMENTS

I would like to thank my supervisors Prof. Andrew Green, Dr. Errol Wile and Miss Nonkululeko Dladla, for being there for me every step of the way. Andy, this would have been possible without you, you have been there for me past the point of supervising and for that I have no words to thank you enough. Errol thank you for your guidance and undivided attention, you have given me a push in situations where I needed a push. Nkule, thank you for always being there for me when I needed you, for doing and being more than a supervisor, for going that extra mile.

I would like to thank Carlos and Nigel, you guys became my additional supervisors. Whatever I needed, you guys would stop everything and assist me and for that I am eternally grateful.

Thank you to my postgrads. To Lauren for constantly checking up on me, telling me I can do it every step of the way. To Arissa and Kreesan, whom we shared the stress, we have finally crossed the finish line. How can I forget about you Thami, every day with you is filled with laughter and fun. Thank you for always bringing me coffee and sugar from home, I'm sure mother got tired.

Many thanks to my rugby teammates, each and every one of you never stopped believing in me, motivated me when I felt this is impossible.

I would like to thank my family abundantly. The one thing I needed the most to finish was space and everyone respected and gave me that, so thank you. For the motivating messages and calls. For the support and love when I was at my lowest. For always being there for me.

Table of Contents

List of Figures and Tables

CHAPTER 1

Introduction

Sea level changes shape the continental shelves, as they are submerged during warmer interglacial periods and emerge in glacial periods (Bosman, 2012). The submerged shorelines of continental shelves provide stratigraphic evidence of the response of the entire littoral zone, as it migrates up the profile during phases of sea-level rise. Pretorius et al. (2016) state that submerged barrier systems provide information on the rate of relative sea-level rise, the rate and effectiveness of transgressive ravinement processes, and how these interact to produce and preserve the stratigraphy of continental shelves. All of this can be provided by detailed examinations of the sedimentary and stratigraphic architecture of submerged shoreline deposits. In addition, comparisons can be drawn between these features and present day systems in terms of accumulation rates, volumes and even climatic conditions (e.g. Cawthra et al., 2014).

Likewise, the examination of high-resolution seismic and backscatter records of shelves reveals much regarding the evolution of the shelf throughout the glacial interglacial cycles, together with the response of the shelf sedimentary regime to oceanographic forcing and changes in sediment supply (e.g. Green, 2009).

This study provides a detailed stratigraphic and geomorphological study of the East London continental shelf of South Africa. The project is framed by broader studies that are attempting to link seafloor geomorphology and biodiversity in the context of South Africa's flagship marine science programme, the African Coelacanth Ecosystem Programme. Of key importance to fish assemblages and hard-rock benthic biota, are submerged shorelines, which act as focal points for demersal fish populations (Winker et al., 2014) and anchor sites for sessile invertebrate communities and importantly cold-water corals (e.g. Sink and Samaai, 2009). In this light, this project aims to examine the seafloor geology and geomorphology, using high resolution remote sensing techniques from an area of important biodiversity (Solano-Fernandez et al., 2012), where little is known regarding the shelf. In

particular, submerged shorelines are examined, from both a stratigraphic and morphologic perspective, together with the sediment compositions of the adjacent shelf materials.

1.1. Aims and objectives

This dissertation aims to provide a geological interpretation of the formation and evolution of the Eastern Cape continental shelf, with particular emphasis on submerged landscapes and palaeo-shorelines. The study focuses on the area spanning the East London upper continental slope to inner shelf, from Port Alfred in the south to Mazeppa Bay in the north (Fig. 1.1). This encompasses an along coast distance of ~ 180 km. The objectives of this study are:

1. To create a series of ultra-high resolution bathymetry maps in order to examine the seascape for features such as drowned shorelines and unconsolidated sediment accumulations.
2. To relate the seafloor features to geological processes, associated with either sea-level variation, changes in sediment supply and changing climate
3. To place these in a chronostratigraphy as best as possible.
4. To examine the shallow subsurface geology from selected areas, tie this to the bathymetry and recreate the evolving geological conditions.
5. To examine the seafloor texture using co-registered backscatter, and to place this into the oceanographic context.

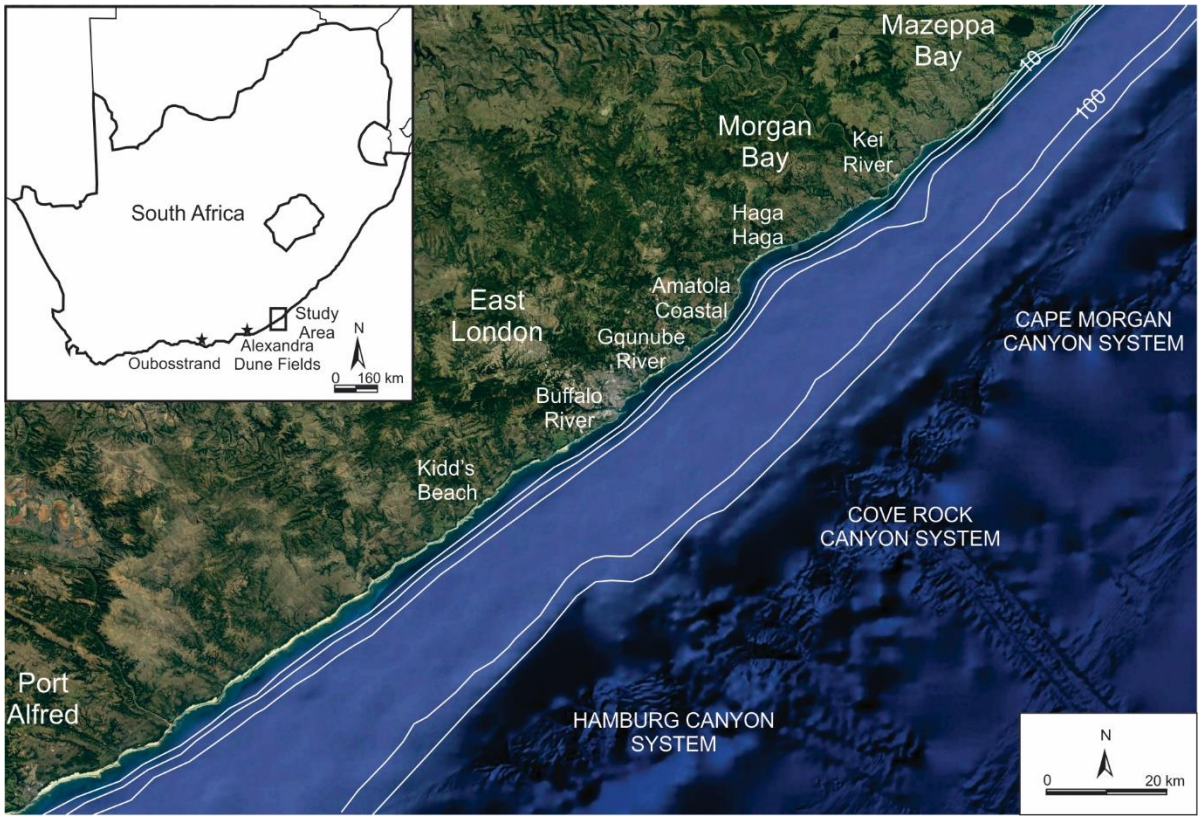

Fig. 1.1. Locality map of the study area spanning the East London continental shelf, from Port Alfred in the south to Mazeppa Bay in the north. The location of Oubosstrand and the Alexandra Dune Fields are indicated by a star.

CHAPTER 2

Literature Review

2.1. Submerged barrier shorelines

Submerged barrier shorelines represent former shoreline complexes that have been preserved as continental shelves were drowned during transgression (e.g., Locker et al., 1996; Gardner et al., 2005, 2007). Their preservation is considered to be enhanced by factors such as coarser grain-sizes (Mellett et al., 2012); early cementation of the barrier form (Green et al., 2013a); gentle antecedent shelf gradient and reduced wave-energy (Storms et al., 2008). The preservation of shoreline sequences is often the result of overstepping of the barrier shoreline during transgression (cf. Carter, 1988; Green et al., 2013). The conditions necessary for overstepping and preservation of overstepped barriers have been debated with much of the argument centred around the degree to which the overstepped barriers are degraded or destroyed in the nearshore zone during overstepping (Rampino and Sanders, 1982).

2.2. A review of shoreline response to relative sea-level rise; Rollover vs overstepping

A number of models have been proposed concerning shoreline or barrier response to rising relative sea-level (RSL) and the resultant geomorphological and stratigraphic signatures produced on the newly formed continental shelf. Well-established models tend to refer to barrier behaviour and modification on low-gradient shelves with a gradient of ~0.01^0 (e.g. Swift, 1968, 1975; Trincardi et al., 1994; Storms et al., 2008; Nordfjord et al., 2009). Recently, the mainstream theory suggests that rollover controls the behaviour of barrier-lagoon systems; (Fig. 2.1b; Swift, 1968, Swift et al., 1991, Belknap and Kraft, 1981). The process of rollover involves the continuous landward retreat of the shoreline which keeps pace with the rate of transgression through a combination of aggradation and landward migration. Wave and tidal ravinement processes entirely rework the barrier-lagoon

deposits, typically resulting in little preservation of these in the offshore sector (Swift and Moslow, 1982; Leatherman et al., 1983).

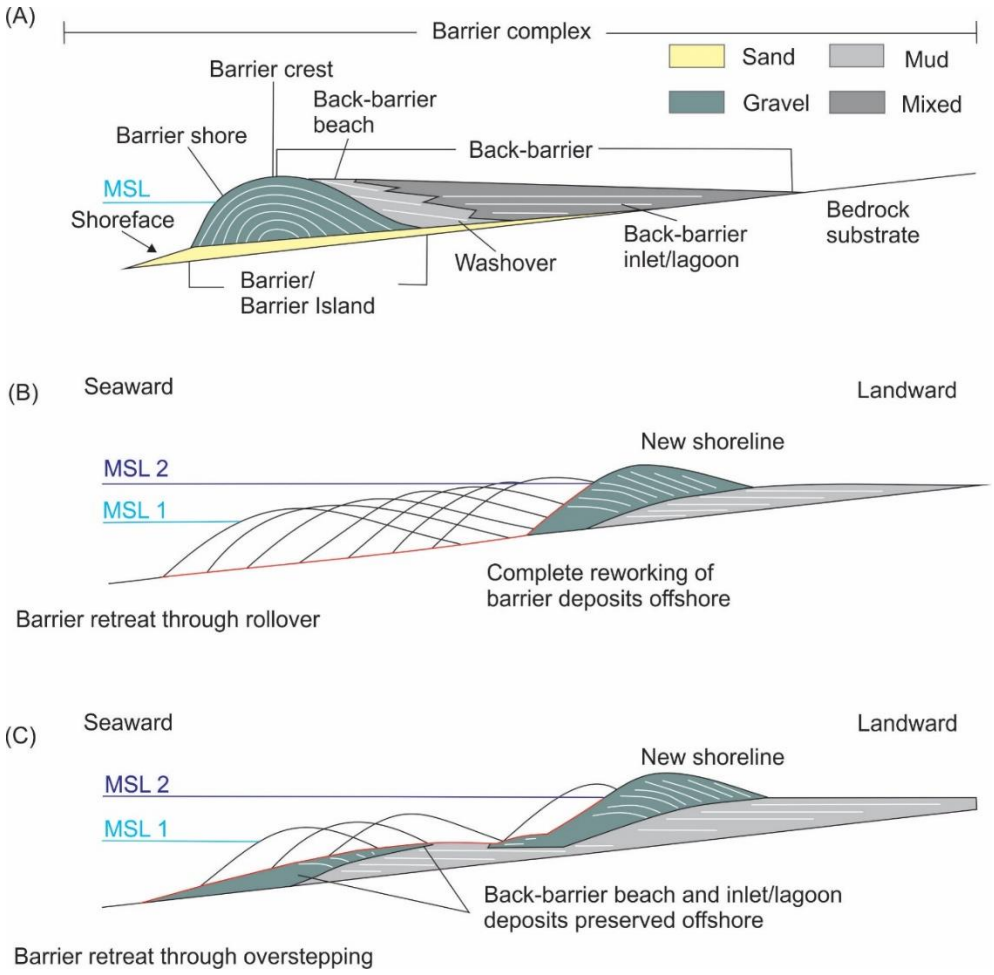

Fig. 2.1. Barrier migration illustrating: a) the main components forming a typical barrier or barrier island system, followed by two primary mechanisms of barrier movement, namely b) rollover and c) overstepping. Modified after Mellett et al. (2012).

Alternatively, barrier overstepping occurs where barriers fail to keep up with the pace of rising sea-levels and are ultimately stranded on the continental shelf as sea level continues to rise over them (Fig. 2.1c; Curray, 1964; Swift, 1968; Rampino and Sanders, 1980). This also involves the vertical growth of the barrier-complex as sea-levels rises (through aggradation) and simultaneous enlargement and trapping of sediment in the lagoons that constrain these barriers and facilitates their overstepping (Storms et al., 2008). The previously formed barrier-complexes tend to be either partially or fully preserved on the shelf, when the shoreline is displaced landward (Rampino and Sanders, 1980, 1982;

Leatherman et al., 1983; Forbes et al., 1991; Storms et al., 2008; Hijma and Cohen, 2010). Mellett et al. (2012) further subdivided this overstepping model into: (1) "*Sediment surplus overstepping";* under conditions of rapid RSL rise with minimum wave reworking, near complete preservation of barrier complexes may occur. Resulting in almost complete preservation of the barrier complexes; and (2) "*Sediment deficit overstepping"*; the shoreline migrates landward in an intermittent fashion and lower degree of preservation can be expected.

These barriers are typically truncated by the wave ravinement surface (wRS, the erosional surface that forms during landward migration of the beachface and shoreface due to rising sea level; e.g. Cooper et al., 2016; 2018; Green et al., 2017). Above the ravinement surface, deposits of the latest transgressive systems tract and highstand systems tract may be less well developed in gentle gradient settings, as compared with the thick post-ravinement transgressive deposits of steeper gradient shelves (e.g. Salzmann et al., 2013). Conditions for the drowning of barrier complexes in these circumstances are considered by Cattaneo and Steel (2003) to be unfavourable.

2.3. Shoreline trajectory

With regards shoreline behaviour amid transgression, the fundamental hypothesis suggests that shoreline trajectory is the essential factor in determining the measure of erosive ravinement that may occur and thus, also controls the ensuing level of preservation (e.g. Helland-Hansen and Gjelberg, 1994; Cattaneo and Steel, 2003). Taking into account relative sea-level flux, sediment supply and antecedent topography, shoreline trajectory is defined as the cross-sectional path of shoreline migration up depositional dip (Helland-Hansen and Gjelberg, 1994). The antecedent topography of the area will dictate both the ravinement shoreline gradient and the resulting topographic relief.

When erosion predominates, few transgressive deposits are deposited. Typically, this occurs when shoreline trajectory coincides with, or is at a low angle, when compared to the surface being transgressed. In this circumstance, the rates of RSL rise are rapid, the transgressed topography is of a low gradient or the rate of sediment supply is low. On the other hand,

extensive accumulations of transgressive stratigraphies with high preservation rates are deposited when a shoreline trajectory is steeper than the transgressed stratigraphy. The transgressed topography is steep or under high sediment supply conditions, when the rate of relative sea-level rise is gradual (Cattaneo and Steel, 2003). In effect, steeper antecedent settings are predisposed to less erosion.

2.4. Barrier preservation potential

Various factors contribute to the preservation potential of a barrier system i.e. the degree to which the system is eroded during transgression. The long-term advancement of coastal barriers and their related back-barrier environments is dependent upon *barrier volume*, the coastal physiography, the *extent of lithification* within the barrier and the *energy setting* (wave, tide and current dependent; Swift, 1968; Forbes et al., 1990, 1991; Forbes, 1995). Coastal physiography is a function of numerous factors including *bathymetric relief, coastal alignment*, *degree of exposure*, *accommodation space, headland control, the geometry of the shoreface*, *compartmentalisation* and *depth of reworking* (Swift, 1968; Forbes et al., 1990, 1991; Forbes, 1995). A further contributing factor associated with the destruction or preservation of coastal deposits during transgression is the presence or absence of a *sediment lag* mantling the shoreface (Swift, 1968). The sediment lag may act to armour, or otherwise protect, the barrier deposits from ravinement. Another principal variable influencing preservation potential is sediment size. Gravel-dominated barriers have longer relaxation times and are thus more resilient than sandy systems and are more likely to be preserved (Long et al., 2006). Tidal range will also play a pivotal role in preservation potential. The lower the *tidal range*, the more probable it becomes that a barrier-island will be preserved during overstepping due to the limited tidal currents contributing to the overall energy setting of the system (Storms et al., 2008). Under transgressive conditions, based on the *rate of sea-level rise,* the shoreline trajectory may be either steepened or flattened and as discussed previously, will influence the evolution and preservation of barrier shoreline system.

2.5. Lagoon systems

A coastal lagoon is defined by Bates and Jackson (1980) as a shallow stretch of seawater, near or interacting with the sea, and partly or completely separated from it by low, narrow elongate strips of land, such as reefs, barrier islands, sandbanks or spits. Lagoons commonly stretch out parallel to the coast, as opposed to estuaries, which are orientated roughly coast-perpendicular. Numerous lagoons have no significant freshwater runoff; however, some coastal embayments that generally fulfil the definition of a lagoon do receive river discharge (Bates and Jackson, 1980). Amid storms, sediment is washed from the front of the barrier, over into the sheltered lagoon and conserved as landward-dipping, current-rippled to planar laminated 'washover fans' (Fig. 2.2; Howell and Flint, 2003).

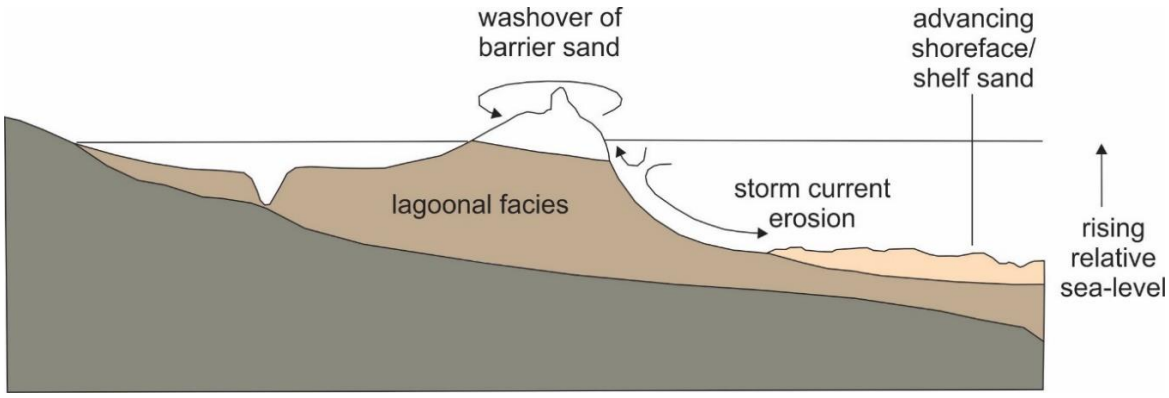

Fig. 2.2. Schematic cross-section through a barrier island showing processes operating during landward migration of the barrier as a result of relative sea-level rise (Modified after Reinson,1992).

2.6. Incised valleys

Incised valley systems as defined by Zaitlin et al. (1994) are fluvially- or glacially-eroded, elongate topographic lows indicated by an abrupt basinward shift of depositional facies across a basal sequence boundary of regional extent. They form in response to base level fall which exposes the continental shelf to fluvial erosion. Later infilling during the subsequent sea-level rise of a transgressive cycle forms and important part of the transgressive systems tract. As coastal depressions, incised valleys shield sediments from

removal by ensuing transgressive erosion and give the most complete sedimentary record of the lowstand through transgressive systems tracts (Thomas and Anderson, 1994; Payenberg et al., 2006).

2.6.1. Wave dominated incised valleys

According to Dalrymple et al. (1992), wave dominated estuaries are characterised by a predictable spatial organisation of facies that exist in response to convergence of fluvial and marine depositional processes. This results in a tripartite facies distribution that typically comprises an outer, seaward zone occupied by sandy sediments of marine origin, a central zone of fine-grained sediment derived from suspended river bed load and autochthonous biological sources, and a landward tidal-fluvial zone of terrestrial derived deposits. The tidal influence is small and the mouth of the system experiences relatively high energy (Dalrymple et al., 1992). Examples include the James estuary in Virginia (Nichols et al., 1991); the Gironde estuary (Allen, 1991; Allen and Posamentier, 1993), estuaries along the southeast coast of Australia (Bird, 1967; Reinson, 1977; Roy, 1984; Nichol, 1991), the onshore and offshore incised valleys of SE Africa (Cooper, 2001; Green, 2009; Green et al., 2013b). Ancient examples include the Crystal and Sundance/ Edson valley-fill deposits of the Viking Formation, Alberta (Reinson et al., 1988; Pattison, 1992) and the Lloydminster member of the lower Cretaceous Manville Group of west-central Canada (Zaitlin and Shultz, 1990).

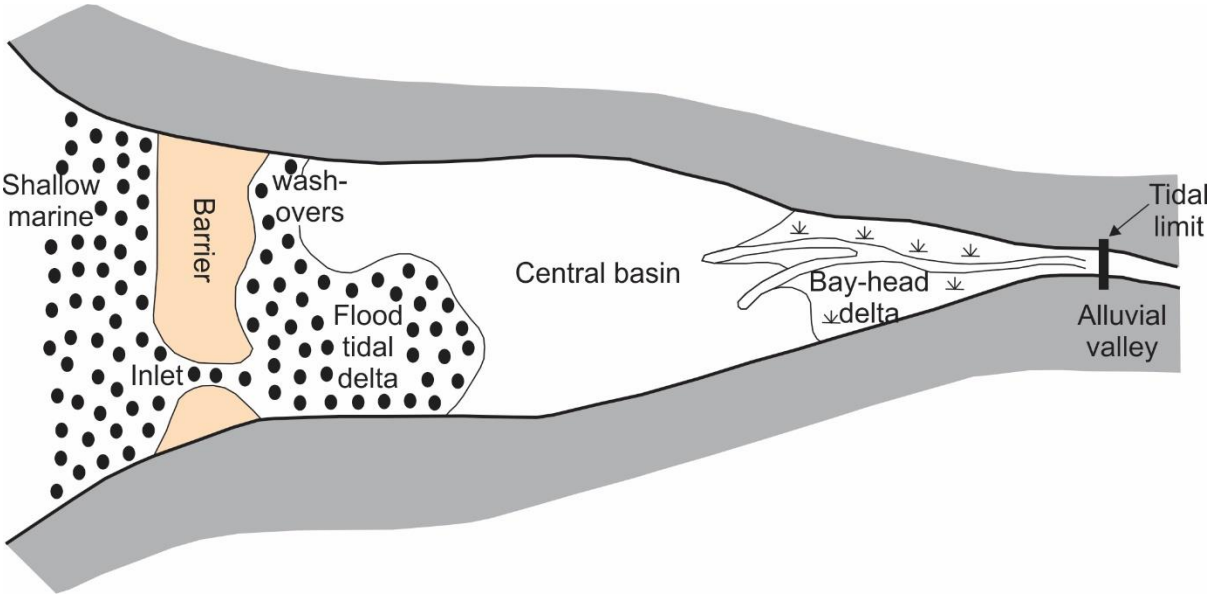

Fig. 2.3. The tripartite zonation of facies in wave-dominated estuaries (modified from Dalrymple et al., 1992).

CHAPTER 3

Regional setting

3.1. Regional setting

The continental margin of southeast Africa corresponds to a shear zone along which South America separated from southern Africa during the initial opening of the South Atlantic (Scrutton and Du Plessis, 1973). Regionally, it is exceptionally straight and narrow, but on a local scale, there are extensive variations in morphology, especially in the distribution of canyons and other irregularities on the continental slope (Flemming, 1981; Dingle et al., 1983).

During the Neogene and Quaternary periods, the South African coast has provided a significant sink with regards to the deposition and accumulation of marine, aeolian and lacustrine sediments (Dingle et al., 1983). The cohesion of this coastline is fragmented by a series of zeta (half-moon) bays of which their origin is related to the brittle deformation phases associated with Gondwana break-up (Watkeys, 2006).

Successive and widespread erosion of the hinterland delivered Cretaceous and younger sediments to the offshore, preserved in the Mesozoic offshore basins. Post-Cretaceous uplift, following the tectonic activities of Gondwana, has resulted in variable rates of Cenozoic land-level changes. Several periods of significant, and rapid, uplift resulted in the formation of pediplains and erosional surfaces (Partridge and Maud, 1987). In contrast, to Partridge and Maud's (1987) episodic uplift model, several recent studies using cosmogenic nuclides and fission-track analysis (Bierman and Caffee, 2001; Luft et al., 2005; Tinker et al., 2008a, b; Kounov et al., 2007) have cited evidence for slow and more uniform rates of erosion during the Cenozoic. The onshore Southern Coastal Plain is capped by periodic silcretes and saprolite profiles that point to a lengthy period of exposure. Offshore, the subsequent fluctuations in the Neogene and Pleistocene sea level, planed the softer Cretaceous sediments and sedimentary rocks (Compton, 2011).

The East London shelf break occurs between 110 m and 120 m depth, with a shelf width that varies between 19 km off the Kei River mouth (north) and 23 km off the Great Fish Point (south). This is narrower and slightly shallower than the world average of 75 km and 130 m, respectively (Flemming, 1981). The platform represents a tectonically raised coastal shelf bevelled by wave abrasion in Late Cretaceous to Early Tertiary times, as revealed by locally preserved, shelly limestone remnants of Palaeocene-Eocene age near East London further to the east (Lock, 1973).

The most important factor in the Neogene development of the outer continental margin of the study area are the large scale slumps and canyons forming immediately after deposition of a stratum. The foot of the continental slope has been shifted up to 25 km basinward by slope wasting and allochthonous mass movement which has constructed extensive continental rise lobes (Dingle and Robson, 1985). Shelf break breaching by canyon heads plays an essential role in the transferring sediment entrained in the Agulhas Current from the continental shelf to the deep ocean basin (Flemming, 1981). The recent sedimentary history of the southern part of the Natal Valley is thought to have been strongly influenced by the distribution of canyons and related continental slope features (Dingle et al., 1983). Flemming (1981) noted that in spite of the several canyon heads that dissect the shelf break, none penetrate far into the shelf and further considered that the locally complex shelf microtopography is caused mainly by Neogene sedimentary features.

Kidd's Beach is considered a prominent coastal offset, and to the south of which, lie three canyon systems (Dingle and Robson, 1985). Each of these has several branches which unite before they advance onto the continental rise at about 3500 m and their sinuous extensions reach the outer edge of the rise at depths of between 4000 m and 4300 m. Extending to the shelf break are the Hamburg and Cove Rock systems, with a third, the Stalwart Canyon not traced shallower than ~ 2000 m (Dingle and Robson, 1985).

3.2. Wind regime and wind-driven circulation

The continental margin of southeast Africa is classified by a high-energy environment (Davies, 1972) dominated by south-westerly swells. The annual mean percent probability of

swell >4 m is about 39% in the south, varying from 26% in March to 48% in August. Thus, swell intensity decreases towards the lower latitudes.

Winds exceeding 8 m/sec are reached with frequencies approaching 60% throughout the year, whereas speeds in excess of 20 m/sec are attained with a frequency of 5% in late summer and up to 20% in late winter. In the case of swell, the frequency of strong winds decreases significantly towards the lower latitudes. There is a periodic alternation between the north-easterly and south-westerly winds, with the latter being dominant over most of the year (cf. Smith, 1961). The strong winds experienced during the late winter months are formed in the wake of high-intensity, low-pressure systems in association with the climate belts by at least 5° latitude (cf. Davies, 1972; Taljaard, 1972).

During south-westerly gales, local wind-generated surface waves and nearshore wind-stress currents spread north-eastward, against the Agulhas Current and parallel to the coastline. The formation of destructive giant waves along the shelf margin may be formed by the propagation of high swells into the current (Mallory, 1974; Schumann, 1976; Smith, 1976). North-easterly winds create surface waves and wind-stress currents which go with the current. As much as the north-westerly and south-easterly winds are not frequent, Flemming (1980) observed wave ripples in coarse sands and gravel at depths >50 m on the southeast African continental shelf, suggesting occasional heavy swells from the southeast.

3.3. Influence of the Agulhas Current

Along the east coast of southern Africa, the Agulhas Current is the most important factor controlling sediment dispersal. Fed by the Mozambique Current, the East Madagascar Current and the Agulhas Return Current (Fig. 3.1; Duncan, 1970; Flemming and Kudrass, 2017), this forms a vigorous western boundary current. The Agulhas Current is one of the few fast-flowing ocean currents found close to a coastline for appreciable distances (over 1000 km). This is due to the extremely narrow continental shelf. Just beyond the shelf break, surface current velocities of >2.5 m/sec have been reported for the core of the current (Pearce et al., 1978). The Agulhas Current is inherently unsteady, just like other similar geostrophic flows. The combined effects of local wind stress, meandering and lateral

migration are the probable cause of velocity fluctuations (cf. Anderson, 1965; Darbyshire, 1972; Pearce et al., 1978). This unsteadiness provides the mechanism for large-scale sediment supply into the central-shelf sandstream (Flemming, 1980).

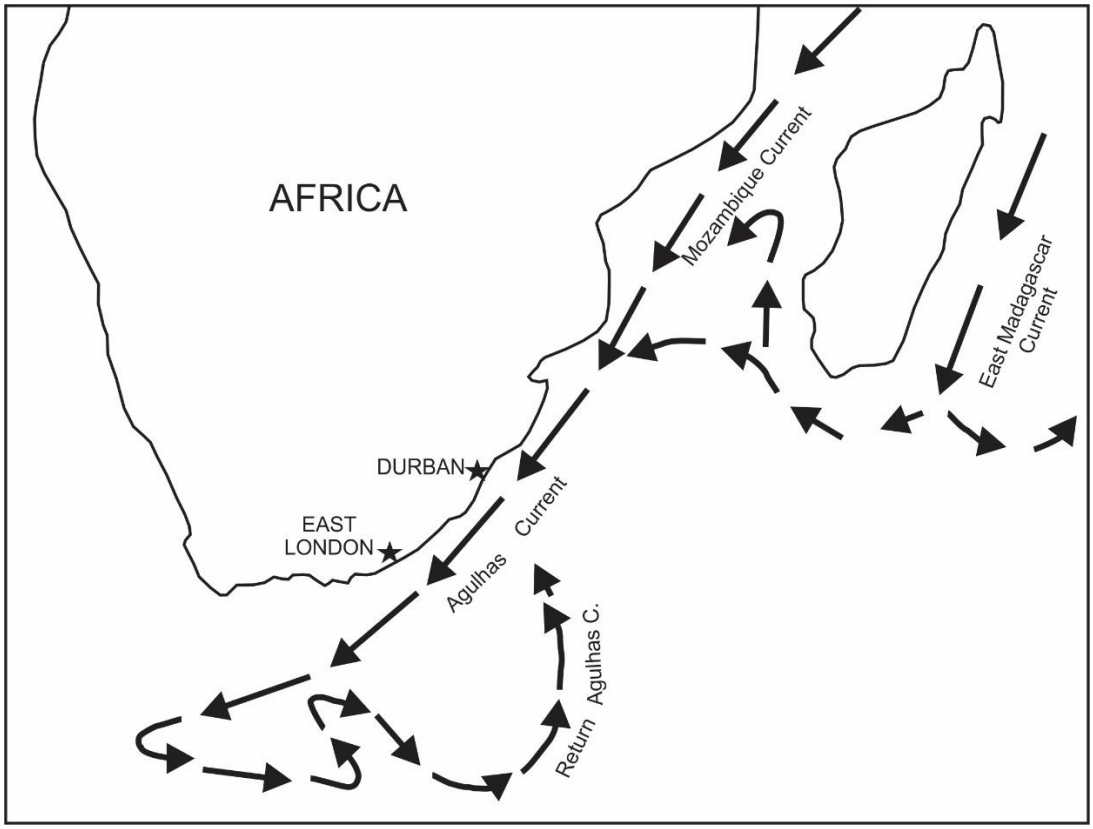

Fig. 3.1. The regional setting of the Agulhas Current setting and, its relationship with the Mozambique Current, the East Madagascar Current and the Return Agulhas Current (Modified after Flemming, 1981).

The relationship between the course of the current and the orientation of the shelf break is an important control on shelf sediment dispersal. Generally, the current is found near the shelf break. Since the momentum of the flow prevents an adjustment to abrupt topographic changes, at each structural offset the current overshoots the shelf break and proceeds over deeper water (Flemming, 1981). In the lee of structural offsets, clockwise eddies have been observed. The eddies are primarily due to the topographically induced velocity structure of the Agulhas Current (Gill and Schumann, 1979). These eddies are particularly responsive to atmospheric forces in the wake of coastal low pressure fronts (Pearce, 1977; Bang and Pearce, 1978). In the south off Algoa Bay there is no eddy systems, but south-westerly winds often produce inshore counter currents (Harris, 1978).

There is no evidence for a notable tidal component in the flow. Spring tide ranges vary from 1.7 to 1.9 m and co-tidal lines run parallel to the coastline, therefore adding little to the coast-parallel flow of the Agulhas Current (Flemming, 1981).

3.4. Sediment supply

With regards sediment dispersal, information about sediment sources, amount of material supplied and the hydraulic properties of the sedimentary particles is required. Of interest are four main sources of sediment, the fluvial supply, modern and relict biogenic products, coastal and shallow-marine erosion and authigenic mineral production at the sea-bed (Flemming and Hay, 1988). The most important source of terrigenous sediment is fluvial discharge, with river mouths marking the major input points. The major fluvial contributors to the study area are the Kei, Gqunube and Buffalo rivers. Biogenic products in the form of bioclastic material is a second significant contributor. On a regional scale there are is no evidence for massive coastal erosion (Flemming, 1981). The local loss of sand during severe storms is usually replace by onshore movement of sediment during fair weather periods (Flemming, 1981).

Authigenic mineralization is not prominent along the east coast, although some glauconite is carried into the south, where periodic or episodic inshore counter currents erode a large glauconite reservoir situated off Algoa Bay, to the south of the study area (Bremner, 1978).

3.5. Geological Setting

3.5.1. The Karoo Supergroup

The study area is covered by the sedimentary rocks of the Beaufort and Ecca Group found in the south-eastern part of the Karoo basin (Johnson et al., 1997).

3.5.1.1. The Ecca Group

The Permian Ecca Group comprises a total of 16 formations (Johnson et al., 2006) of which the Ripon Formation is observed landward of the Buffulo River mouth (Fig. 3.2).

The Ripon Formation is generally a 600-700 m thick succession consisting of poorly sorted, fine- to very fine-grained lithofeldspathic sandstones alternating with dark-grey clastic rhythmites and mudrocks (Johnson and Kingsley, 1993). In the eastern region of the basin, the formation can be subdivided into a lower Pluto's Vale Member (mainly sandstone), a middle Wonderfontein Member (mudrock/rhythmite) and upper Trumpeters Member (alternating sandstone and mudrock; Kingsley, 1977; 1981; Johnson and Kingsley, 1993).

Deformation structures include load casts, flame structures, convolute bedding, sandstone dykes and sills, and slump structures (Johnson et al., 2006). Various trace fossils, including tracks, trails, tubes and burrows, occur sporadically throughout the Ripon Formation (Anderson, 1974; Kingsley, 1977), generally reflecting deep-water conditions. Palaeocurrent data suggests a north-northwesterly transport direction (Johnson et al., 2006).

3.5.1.2. Beaufort Group

The Beaufort Group is composed of the lower Adelaide Subgroup and an upper Tarkastad Subgroup.

3.5.1.2.1. Adelaide Subgroup

The Late Permian Adelaide Subgroup, in the southeastern part of the basin, includes the Koonap, Middleton and Balfour Formations (Johnson et al., 2006). The Koonap Formation is absent from the study area. The Middleton Formation is characterised by abundant red mudstones, and an arenaceous Oudeberg Member constitutes the base of the Balfour Formation (Johnson et al., 2006).

The Adelaide Subgroup reaches a maximum thickness of about 5000 m and consists of alternating blush-grey, greenish-grey, or greyish-red mudrocks and grey, very fine- to medium-grained lithofeldspathic sandstones (Johnson et al., 2006).

The mudrocks in the Adelaide Subgroup are generally massive Calcareous nodule and concentrations occur in mudstones throughout the Beaufort Group (Johnson et al., 2006). Terrestrial vertebrate fossils are common, with fish remains, molluscs, invertebrate burrows and trails, silicified wood and stem impressions that occur sporadically throughout the group (Johnson et al., 2006). Well-preserved leaf impressions (mainly Glossopteris) are also common in the Daggaboersnek Member (Riek, 1973, 1976).

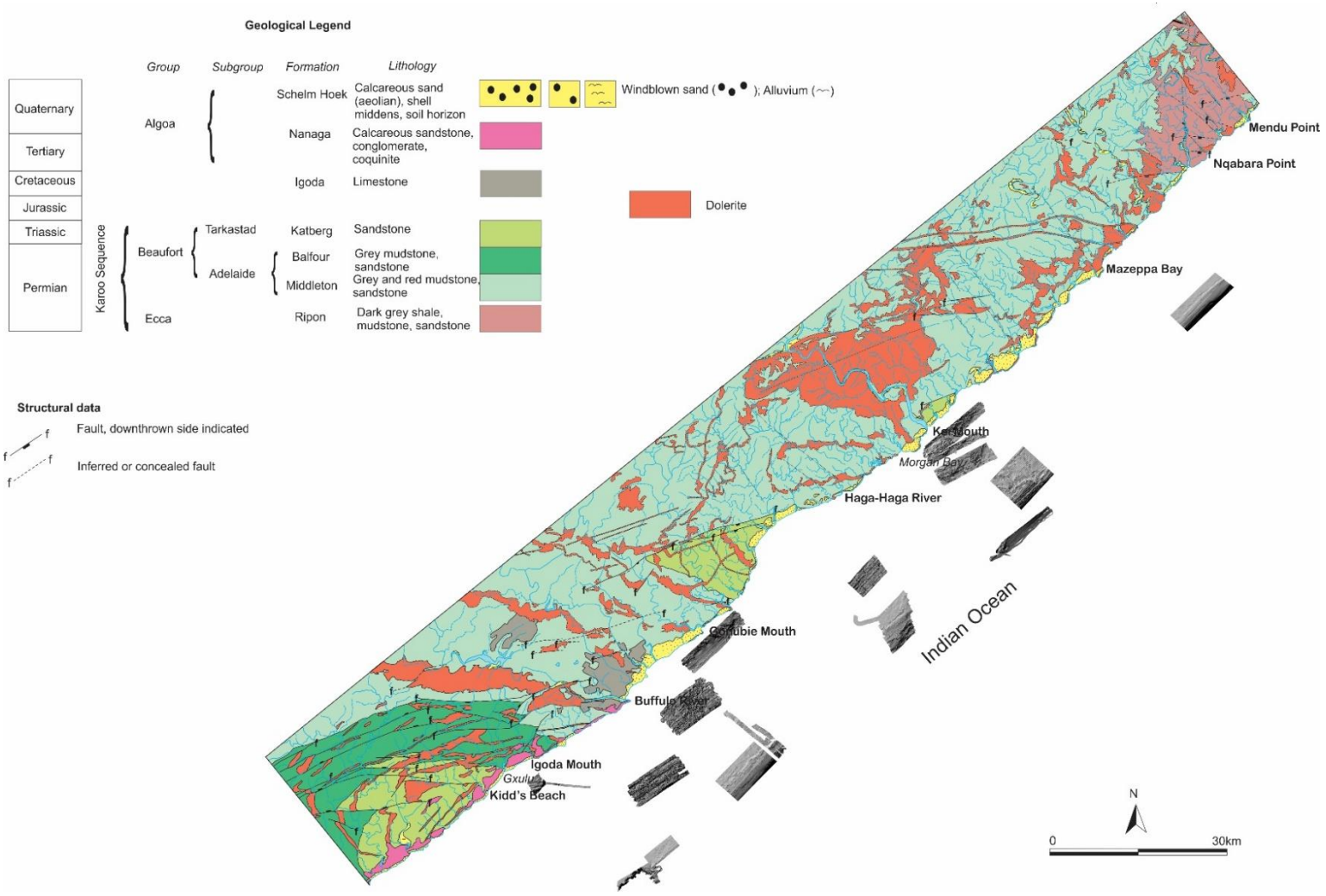

Fig. 3.2. Geological Map of East London. Showing the various formations from the Permian age through to present day. The study area shown by bathymetry. Modified from the 1:50 000 sheet published by the Council for Geoscience.

3.5.1.2.2. Tarkastad Subgroup

The Tarkastad Subgroup is defined by a greater abundance of both sandstone and red mudstone than the Adelaide Subgroup. It comprises a lower Katberg Formation (sandstone-rich) and an upper Burgersdorp Formation (mudstone-rich) which is absent in the study area (Fig. 3.2; Johnson et al., 2006). The Katberg Formation occurs in small coastal exposures near East London and is made up of 90% sandstones. The sandstones are fine to medium grained, with scattered pebbles up to 15 cm in diameter present in the coastal outcrop, and light brownish grey in colour. Intraformational mud-pellet conglomerates are common in the Katberg Formation (Johnson et al., 2006).

3.5.2. Onshore Post-Karoo Mesozoic Deposits

Isolated Jurassic and Cretaceous deposits occur along the eastern and southern margins of South Africa. These deposits are, for the most part, remnants of once thicker and more laterally extensive successions that accumulated in complex graben and half-graben basins. These basins formed along the margins of the newly developed African continent in response to regional extension associated with the break-up of Gondwana (Shone, 2006). Of these deposits, the Igoda Formation is commonly cropping out in the study area (Dingle et al., 1983).

3.5.2.1. Igoda Formation

The Igoda Formation occurs along the Igoda River mouth southwest of East London, comprising a conglomerate overlain by 20 m of calcareous, glauconitic sandstone that contains a restricted assemblage of corals, echinoderms, bivalves, brachiopods and foraminifera, together with the ammonite genus *Baculites* (Klinger and Lock, 1979).

3.5.3. Algoa Group

The name Algoa Group was given to the Cenozoic strata that extend eastwards from Oubosstrand to East London by Le Roux (1990a). This group has six formations of which two are present in the study area, based on the 1:250 000 geological map from the Council for Geoscience (Fig. 3.2).

3.5.3.1. Bathurst Formation

The Bathurst Formation is found between Port Elizabeth and East London, situated on a slightly tilted marine surface of erosion (Partridge and Maud, 1987). The formation ranges in elevation from 75 to 375 m between Bathurst and East London and comprises soft marine limestone overlain by pebbly coquina, in some places include a basal beach deposit containing silcrete clasts (Le Roux, 1990b). The formation rests unconformably on Karoo Supergroup bedrock (Maud and Partridge, 1990) and is dated to the middle Early Eocene or earliest Middle Eocene (Maud et al., 1987).

3.5.3.2. Alexandra Formation

The Alexandra Formation is located near Colchester, 37 km northeast of Port Elizabeth, although it occurs largely to the north of Algoa Bay. The Formation comprises a basal conglomerate layer or bed of oyster shells, overlain by interbedded calcareous sandstone, pebbly coquina and thin conglomerates. The sandy upper part of the succession consists of horizontally bedded as well as planar and trough cross-bedded calcareous sandstone deposited in shoreface, foreshore, infralittoral and estuarine environments (Le Roux, 1987a, b). The maximum thickness of this formation is 18 m and is probably Late Miocene to Pliocene in age (Siesser and Dingle, 1981). The deposition of the Alexandra Formation was in response to series of Middle Miocene to Pliocene marine transgression/regression cycles (Le Roux, 1990b).

3.5.3.3. Nanaga Formation

This formation occurs extensively in the northern hinterland of the Algoa Bay and along the coast to the west of Port Elizabeth (Fig. 3.2). It comprises coastal palaeo-dune fields, with medium-grained, cross-bedded, calcareous sandstones and calcretes up to 250 m thick (Le Roux, 1992). The Nanaga Formation may overlie the Palaeozoic Cape Supergroup, the Cretaceous Uitenhage Group or the Cenozoic Bathurst or Alexandra Formations. The estimated age of this formation is Pliocene to Early Pleistocene (Le Roux, 1990a).

3.5.3.4. Salnova Formation

This formation is sporadically developed and rests on a wave-abraded surface, truncating rocks of the Uitnhage and Table Mountain Groups and is unconformably overlain by Late Pleistocene to Recent aeolian deposits and soils (Le Roux, 1991). The Salnova Formation incorporates reworked Alexandra Formation coquina and conglomerate, an abundance of crustacean and echinoid remains and poor consolidation and cementation. The lithologies include calcareous sand, sandstone, conglomerate and coquina. The total thickness ranges from 1.6 to 6.5 m. It records Quaternary and possibly Late Pliocene eustatic sea-level fluctuations (Le Roux, 1991).

3.5.3.5. Nahoon Formation

The Nahoon Formation aeolinites rest on wave-truncated Palaeozoic and Mesozoic rocks, as well as conformably to disconformably on the Salnova Formation foreshore/upper shoreface calcarenites and conglomerates, just below present mean sea level (Le Roux, 1989). This formation is overlain by recent aeolian sands or soil and is patchily developed along the coastline. The Nahoon formation is found in East London, where large parabolic dunes up to 50 m high comprise well-consolidated, calcareous sandstone with internal palaeosols. The shelly material in the sandstone is dated using the luminescence and U-Th dating, giving the age of ~200 ka (Le Roux, 1989). The wave-cut benches are at 4 to 5 m

above mean sea level and a coquina of assumed Marine Isotope Stage 5e (last interglacial) age (MIS), discussed in section 2.6.3.

3.5.3.6. Schelm Hoek Formation

The most recent phase of aeolian sedimentation in the Algoa Group is recorded by the Schelm Hoek Formation. The type area is formed by the Alexandra and Schelm Hoek coastal dune fields east of Port Elizabeth, ~ 150 km south of East London. These dune fields vary from a few hundred metres to 3 km in width. The unconsolidated, calcareous aeolian sand ranges up to ~100 m in thickness, with locally developed palaeosols and Late Stone Age middens (Illenberger, 1992). Transverse dune forms predominate, with longitudinal, barchan and parabolic dunes also present. Accumulation of this formation has been ongoing since about 6.6 ka, when the sea level approximately reached its present elevation (Illenberger, 1992).

3.6. Sea-level changes

Tectonic uplift and subsidence may have influenced local changes in relative sea level along the coastal plain of southern South Africa (Compton, 2011). Nevertheless, in comparison to the large amplitude variations in global sea level on a glacial to interglacial cycles, these factors are assumed to have been insignificant for the coastline (Compton, 2011). This assumption is supported by the sea level curves derived from the South African margin which reflects general agreement with global records since the Last Interglacial (Ramsay and Cooper, 2002; Carr et al., 2010) and for the timing of sea level fluctuations since 440 Ka (Compton and Wiltshire, 2009). The composite global relative sea level curve of Waelbroeck et al. (2002) spans the last 450 000 years to present, a collection based on statistical comparison between relative sea level estimates derived from corals, other evidences and high-resolution $\delta^{18}O$ records. This shows repeated highstand-lowstand cycles that have caused repeated cross shelf fluvial incision during regression and subsequent wave-base planning during transgression. Superimposed on this are periods of stepped sea-level rise,

most notably during the Holocene deglaciation (see discussion chapter, Green et al., 2014; Pretorius et al., 2016).

3.6.1. Quaternary sea level variations in South Africa

In South Africa, several proxy data have been used to reconstruct past sea levels (e.g. Norström et al., 2012). The age constraints are based mainly on radiocarbon or Optically Stimulated Luminescence (OSL) dating of exposed marine facies or shoreline indicators (e.g. Ramsay, 1995; Compton, 2006; Carr et al., 2010), in addition palaeo-environmental indicators in lagoon and estuary sediments (e.g. Baxter and Meadows, 1999). During the last 7000 years, sea level has fluctuated no more than ± 3 m (Miller et al., 1993; Ramsay, 1995; Baxter and Meadow, 1999; Compton, 2001), compared to sea level fluctuation of greater than 100 m over periods of thousands of years during glacial to interglacial cycles (Ramsay and Cooper, 2002; Cutler et al., 2003).

In South Africa during the last interglacial (MIS-5e), sea level was approximately 6 to 8 m higher than present day (Ramsay et al., 1993). Sea level fell to about -50 m between 95 Ka and 54 Ka BP, followed by a subsequent transgression to -25 m at 25 Ka BP. The prolonged regression that followed the last interglacial, occurring over the next 7000 years that ended in the Last Glacial Maximum (LGM) lowstand of -125 m below Mean Sea Level (Green and Uken, 2005). The Flandrian Transgression (18 Ka to 9 Ka BP) followed, where sea level rose rapidly to the contemporary MSL (Ramsay and Cooper, 2002). During the Holocene Epoch sea levels gently fluctuated around the elevation of present day MSL (Ramsay, 1995).

The global sea-level rose due to increasing temperatures, glacial melting and large volumes of water within the world's oceans (Norström et al., 2012). The available sea level curves in the southern African region place the Holocene sea level maximum between 6500 cal BP (Miller et al., 1993; Compton, 2006) and 5000 cal BP (Ramsay, 1995; Baxter and Meadows, 1999; Ramsay and Cooper, 2002) with an elevation of ~2 to 5 m above MSL as suggested by Norström et al. (2012).

3.6.2. Meltwater Pulses and the global eustatic record

Meltwater pulses (MWPs), allow for a sudden increase in sea level as they represent stages of increased melting during deglaciation. Much dispute surrounds the timing and existence of meltwater pulses (see for example the references of Okuno and Nakada, 1999; Peltier, 2005; Peltier and Fairbanks, 2006; Stanford et al., 2006). This is due to the differences in the reconstructed sea-level variations between the coral-based records of Tahiti (Okuno and Nakada, 1999), and Barbados (Peltier and Fairbanks, 2006). The Tahiti records do not recognise a MWP-1B, though MWP-1A is evident. Furthermore, modelling of the ice sheet volumes over time, coupled to the global isostatic adjustments of the oceans satisfies the observations for Barbados, but is inconsistent with late-glacial sea-level observations at Tahiti. Recent sedimentological observations by Green et al. (2014) and Pretorius et al (2016) confirm that both MWP-1A and B affected the shelf of South Africa.

The Quaternary sea-level changes in Southeast Africa have been geo-eustatic in nature and are linked to climate variations, such as changes in ice volume in the northern hemisphere (Tankard et al., 1982; Dawson, 1992; Bradley, 1999; Siegert, 2001; Pillans and Naish, 2004). The melting of the icebergs accompanying the end of the OIS-2 glaciation (~ 18 000 yr BP) resulted in a rise in global sea-levels from as much as 120 m (e.g. Eitner, 1996; Siegert, 2001; Lambeck et al., 2002a; 2002b) to 130 m (e.g. Ramsay and Cooper, 2002).

On a global scale the Flandrian transgression occurred via several smaller decadal scale warming events known as Dansgaard-Oescher events, constrained to the northern hemisphere (Voelker, 2002), and several of larger high-magnitude meltwater pulse (MWP) events (e.g. Fairbanks, 1989; Bard et al., 1996; Okuno and Nakada, 1999; Liu and Milliman, 2004; Liu et al., 2007). The most noticeable of these is MWP-1A, which spanned depths of between 96-76 m and occurred between 14.3-14.0 ka BP; and MWP-1B during which sea-levels rose from depths of 58-45 m between 11.5-11.2 ka BP (Liu and Milliman, 2004). These correspond with rates of transgression of roughly 60 mm a-1 and 43.3 mm a-1 respectively.

The meltwater pulses were between colder climatic periods of slow or static sea-level known as slowstands (e.g. Kelley et al., 2010) and stillstands. A slowstand associated with

the Younger Dryas event occurred from ~12.7-11.6 ka BP in which the rates of RSL rise were primarily diminished (Camoin et al., 2004; Stanford et al., 2011).

In South Africa, the Flandrian transgression occurred between 18 000 and 9 000 yr BP and caused a large amount of the exposed shelf sands to be eroded before sea level stabilised at its present level between 7 000 to 6 000 yr BP (Ramsay and Cooper, 2002). Sea level rose to +2.75 m for a duration of 2 500 yr before reaching the mid-Holocene high sea-level of +3.5 m approximately 4 500 yr BP (Ramsay, 1995, 1997). Sea level declined to -2 m by ~ 2 000 yr BP before rising again to + 1.5 m around 1 610 yr BP (Ramsay and Cooper, 2002). Lastly, the sea level reached its current level approximately 900 years ago and appears to be slowly rising as deglaciation continues (Ramsay, 1995; Cooper, 2002).

CHAPTER 4

Methods

Figure 5.1 illustrates the data collection sites outlined below. Ultra high resolution seismic data were collected aboard the RV Meteor cruise M123 in February 2016. The data were acquired with an Atlas PARASOUND parametric echosounder using a primary low frequency of 4 kHz. Data were recorded on a master PC, where the navigation feed was incorporated into the seismic header using the Atlas HYDROMAP software. Navigation was achieved using a differential GPS (DGPS) capable of ~ 0.1 m accuracy in the X and Y domains.

The data were processed with Atlas PARASTORE, where the sea bottom was tracked, the data filtered and swell corrected, time varied gains were applied, and the processed data exported in SEGY format. All data were then interpreted in IHS Kingdom Suite.

Multibeam data were collected using two different systems. Data offshore Morgan Bay, East London shelf edge and the Mazeppa Bay area were collected in 2009 using a Reson 7125 high resolution multibeam echosounder coupled to a DGPS and Applanix POS-MV motion reference unit. The data were collected and processed by Marine Geosolutions Pty Ltd., and resolve to a 1 x 1 m grid, with a depth resolution of ~ 30 cm. Backscatter data were collected simultaneously with a Klein 3000 side scan sonar system with a scan range of 75 m using the 500 kHz channel. The data were processed using the Klein SonarPro software, where the bottom was manually tracked, the data were filtered with time varied gains applied, the channels colour balanced and the nadir zone removed for seamless mosaicking. The final data set resolve to a mosaic pixel approximating 1 x 1 m.

The second set of multibeam data were collected in September 2016 using the African Coelacanth ecosystem Programme's system. This encompassed a Reson 7101 Extended Range high resolution multibeam system, coupled to a hemisphere VS330 GNSS receiver and a SBG Systems Ekinox-D INS motion reference unit. Continuous sound velocity measurements were made at the sensor head with a Reson SVP-70 probe, and sound velocity profiles for the water column were collected hourly suing a Teledyne ODOM Digibar S500M. These were integrated into the data suing the Qinsy software package. All soundings were reduced to mean sea level during processing, where the data were cleaned

and the motion reference unit measurements incorporated to eliminate heave, pitch and yaw of the sensor head. The final data were output as a 5 x 5 m resolution grid, with a depth resolution of ~ 50 cm. Co-registered pseudo side scan sonar data were collected as Snippets for backscatter mapping, the final output of these on the same horizontal scale as the bathymetry data. Data were then visualised in ArcGis 10.4.

Seafloor materials were sampled using a benthic sled, a Shipek grab and a dredge, depending on the substrate; rocky substrate necessitated a dredge as opposed to the less consolidated materials such as mud and sandy material/gravels. Sampling was mainly done for biological purposes and as such, not all the bathymetric and backscatter features observed were sampled.

In an attempt to provide a geochronological framework for the upper sedimentary packages, bulk sediment and intact coralline material were selected for 14C dating using accelerator mass spectrometry (AMS). Calibrated ages were calculated using the Southern Hemisphere atmospheric curve SHCal13 (Hogg et al., 2013). A reservoir correction (DeltaR) of 161 +/- 30 was applied to the rhodolithic material, whereas no corrections were applied to bulk organic matter. All analyses were performed by Beta Analytic in their Florida radiocarbon facilities.

CHAPTER 5

Results

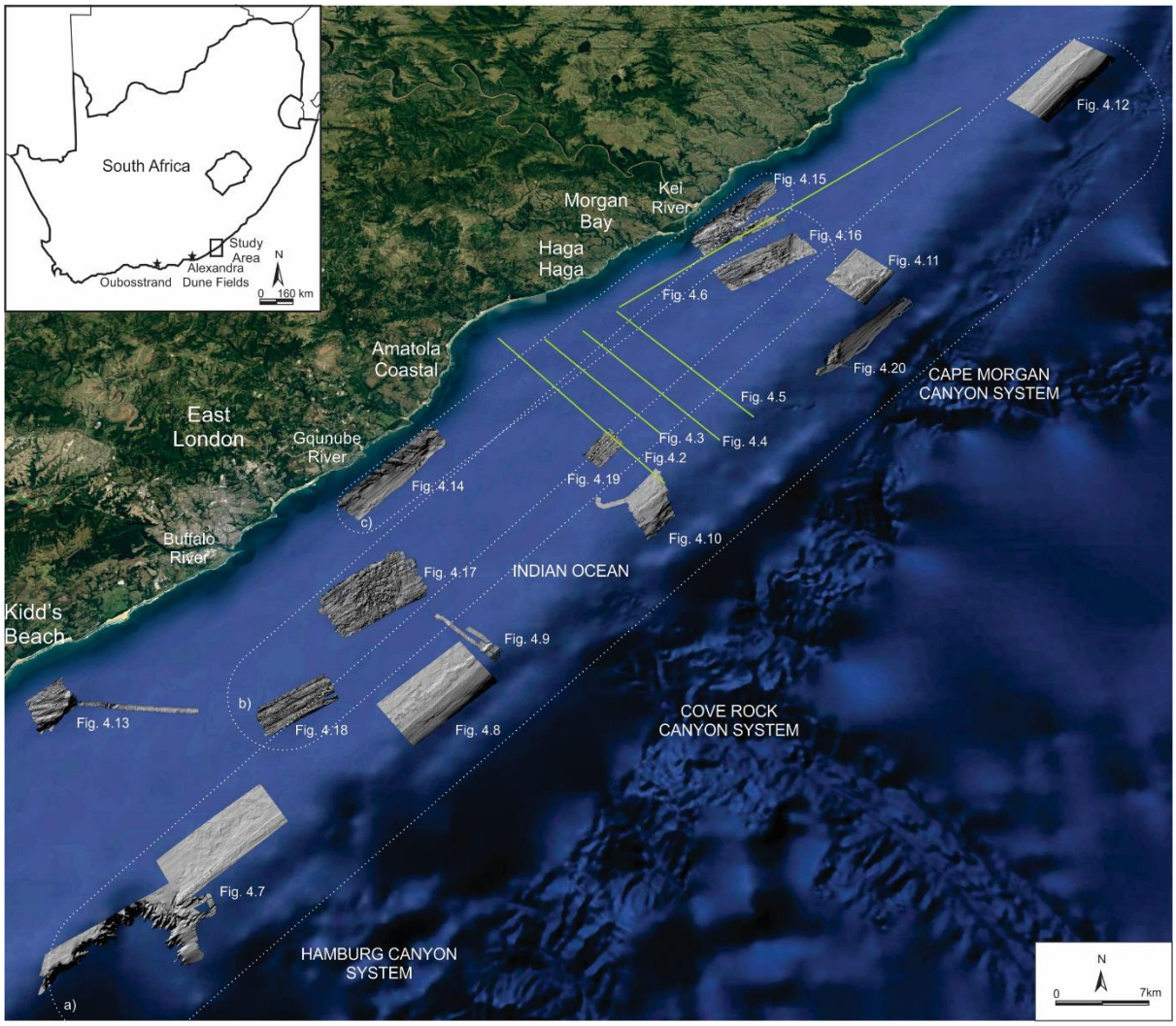

Fig. 5.1. Locality map of the East London continental margin, with seismic sections depicted in Fig. 5.2 to Fig. 5.6, the spread of data between targeted bathymetric blocks, and the canyon systems. The location of Oubosstrand and the Alexandra Dune Fields are indicated by a star.

This chapter consist of four subchapters; seismic stratigraphic observations, multibeam bathymetric descriptions, Side scan sonar and coregistered backscatter examinations and descriptions of the benthic samples.

5.1. Seismic Units (Table 5.1)

The position of the seismic lines are shown on the shown on the locality map above (Fig. 5.1), from figure 5.2 to figure 5.3.

5.1.1. Unit A

Unit A is observed in all seismic profiles and is the oldest unit resolved. It comprises a set of prograding, oblique parallel, high amplitude and continuous reflectors (Fig. 5.2, 5.3, 5.4, 5.5 and 5.6). High amplitude and continuous reflection. This unit is truncated by sequence boundary 1 (SB1), an undulating surface marked by several incised valleys. The valley dimensions reach depths and widths of ~ 78 m and up to 660 m respectively. In some areas, Unit A is truncated by SB2, a planar, gently seaward-dipping erosional surface with localised scours that truncates much of the stratigraphy.

5.1.2. Unit B

Unit B is recognized throughout the study area and comprises variable amplitude, hummocky- aggrading to acoustically transparent, low continuity reflectors and is ~ 3 m thick (Fig. 5.6). Unit B rests directly on SB1 and is truncated by SB2. Where Unit B does not occur, SB2 merges with SB1 to create a composite erosional surface (Fig. 5.2 and 5.5).

5.1.3. Unit C

Unit C is likewise pervasive throughout the study area. It comprises variable amplitude, aggrading to acoustically transparent, low continuity reflectors (Fig. 5.2a and 5.6) and is erosionally truncated by SB2. Unit C manifests as a fill facies that onlaps incisions into the underlying unit A, within surface SB1. It represents fills that are approximately 16 m thick, characterised by a wavy aggrading reflector geometry that forms a drape fill of alternating high and low amplitude reflectors with various degrees of continuity (Fig. 5.2a and 5.6)

5.1.4. Unit D

Unit D comprises a series of acoustically opaque, rugged-relief pinnacles (Fig. 5.2b and 5.3a). Occasional internal structure is evident (Fig. 5.3a), in such cases the internal reflectors are progradational. The unit has a gentle, dipping seaward surface and a more gently inclined landward face. SB2 truncates the upper portions of the unit, the base of which mantles SB1 (Fig. 5.2 and 5.3).

5.1.5. Unit E

Unit E comprises an acoustically transparent unit that onlaps Unit D to landward (Fig. 5.2b and 5.3a). The upper truncating surface (SB2) is rugged (Fig. 5.2b). The unit consists of occasional chaotic, low amplitude reflectors (Fig. 5.2b and 5.3a) which onlap small irregularities in SB1 (Fig. 5.2b). This unit incise into the underlying Unit A (Fig. 5.3a). It is approximately 8 m thick.

5.1.6. Unit F

Unit F rests on SB1 and truncated by SB2. Deposited at the break in slope at the toe of the pinnacle of Unit D. Its upper portions are truncated by Unit G1 (Fig. 5.4), if not Unit G2 (Fig. 5.2, 5.3 and 5.5). The Unit's internal reflector configuration is mostly acoustically transparent (Fig. 5.3a). Occasional low amplitude reflectors form high-angle prograding packages (Fig. 5.4). This unit ranges from about 4 m to 12 m in thickness.

5.1.7. Unit G

Unit G comprises a shore attached sediment wedge that has an onlap/downlap relationship of the reflectors (Fig. 5.2, 5.3, 5.4, 5.5 and 5.6). The reflector sets are dominantly progradational and can be subdivided into Unit G1 and Unit G2. Unit G1 is characterised by hummocky bottomset reflector that merge into tangential to sigmoidal topset reflectors (Fig. 5.3a and 5.4) with varying amplitudes and continuity. Unit G2 consists of high

amplitude and continuity, tangential oblique prograding-aggrading reflector sets (Fig. 5.3). In coast parallel orientation, Unit G2 forms two elongate drift packages (Fig. 5.6). These each span ~ ≥ 2000 km in a coast-parallel manner. These are separated from each other by a high point of Unit D and the acoustic basement. The two drift packages comprise sigmoid oblique reflectors that vary in terms of their dip angle (less than 1^0) and dip in a coast-parallel direction in opposing directions (Fig. 5.6).

5.1.8. Unit H

Unit H is a mound of intermediate to high amplitude reflectors that can be further sub-divided into Unit H1 and H2. Unit H1 comprises a chaotic to hummocky internal structure with discontinuous and discordant reflectors of variable amplitudes (Fig. 5.2d, 5.3b and 5.5). Unit H2 (Fig 5.4) consists of landward dipping reflectors which gradually become acoustically opaque to landward. This unit rests on Unit G1 in place of unit G2 which appears to be an up-dip correlative.

Table 5.1. Seismic stratigraphy detailing unit morphology, internal reflector characteristics, bounding surfaces and interpretation

Unit		Underlying surface	Description	Stratal relationship	Thickness (m)	Interpreted depositional environment
Unit H	H2	SB2	Mound	landward dipping reflectors, gradual transition from acoustically transparent to opaque in a landward direction	11	Shallow-marine
	H1	SB2	mound	chaotic to hummocky internal structure with discontinuous and discordant reflectors of variable amplitudes	8-12	Shallow-marine
Unit G	G2	SB2	shore attached sediment wedge	high amplitude and continuity, tangential oblique prograding-aggrading reflector sets	10	Reworked shoreface
	G1	SB2	shore attached sediment wedge	hummocky bottomset reflector that merge into tangential to sigmoidal topset reflectors	9	Prograding shoreface
Unit F		SB1	Sediment wedge	mostly acoustically transparent, occasional low amplitude reflectors form high-angle prograding packages	4-12	Beachrock and aeolianite rubble
Unit E		SB1	Drape package bound landwards by high-relief pinnacle structures	acoustically transparent unit, with occasional chaotic, low amplitude reflectors	8	Back-barrier lagooonal deposits
Unit D		SB1	rugged-relief pinnacles welded onto basement rock	acoustically opaque, rugged-relief pinnacles, occasional progradational internal reflectors	8-12	Barrier system (Palaeo-coastline)
Unit C		SB1	Well-developed onlapping drape package	wavy aggrading reflector geometry	16	Incised valley
Unit B		SB1	Land-attached sediment wedge	variable amplitude, hummocky- aggrading to acoustically transparent, low continuity reflectors	3	Outer to mid-shelf
Unit A		n/a		prograding, oblique parallel, high amplitude and continuous reflectors	n/a	n/a

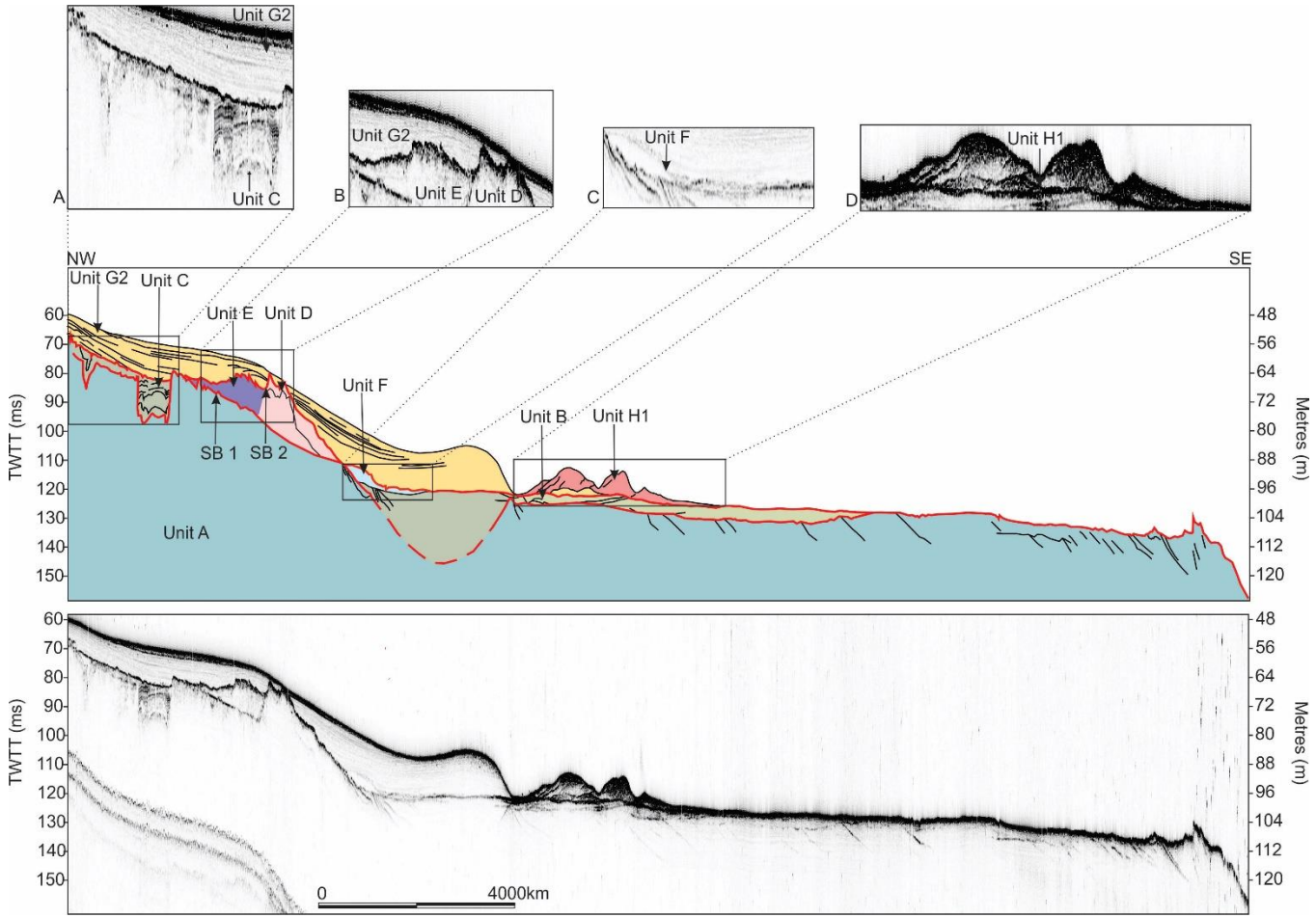

Fig. 5.2. Interpreted (upper) and processed (lower) down-dip seismic images with enlarged raw data from the profile. Section A shows the incised valley and internal reflectors of Unit C and Unit G2. Section B shows Unit E onlaps on Unit D, with both units upper truncating surface rugged. Section C shows Unit F resting on SB1 and truncated by SB2. Section D shows chaotic to hummocky internal structure of Unit H1.

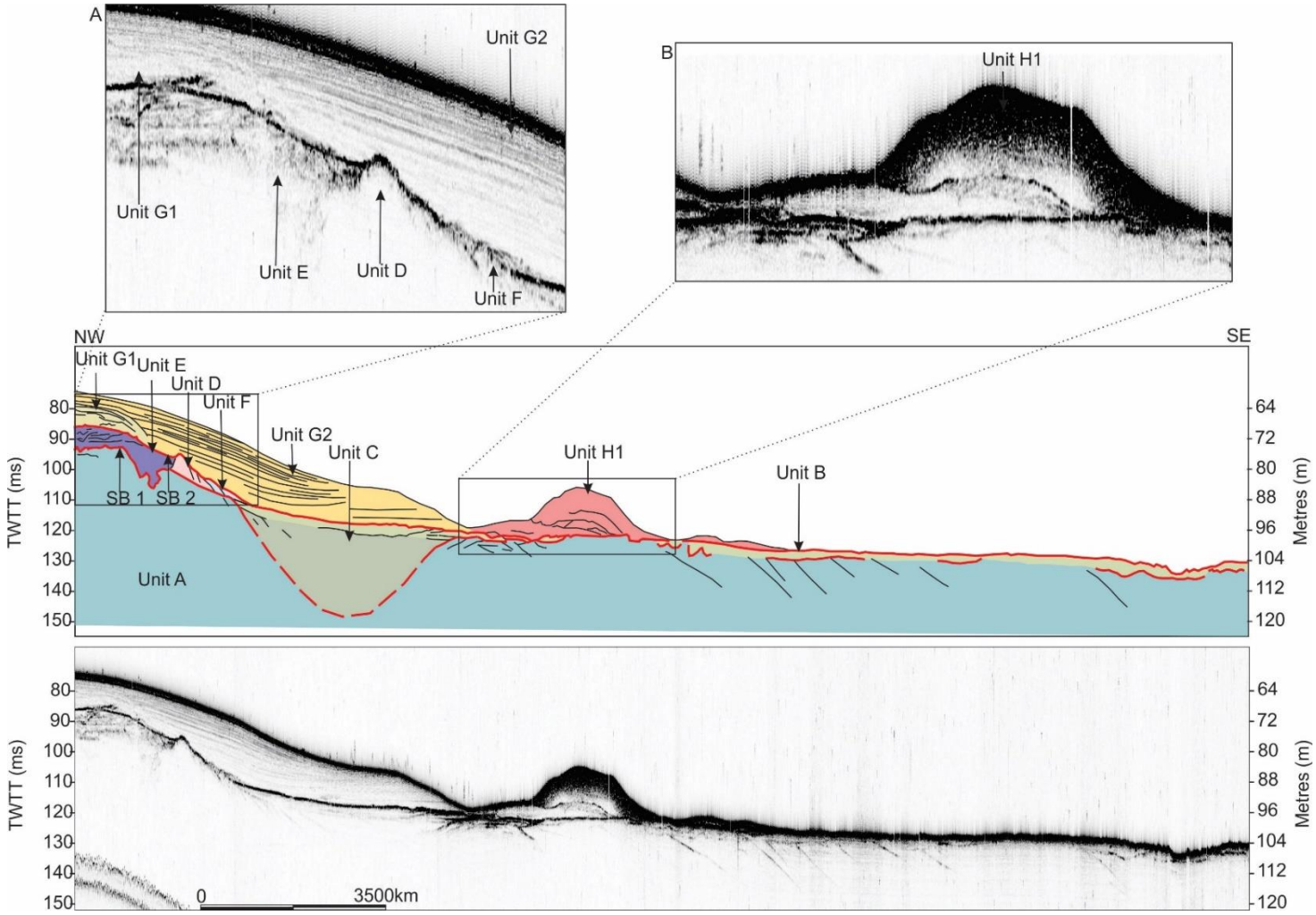

Fig. 5.3. Interpreted (upper) and processed (lower) down-dip seismic images with enlarged raw data from the profile. Inset A shows rugged-relief pinnacles of Unit D, Incision of Unit E into the underlying Unit A, truncation of unit F by Unit G2, and the sediment wedge of Unit G1. Inset B shows the chaotic to hummocky internal structure of unit H1.

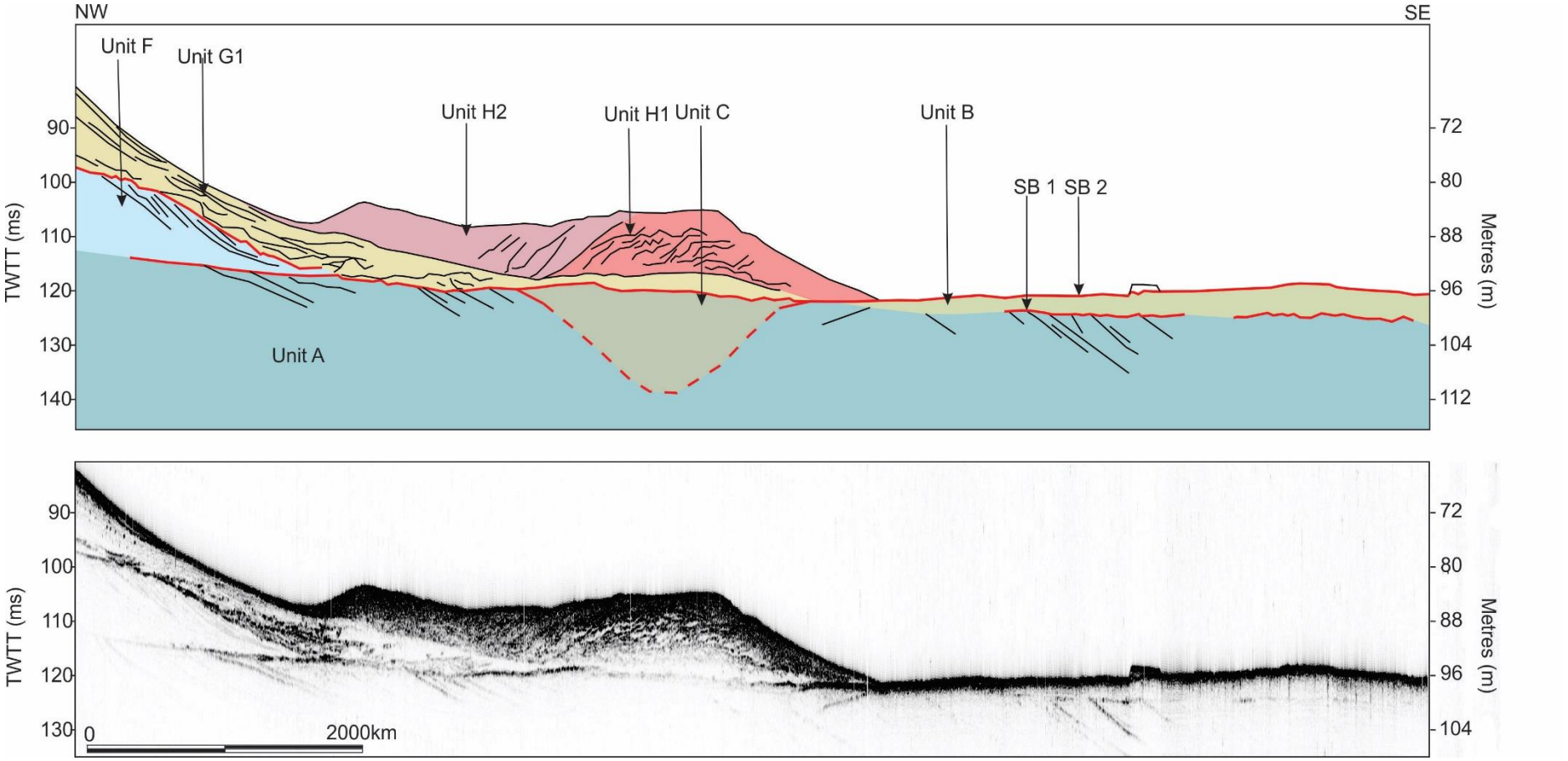

Fig. 5.4. Interpreted (upper), and processed (lower) down-dip seismic images showing Unit H2 resting on unit G1 with the thickest package of Unit F underlying Unit G1. Note the merger of SB1 and SB2 to form a composite erosional surface to landward.

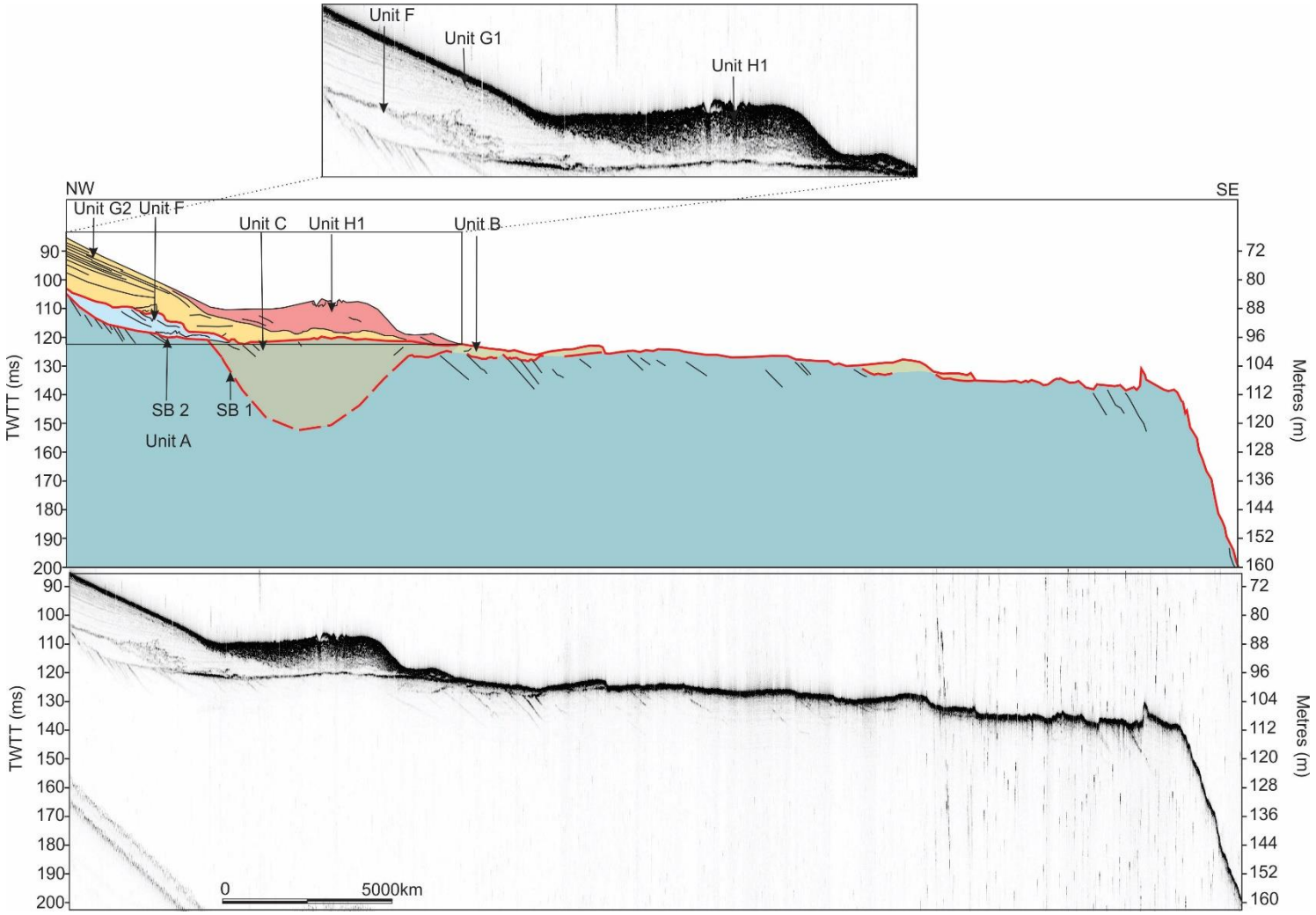

Fig. 5.5. Interpreted (upper) and processed (lower) down-dip seismic images and enlarged raw data from Unit F resting on SB1 and truncated by SB2, the sediment wedge of unit G1 and the chaotic reflectors of Unit H1.

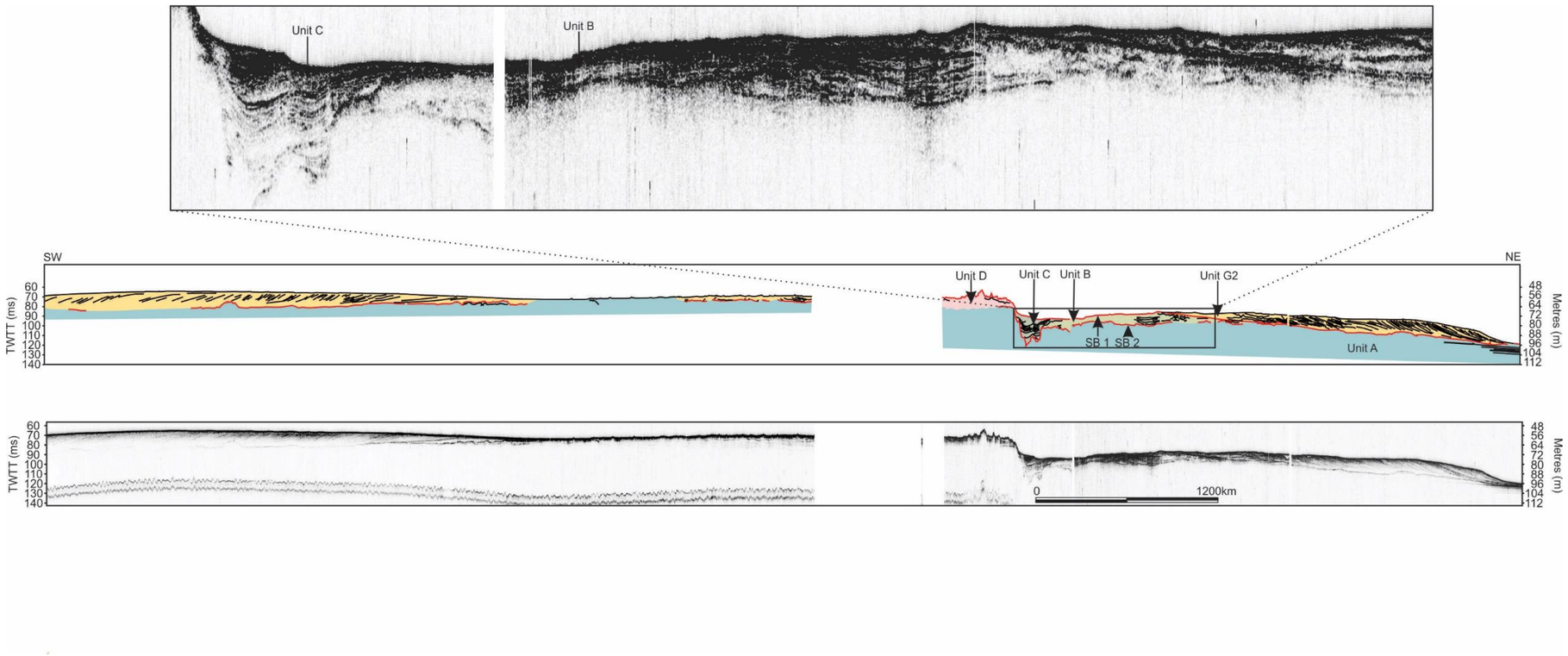

Fig. 5.6. Interpreted (upper) and processed (lower) coast parallel seismic images and enlarged seismic records illustrating the stratigraphy of the study area. The enlarged raw data show variable amplitude, hummocky- aggrading to acoustically transparent, low continuity reflectors of Unit B and the incision of unit C into the underlying Unit A with its variable amplitude, aggrading to acoustically transparent, low continuity reflectors. Both these units are truncated by SB2.

5.2. Bathymetry

5.2.1. Overall physiography

The full extent of the study area encompasses 6 615 km^2 of the East London continental shelf, of which ~ 450 km^2 of shelf was mapped continuously by multibeam bathymetry. In general, the continental shelf is narrow (a maximum of 23 km wide) and widens towards the south of the study area, typically rugged, but with an overall flat profile that dips at ~0.06^o.

The shelf break occurs at an average depth of 100m, but decreases in depth gradually to 110 m south of the Kei River to 140 m south of the Gqunube River. The shelf break is dissected by the Hamburg Canyon complex, previously described by Dingle and Robson (1985), which impinges up to 4 km onto the continental shelf. Notable shelf-wide features include laterally persistent coast-parallel ridges, semi-circular seafloor depressions and the preserved expressions of river valleys on the seafloor. The -100 m to -90 m ridge of unit A can be traced from East London all the way to the Mazeppa Bay. The -60 m ridge is identifiable by arcuate features and arcuate barriers with cuspate extensions offshore the Gqunube River and the Kei River. The Palaeo-Gqunube and Palaeo-Kei Rivers are identified by the remnants of several under-filled incised valley systems.

5.2.2. Seafloor ridges

5.2.2.1. -100 m to -90 m ridge of Unit A (Fig. 5.1a)

The -100 m to -90 m ridge of Unit A marks the continental shelf edge, just inshore of the shelf break. The ridge can be traced from East London all the way north to the Mazeppa Bay over a distance of 130 km. The ridge bifurcates in places to form several ridges from water depths of 88 m to 113 m (Fig. 5.7, 5.8, 5.9, 5.10, 5.11 and 5.12). The -100 m to -90 m ridge of Unit A can reach up to 10 m in height, with widths that range from 120 m to 500 m. A number of circular hollows and elongate depressions within the unit are apparent, each of which is approximately 2 m deep (Fig. 5.11).

Offshore Morgan Bay, the ridge is interrupted by an erosional depression 4 m deep and 840 m wide (Fig. 5.11). the ridge continues farther northward past this erosional gap, where a

number of arcuate ridge features of lesser relief are superimposed onto the landward side of the main ridge form (Fig. 5.11). These create distinct semi-circular seafloor depressions up to 3-4 m in vertical relief. The seafloor to landward of the -100 m ridge is characterised by a topographic depression behind the barrier (Fig. 5.10).

5.2.2.2. -90 m ridge

A lower relief ridge (5 m high and 800 m wide) of limited lateral continuity is observed at 90 m offshore the Gqunube River (Fig. 5.11). Apart from its depth, it exhibits the same morphological characteristics of the deeper ridge and is likewise characterised by a depression behind the barrier with scours approximately 2 m deep (Fig. 5.9).

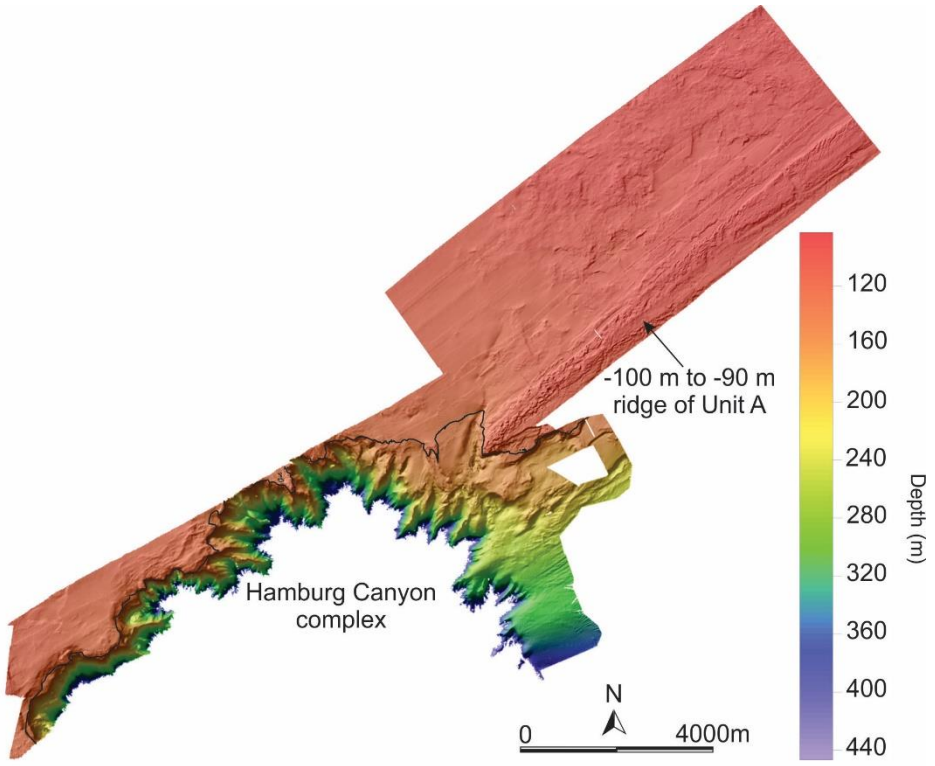

Fig. 5.7. An unknown canyon within the Hamburg Canyon Complex, intersected by the -100 m to -90 m ridge of unit A. The shelf break is marked by the contour at 140 m.

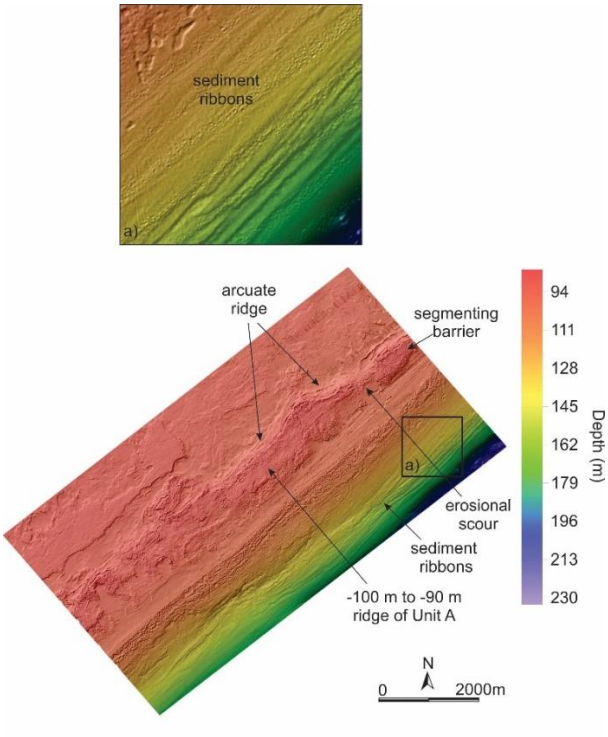

Fig. 5.8. Shows the -100 m to -90 m ridge of Unit A, with its arcuate ridges of the -100 m to -90 m ridge of Unit A separated from the segmenting barrier by an erosional scour.

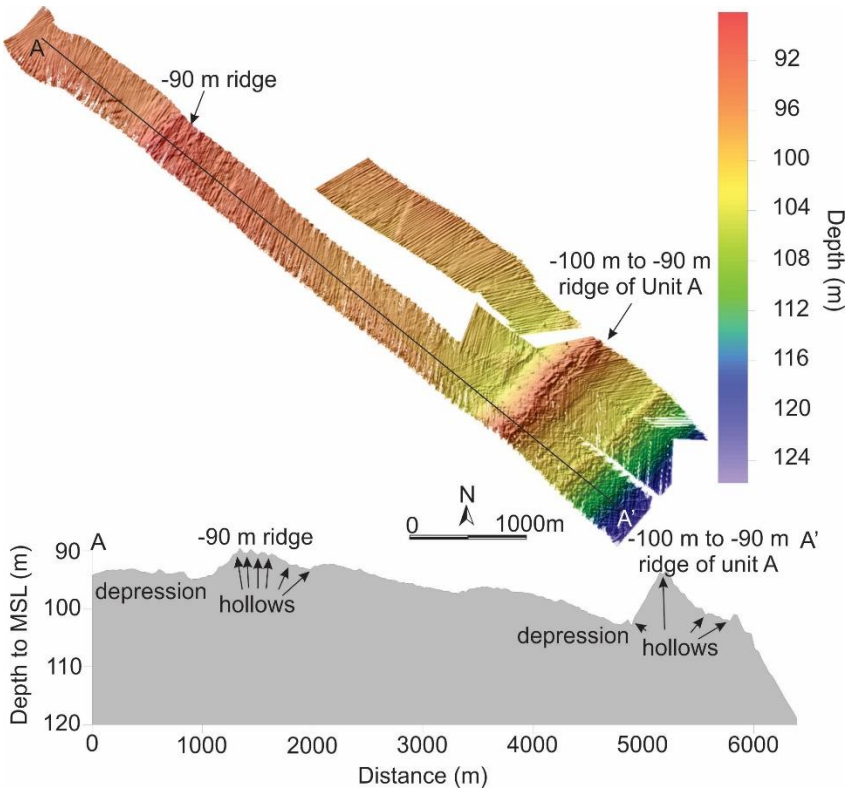

Fig. 5.9. Shows the relationship between the -100 m to -90 m ridge of Unit A and the -90 m ridge.

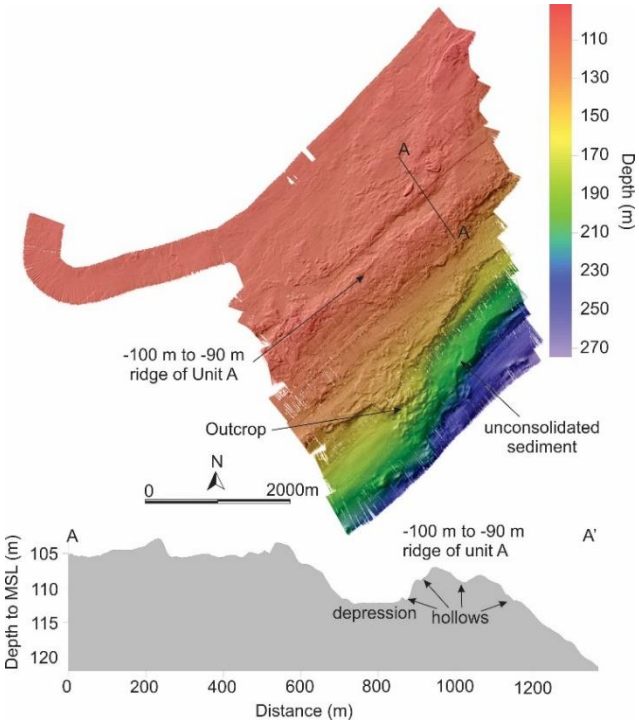

Fig. 5.10. Shows the -100 m to -90 m ridge of unit A, the outcrop beyond the shelf break with sediment accumulated around it.

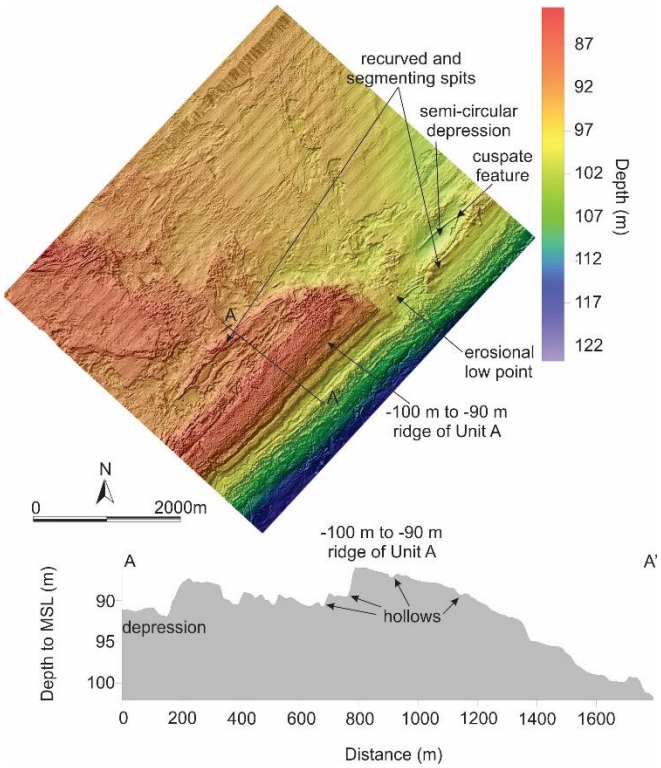

Fig. 5.11. Shows the -100 m ridge of Unit A, together with superimposed recurved and segmenting ridges to landward. Note the semi-circular seafloor depression to landwards, and erosional gap in the barrier.

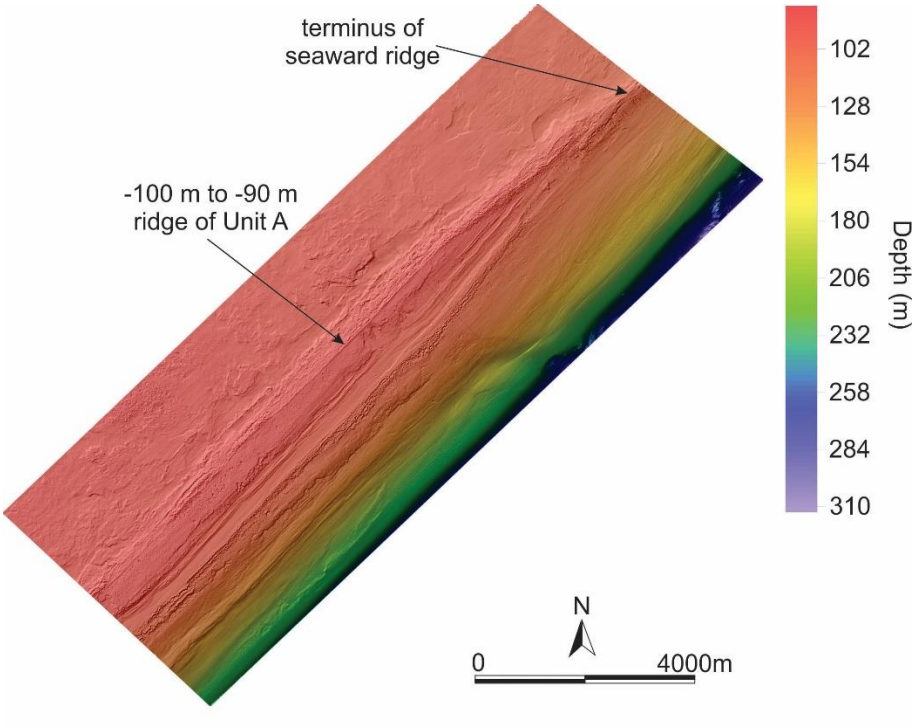

Fig. 5.12. The termination of the -100 m to -90 m ridge of Unit A.

5.2.2.3. –60 m ridge (Fig. 5.1c)

A -60 m ridge is observed offshore Kidd's Beach shelf (Fig. 5.13. 5.14 and 5.15). This ridge is characterised by large-scale arcuate ridges and smaller cuspate features where the ridges intersect. Offshore of the Gqunube River and to landward of the -60 m ridge, outcrops of strongly layered rock with very clear lineaments are apparent (fig. 5.14a). These trend in a WNW-ESE direction and mirror the onshore strata observable from satellite imagery (Fig. 5.14a). Offshore Kidd's Beach the ridge has a marked ledge which is cut into the leading seaward edge of this part of the ridge, increasing its steepness (Fig. 5.13). This ridge has a particularly rugged and undulatory surface (Fig. 5.13). Seaward of the Gqunube Point area, a drumstick-shaped ridge occurs at a depth of 77 m (Fig. 5.14). The overall feature comprises an arcuate seafloor high that trends in a SW-NE direction, terminating in a series of small (14 m high) prograded ridges.

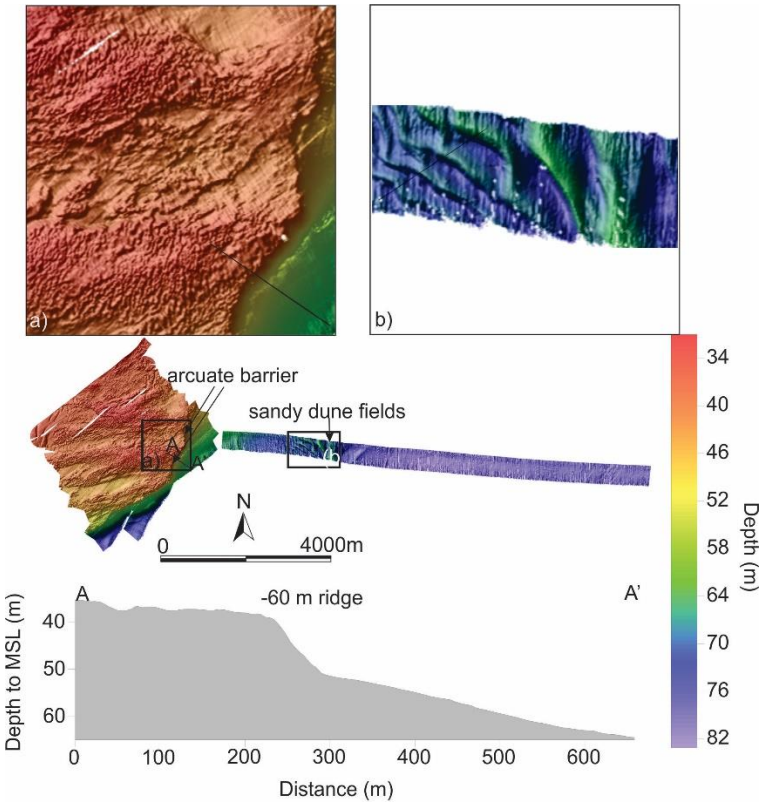

Fig. 5.13. The arcuate barrier forming the -60 m ridge. The rugged undulating surface of the beachrock/aeolianite landward of the ridge. Sandy dune fields that are increasing in size, shallowing in depression depth seaward.

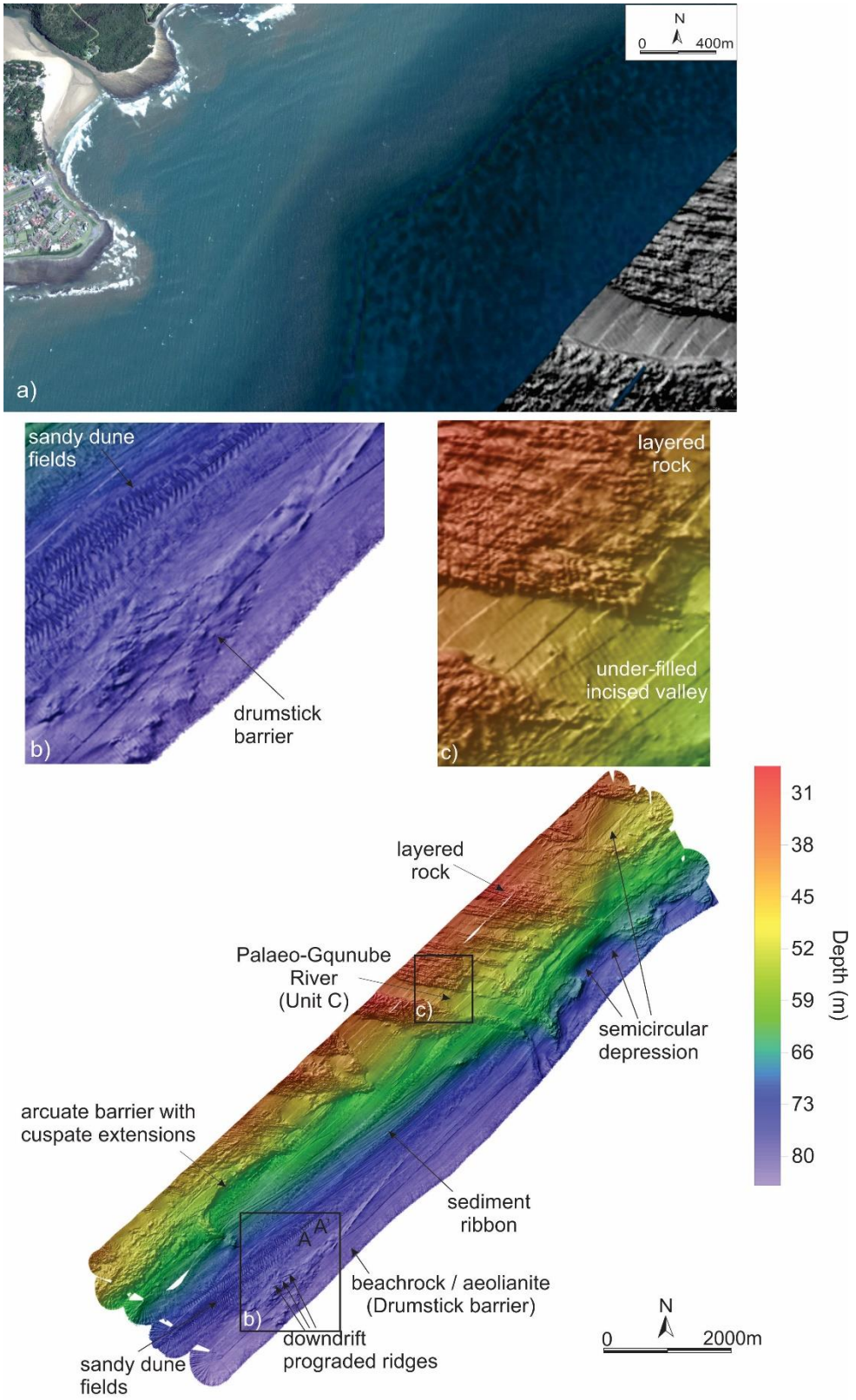

Fig. 5.14. The -60 m ridge marked by an arcuate barrier and cuspate extensions. Layered rock with lineaments are apparent on section a. The drumstick barrier with prograded ridges. The sandy dune fields and sediment ribbon confined by the -60 m ridge and the drumstick barrier shown by b. The under-filled Palaeo-Gqunube River with outcrop of Unit C is outlined by inset c.

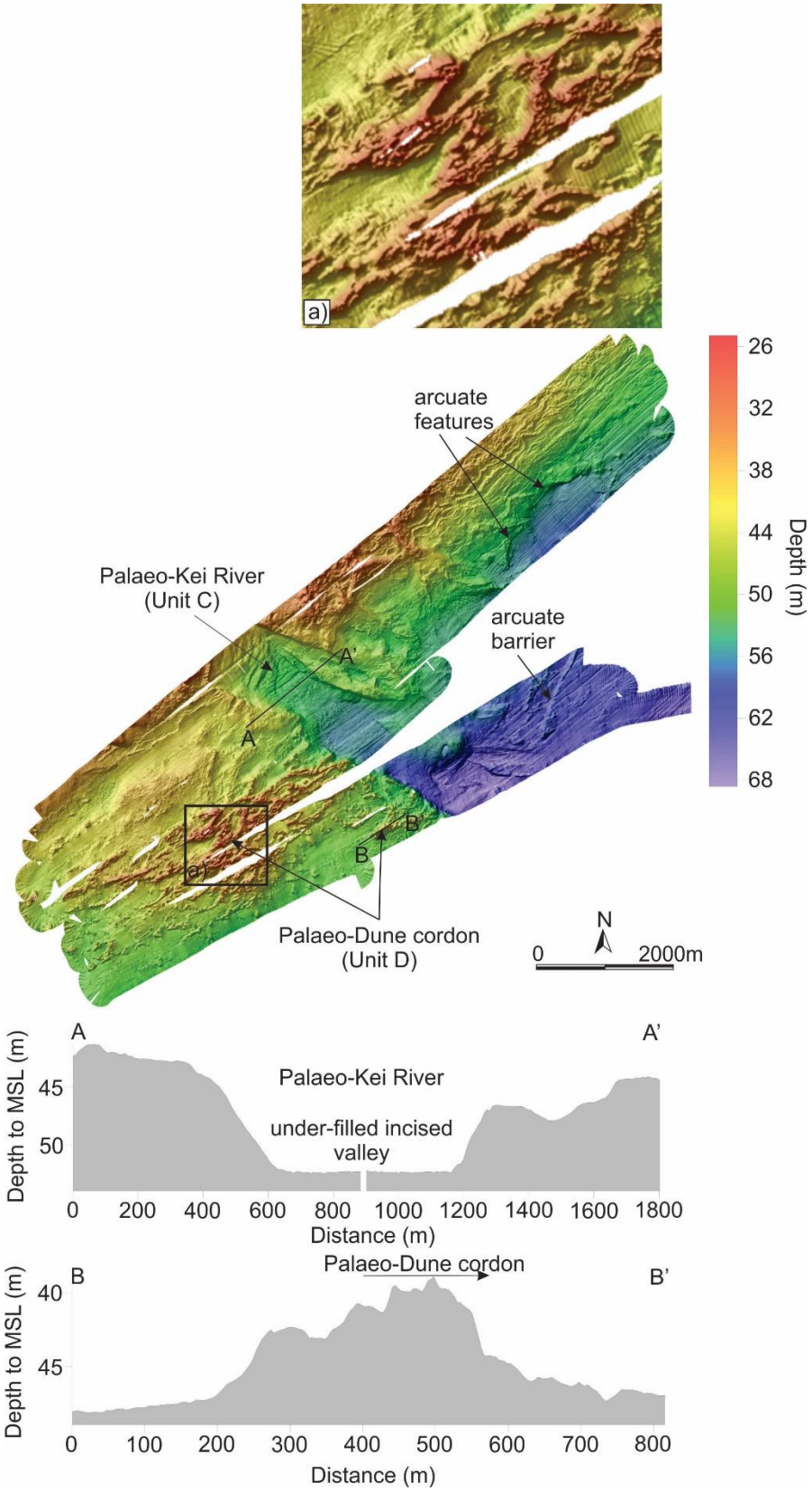

Fig. 5.15. The under-filled incised valley (Palaeo-Kei River), floored by Unit C. The palaeo-dune cordons (parabolic dunes) as Unit D marking the under-filled incised valley.

5.2.3. Unusual seafloor depressions and palaeo-drainage

The palaeo-Kei river extends as an under-filled incised valley, offshore the contemporary Kei River mouth. The under-filled valley merges into a series of large, semi-circular seafloor depressions (Fig. 5.15 and 5.16). These are separated by segmenting arcuate ridges approximately 1.5 to 3 m in height (Fig. 5.15b). The arcuate ridge at a depth of ~ 63m (Fig. 5.15), separates a saddle of seismic Unit D, and borders another seafloor depression (Fig. 5.16). This ridge ranges from 5 to 10 m in height and trends in a NNE-SSW direction (Fig. 5.16). Further seaward, the main ridge of the outer shelf is approximately 6 m in height, and 1.2 km wide, including its recurved and segmenting landward ridges (Fig. 5.11). This ridge forms part of the -100m to -90 m ridge of Unit A (Fig. 5.11). The recurved and segmenting spits behind this ridge increase in size landward and appear to comprise a prograding form (Fig. 5.11). It is notable that the associated semi-circular seafloor depressions decrease in size seaward (Fig. 5.11 and 5.16).

A similar situation exists for the Palaeo-Gqunube fluvial extension. Unfortunately, the multibeam coverage was not as extensive as for the Palaeo-Kei system, however the imagery reveals similar features in the proximal mid shelf such as arcuate ridges which segment semi-circular seafloor depressions and erosional truncations of the -60 m ridge (Fig. 5.14 and 5.17). Further seaward, the ubiquitous -100 m to -90 m ridge occurs with a small erosional scour ~ 3m deep, and 500 m wide (Fig. 5.17). The semi-circular depressions are smaller in size than those found between the Palaeo-Kei lagoon/lake systems (Fig. 5.16 and 5.17).

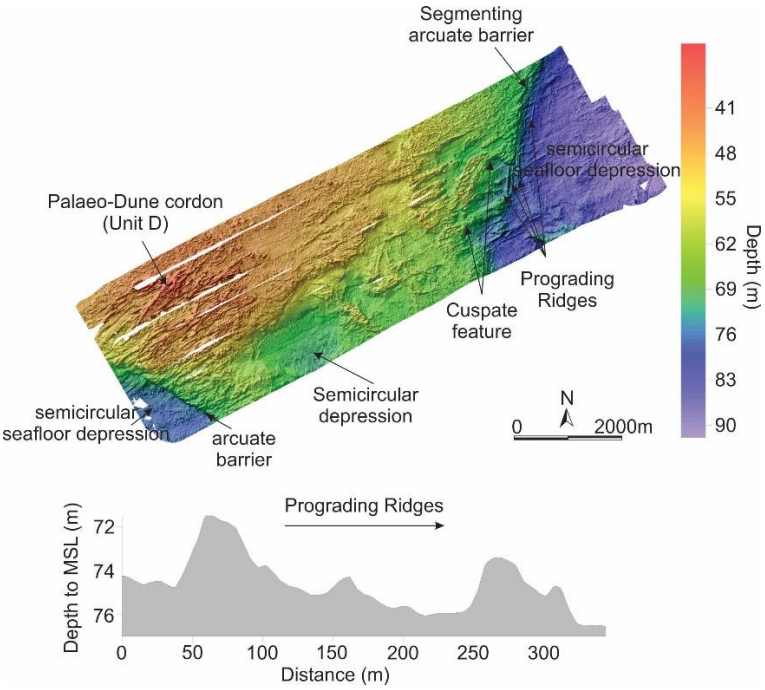

Fig. 5.16. Shows the semi-circular depressions barricaded by segmenting arcuate barriers, with prograding ridges. Large Palaeo-dune cordon.

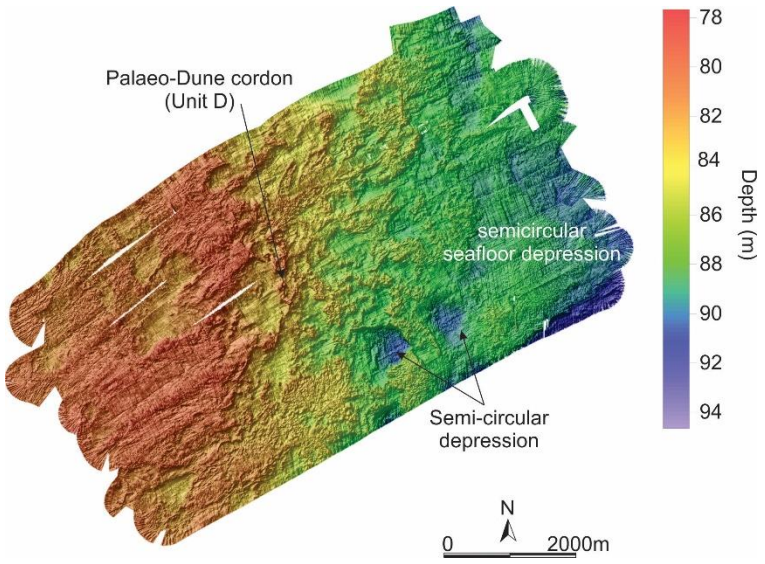

Fig. 5.17. Shows the semi-circular seafloor depression marked by the Palaeo-dune cordon (Unit D) with semi-circular depressions.

5.2.4. Under-filled incised valley systems

The under-filled incised valley systems (Palaeo-Kei River and the Palaeo-Gqunube River systems) cut through some rock units not recognised from the seismic data set, together with the ridges of Unit A. The -60 m ridge is clearly intersected by two river systems (Fig. 5.14 and 5.15). Seismic profiles (Fig. 5.6) show the valley floors to be the surface expressions of unit C. The valleys are approximately 16 m deep (Fig. 5.6) and trend with the regional lineament orientations (Fig. 5.14a). The Palaeo-Kei River is approximately 1.28 km wide and the Palaeo-Gqunube River is approximately 0.33 km wide (Fig. 5.14 and 5.15).

5.2.5. Hardgrounds

A number of low-relief, rocky outcrops exists that separate the -60 m and -100m ridges. These are exposed patches of seismic Units A or B (Fig. 5.15, 5.16, 5.17, 5.18 and 5.19). Localised pinnacles and ridges are common and may attain reliefs of up to 28 m from the seafloor (Fig. 5.15, 5.16, 5.17 and 5.18). These hardgrounds occur in two main groups in the areas mapped; those found offshore the Buffalo River (Fig.5.17 and 5.18), and those found offshore the Kei River (Fig. 5.15 and 5.16). The hardgrounds offshore the Buffalo River rise up to 3m in height, and within these features, parabolic depressions with ridged-rims are common (Fig. 5.18). The long axes of these forms are orientated WSW-ENE. Hardgrounds in the north, offshore the Kei River, have similar features which rise up to 10 m in height, however their long axes trend in a NE-SW orientation (Fig. 5.15 and 5.16).

5.2.6. Unconsolidated sediment and bed forms

Unconsolidated sandy sediments are not widespread on the East London to Kei River shelf. It is apparent from the bathymetry, and backscatter data sets (Fig. 5.10. 5.13 and 5.14; forthcoming backscatter section), that the majority of the mid-shelf appears to be sediment starved, with either bedrock cropping out, or veneers of bioclastic gravel mantling shallow subcropping bedrock. In some areas, sediments do accumulate (Fig. 5.10), many of which are reworked into bedforms as described below.

5.2.6.1 Sandy dune fields

Sandy dune fields are found offshore East London between Kidd's Beach and Gonubie Point at depths of 65 to 75 m (Fig. 5.13 and 5.14). The dune trains found offshore Kidd's Beach decrease in both wavelength and amplitude towards the land (Fig. 5.13); their leeward slope facing SW (fig. 5.13). Offshore Gonubie Point, the dunes are much smaller (wavelength = 40 to 70 m, height = ≤0.8 m) than those offshore Kidd's Beach (Fig. 5.14). These smaller dunes are confined by the -60 m ridge and the drumstick-shaped seafloor high (Fig. 5.14).

5.2.6.2. Sediment ribbons

There are two main areas of sediment ribbons located at different depths, all of which trend in a general SW-NE direction. Offshore Mazeppa Bay and beyond the shelf break, sinuous sediment ribbons at depths of 150 m are found (Fig.5.20). These sediment ribbons are of limited lateral extent and form negative seafloor relief features ~ 10 m wide and 20 cm deep (Fig. 5.8). A shallower set of sediment ribbons occur offshore the Gqunube River between depths of 65 to 70 m in the mid-shelf (Fig. 5.14). These are curved and continuous, orientated more towards the ENE-WSW. These adjoin and merge with the subaqueous dune field described earlier (Fig. 5.14).

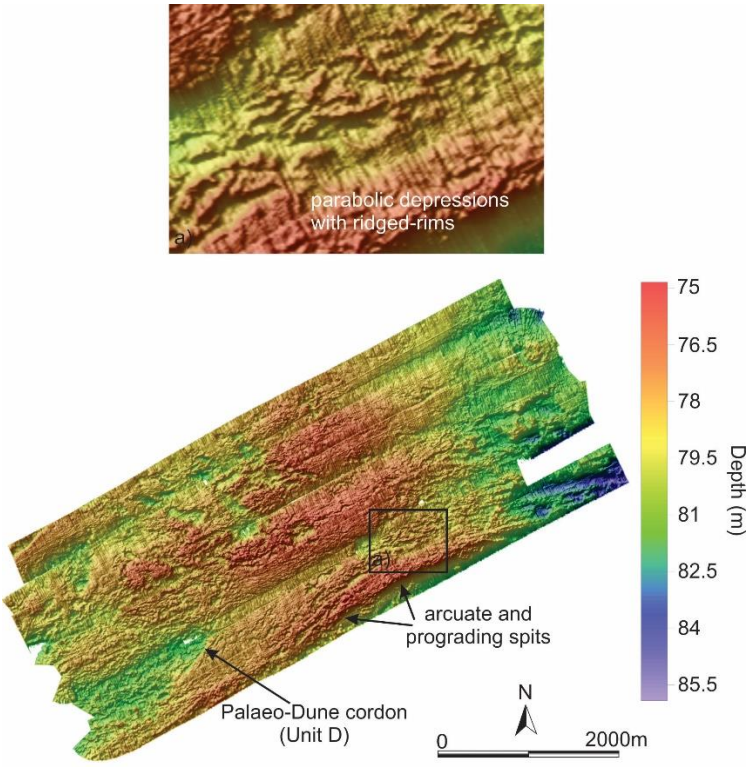

Fig. 5.18. Shows a rugged surface of Unit A or B, forming arcuate and prograding spits.

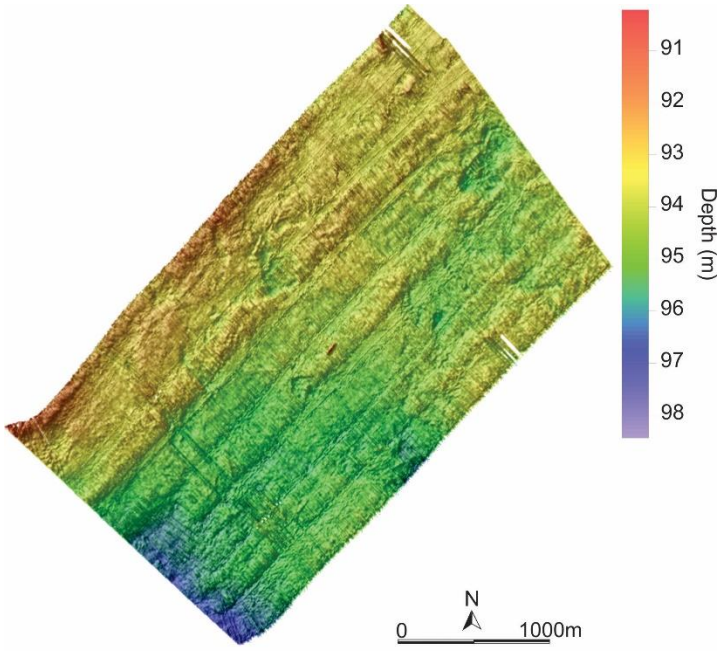

Fig. 5.19. Seafloor comprising outcrop of Unit A or B, with a rugged surface.

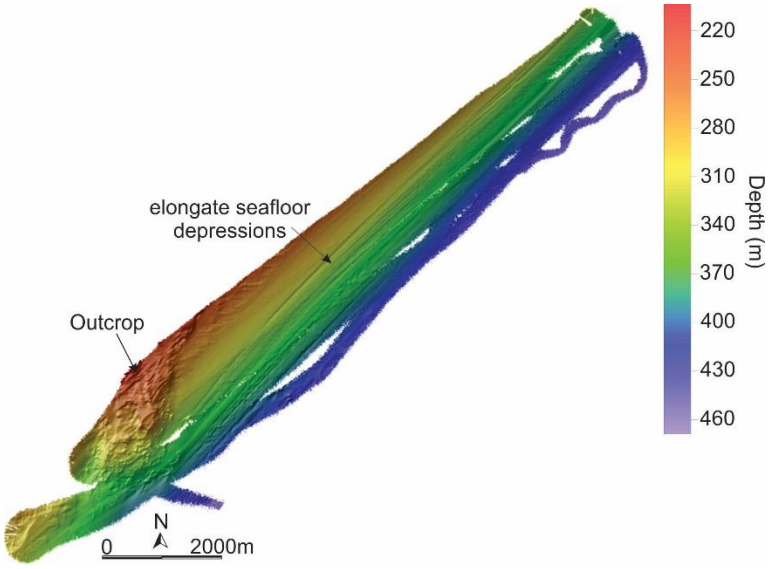

Fig. 5.20. Shows a rock outcropping beyond the shelf break and elongate seafloor depressions.

5.3. Backscatter

Several acoustic facies are evident from the co-registered backscatter data, and are distinguished based on the acoustic backscatter characteristics of the seabed and correlated to some of the corresponding bathymetric features (Fig. 5.21).

5.3.1. Acoustic facies A

Acoustic facies A comprises rugged, high relief, alternating moderate to high backscatter, punctuated by pockets of rippled high backscatter (Fig. 5.22a). Dredge samples collected for the area reveal this to comprise outcrop of beachrock and aeolianite. These outcrops are widespread and are related to the linear seafloor ridges identified in the bathymetry. They are fringed to landward by acoustic facies B (Fig. 5.22), and to seaward, especially in the mid-shelf and shelf edge form as ridges (Fig. 5.23, 5.24a, 5.25, 5.26 and 5.27).

5.3.2. Acoustic facies B

Acoustic facies B reflects smooth-toned, low to moderate backscatter seafloor, punctuated by small, randomly orientated high backscatter patches. Low backscatter seafloor is restricted mainly to the inner and mid continental shelf (Fig. 5.22, 5.23 and 5.28), especially in areas where the shelf is covered by subaqueous dunes. The outer shelf has some patches of moderate-intensity backscatter; however these are quite isolated (Fig. 5.27). Grab samples reveal this to comprise mostly quartz-rich, sandy shelf sediments.

5.3.3. Acoustic facies C

Acoustic facies C is marked by a high backscatter return. This facies can be subdivided into acoustic facies C1 and C2. Acoustic facies C1 occurs as elongate strips of high backscatter (Fig. 5.22a, 5.23, 5.24b, 5.26 and 5.28a). Dredge samples show these to comprise current-planed gravels with gravel streamers or ribbons (*Prof. Sven Kerwath, pers. comm*). On the outer shelf, C1 can merge into C2, as sinuous patches of high backscatter. These are related to the formation of large 3D or sediment starved dunes (Fig. 5.26).

5.3.4. Acoustic facies D

Acoustic facies D comprises rippled, alternating high and low backscatter indicative of rippled bioclastic gravels (Fig. 5.22a, b and c). These may form in patches (Fig. 5.22a) or in thin veneers (Fig. 5.22b).

5.3.5. Acoustic facies E

Acoustic facies E is composed of irregular, high backscatter (Fig. 5.28b). This corresponds to the dune fields recognised in the bathymetry (Fig. 5.13 and 5.14). This facies is restricted to the inner shelf.

5.3.6. Acoustic facies F

Acoustic facies F is marked by high backscatter with subordinate patches of low backscatter (Fig. 5.28c), these comprise bioclastic sediments of variable grain size, ranging from medium sand to pebbles (Fig. 5.29).

5.3.7. Acoustic facies G

Acoustic facies G reflects smooth-toned high backscatter (Fig. 5.22). This is restricted to the most inshore depression of the Palaeo-Kei River, and extends for over 3 km in shore-perpendicular fashion from the shoreline. Dredges of this facies reveal it to comprise stiff mud.

5.3.8. Acoustic facies H

Acoustic facies G grades into Acoustic facies H, an irregular, moderate and patchy backscatter field. Dredge samples from the offshore extensions of the Palaeo-Kei River (Fig. 5.22 and Fig. 5.30), and from Unit D that crops out in a coast parallel fashion (Fig. 5.6), reveal this to comprise extensive and thick deposits of maerle/rhodolith.

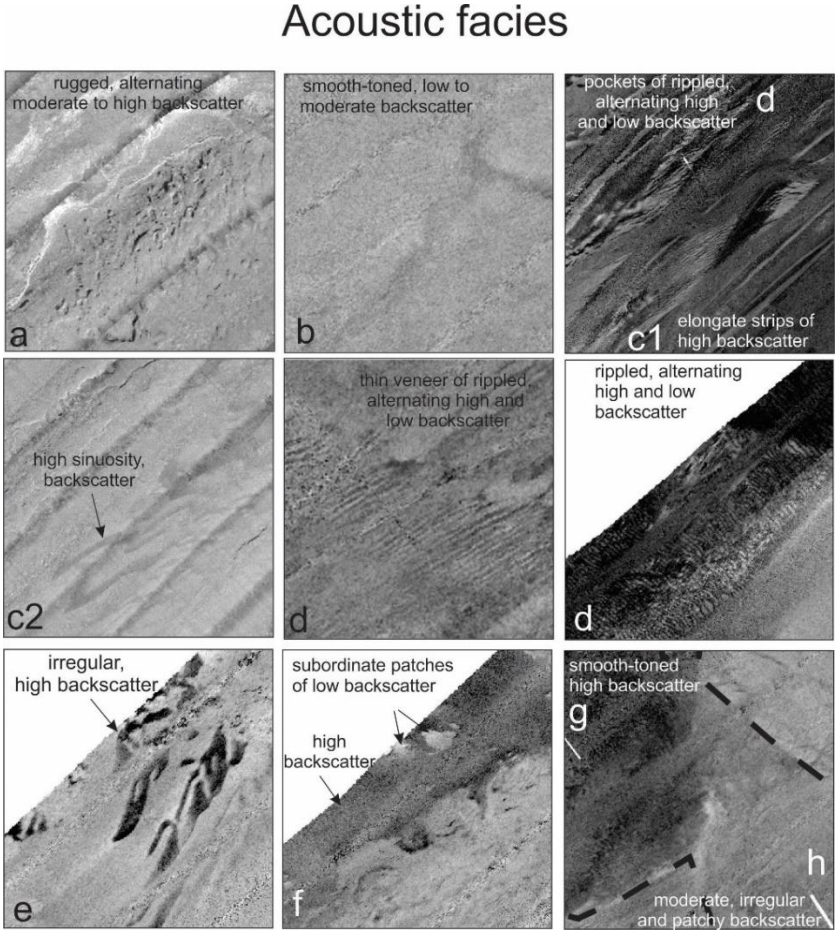

Fig. 5.21. Acoustic facies a-h on the shelf, derived from backscatter data.

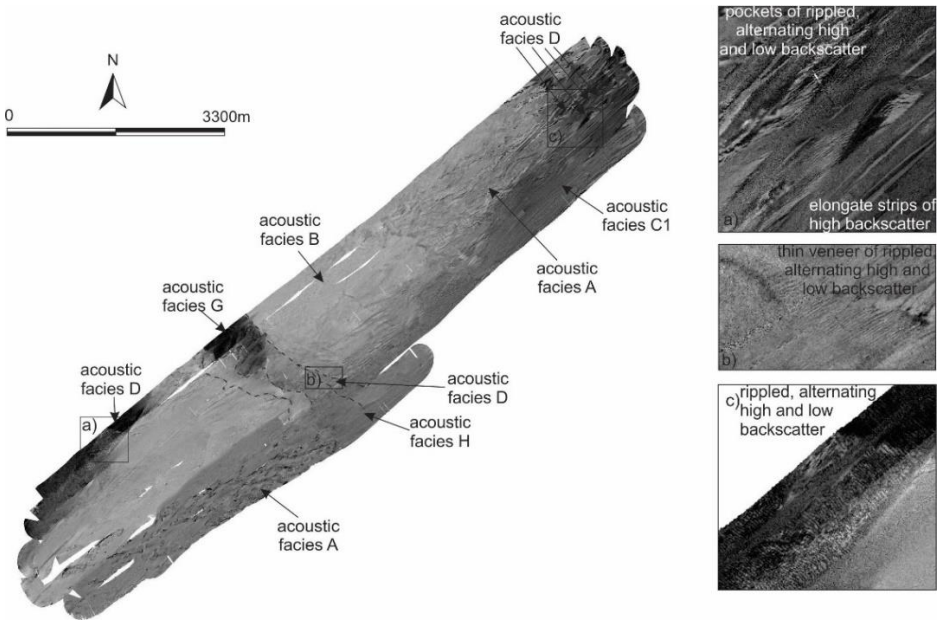

Fig. 5.22. Backscatter map of the inner shelf offshore the Kei River (Morgan Bay). Dotted line outlines the bedrock contact of the Palaeo-Kei River course.

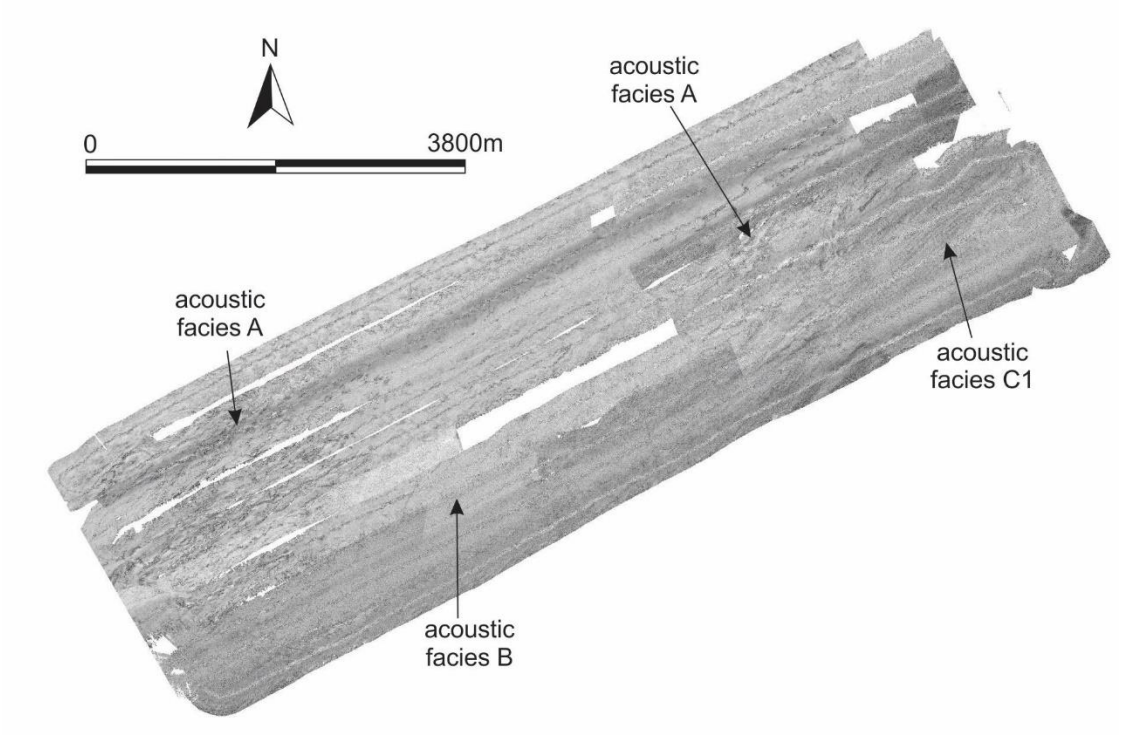

Fig. 5.23. Backscatter imagery from the mid-shelf offshore Morgan Bay.

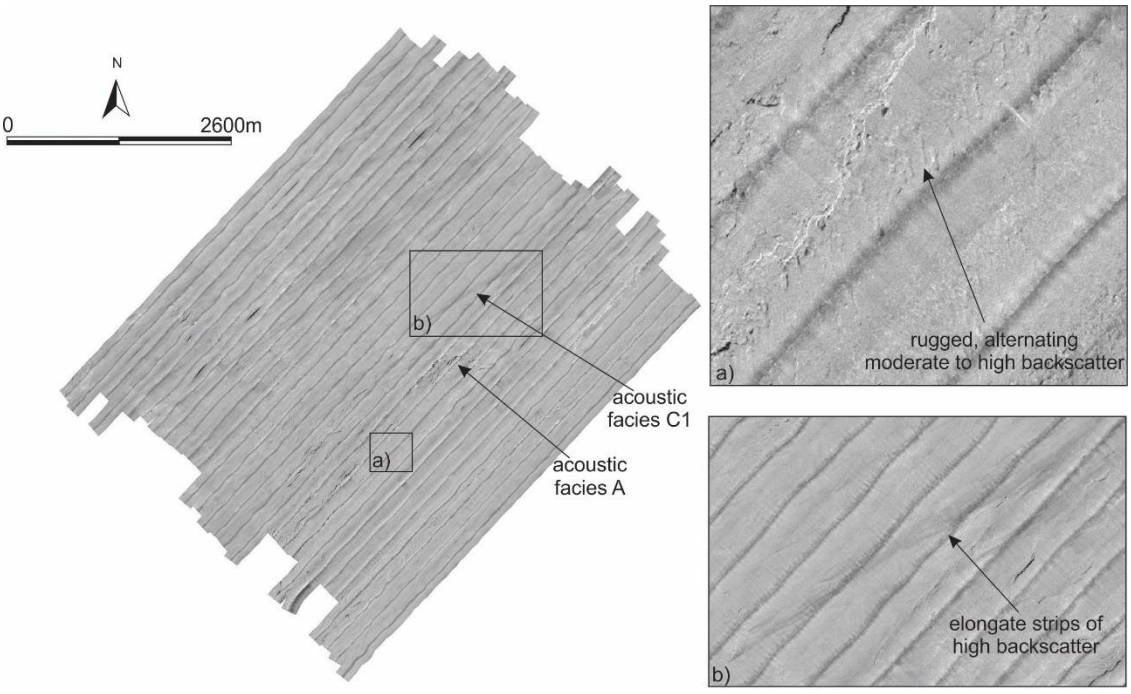

Fig. 5.24. Backscatter imagery from the outer shelf offshore Morgan Bay.

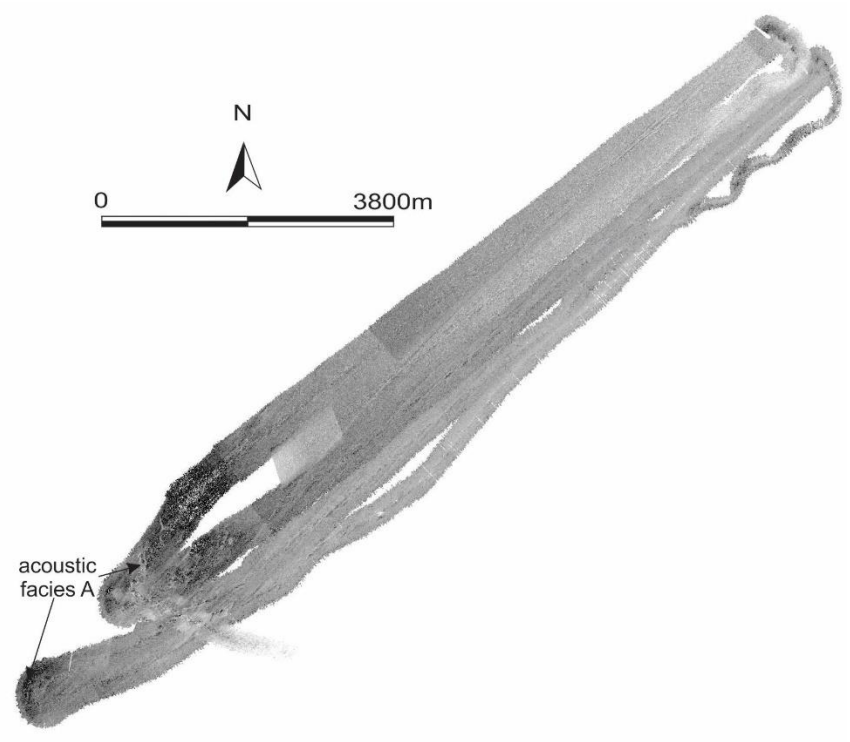

Fig. 5.25. Backscatter image of the upper slope offshore Morgan Bay. The data from these water depths were of insufficient quality to produce very clear facies identifications.

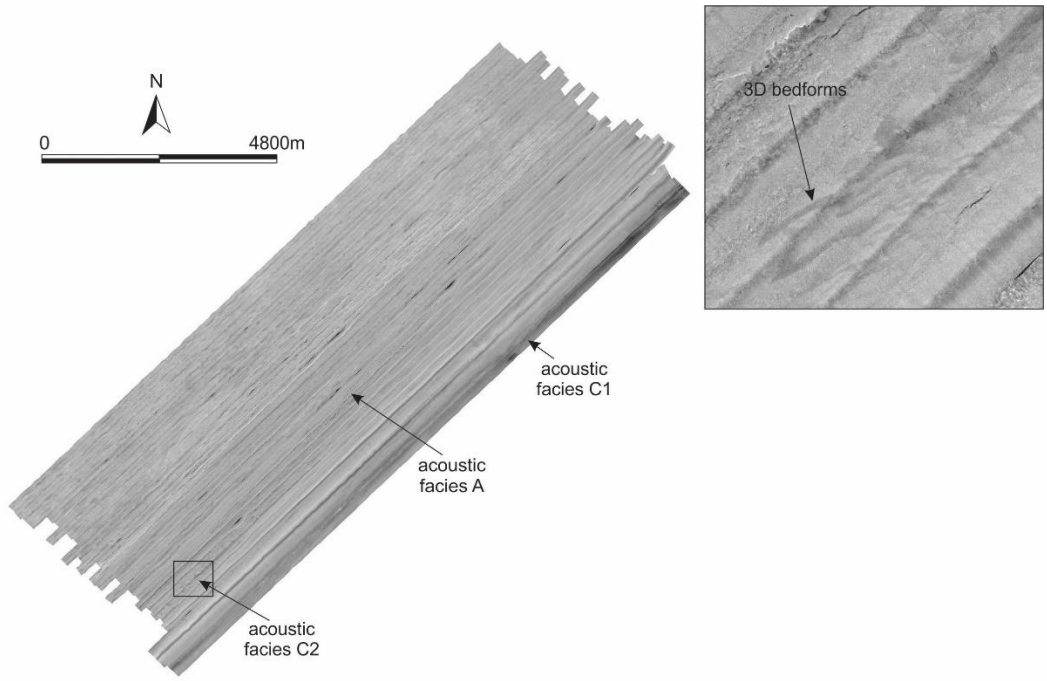

Fig. 5.26. Backscatter imagery from the outer shelf and upper slope offshore Mazeppa Bay.

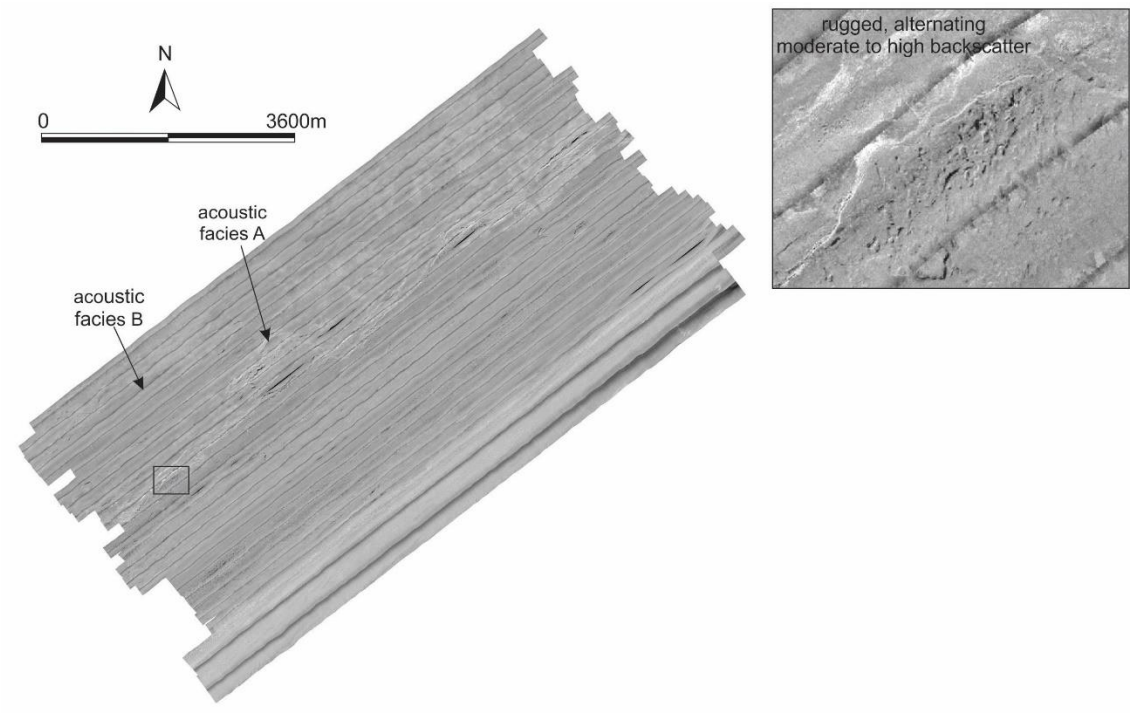

Fig. 5.27. Backscatter image of the mid-outer shelf offshore East London.

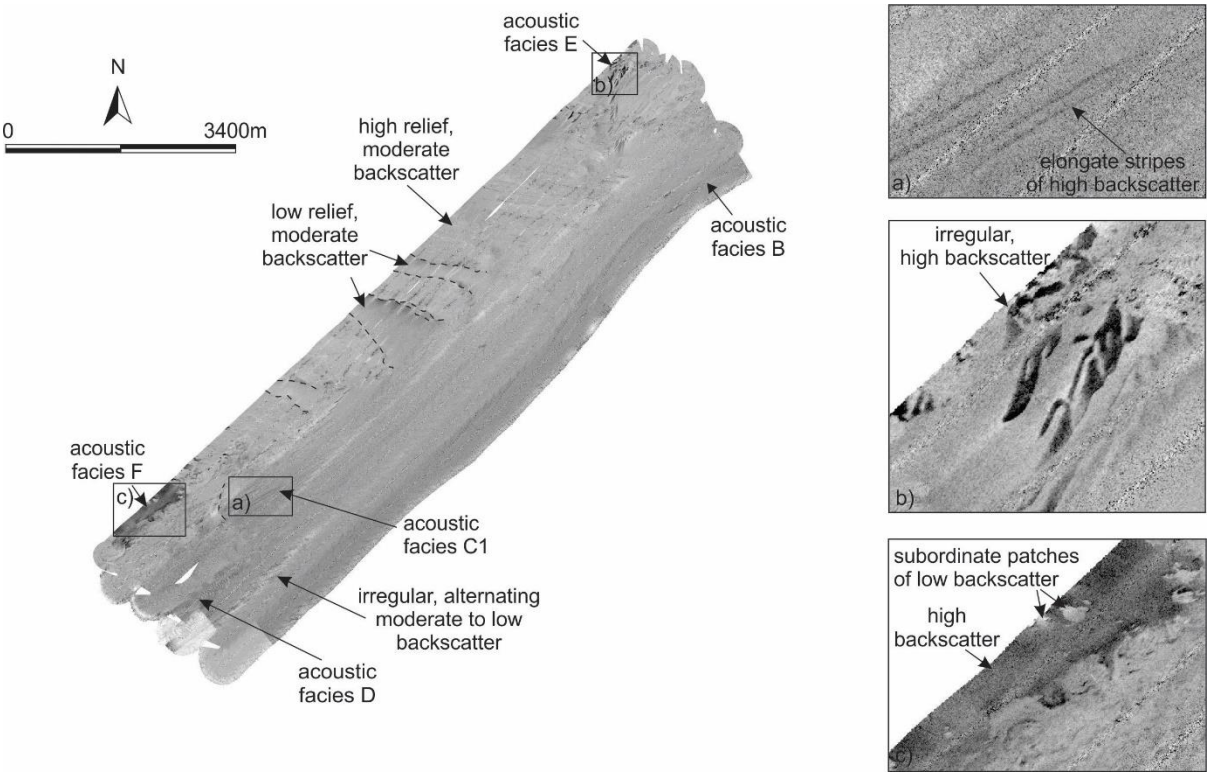

Fig. 5.28. Backscatter image of the inner shelf offshore Gqunube River.

Fig. 5.29. Dredge samples taken offshore East London, south of the Gqunube River. A) bioclastic sediments of grain size ranging from medium sand to pebbles. B) beachrock/aeolianite of Acoustic Facies A.

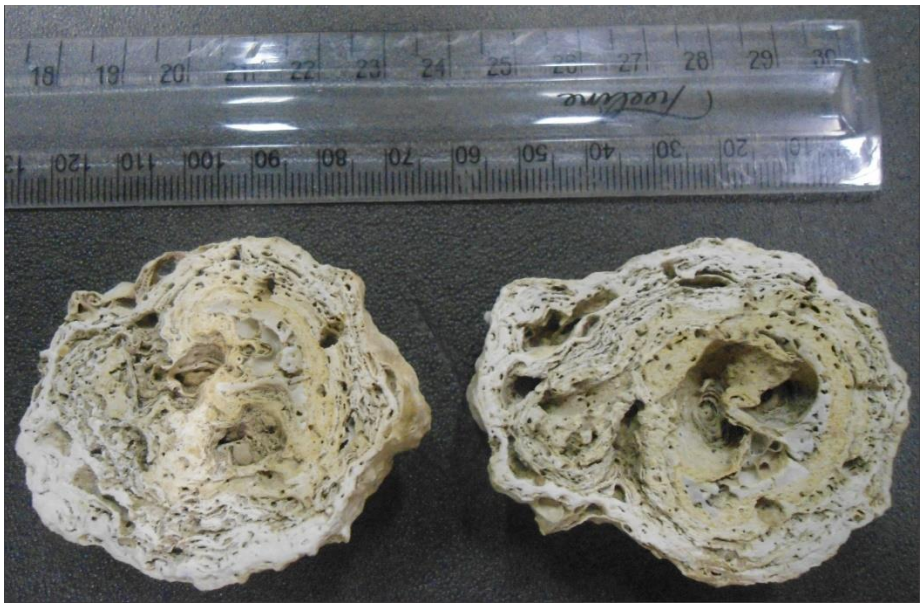

Fig. 5.30. Dredge sample of rhodoliths taken offshore Morgan Bay, on the Palaeo-Kei River incised valley.

5.4. Unconsolidated sediment

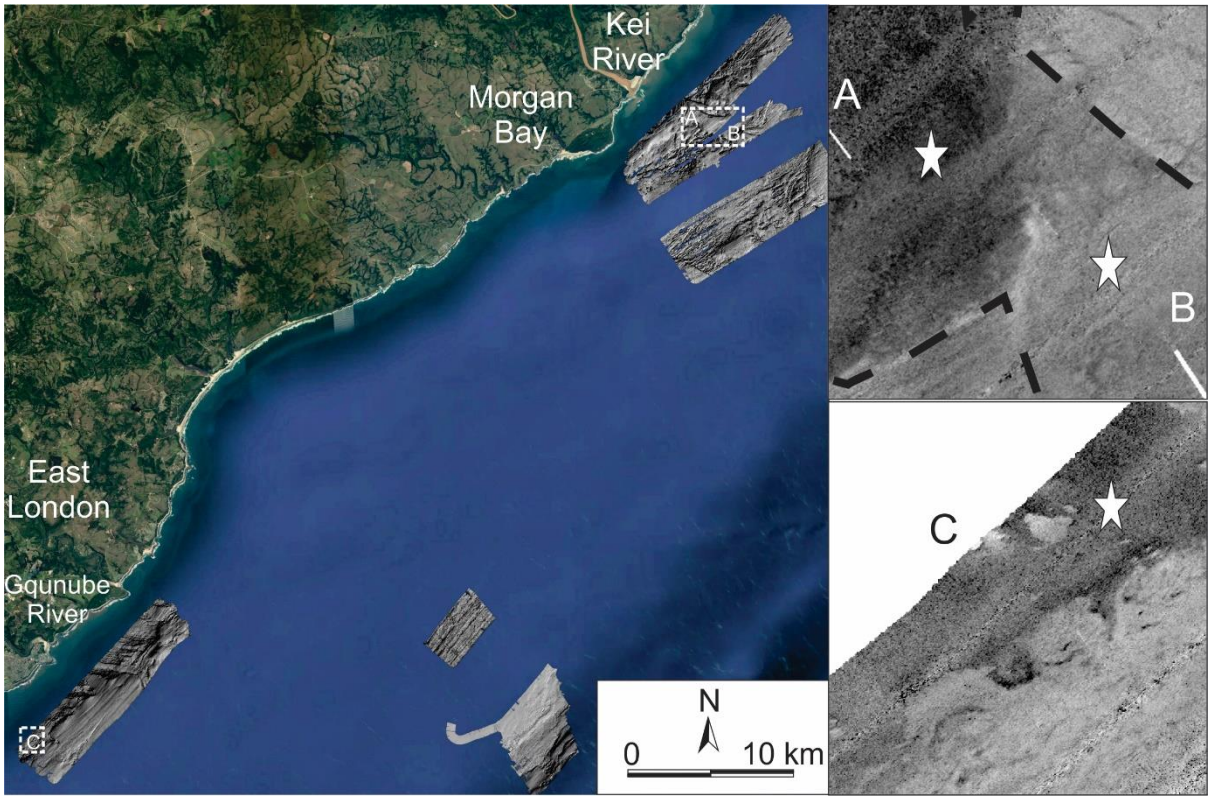

Fig. 5.31. Locality map of the dredge samples. Multibeam bathymetry shows the location of the dredge samples and the corresponding backscatter blowups of the dredge site and acoustic facies. Locations illustrated by stars.

A number of dredge samples have been collected in the study area, three of the most important ones have been indicated in the locality map above (Fig. 5.31).

Very stiff mud was collected offshore Morgan Bay on the under-filled incised valley of the Palaeo-Kei River system extending for over 3 km in shore-perpendicular fashion from the shoreline. Proving that Acoustic facies G is in fact very stiff mud (Fig. 5.21, 5.22 and 5.34) which date to 980-902 cal yr BP.

Rhodoliths of acoustic facies H were sampled offshore Morgan Bay, on the under-filled incised valley of the Palaeo-Kei River system, >3 km from the shoreline (Fig. 5.31). These rhodoliths are ~6 cm in diameter. The interior reflects a bit of a concentric pattern and shelly/skeletal material (Fig. 5.30). Dates of the interior of the rhodoliths ranged from 7406 - 7225 cal yr BP and the surface dates to present day (150 - Post Bomb cal yr BP 0).

Acoustic facies F bioclastic sediments were collected offshore East London, south of the Palaeo-Gqunube River. These bioclasitc sediments are of variable grain size, ranging from medium sand to pebble (Fig. 5.29a). With this sample, pebbles of beachrocks/aeolinates were found which also proves that the adjacent acoustic facies A is made up of beachrocks/aeolinates (Fig. 5.29b).

CHAPTER 6

Discussion

6.1. Seismic Stratigraphic Interpretation

6.1.1. Unit A: Campanian Limestone basement

The oldest unit or acoustic basement, of the study area is composed of Campanian-age limestones of the Igoda Formation. This unit was deposited in response to the Campanian normal regression. This unit is truncated by two surfaces; an undulating surface marked by several incised valleys (SB1) and a planar, gently seaward-dipping erosional surface with localised scours (SB2). This unit compares to the acoustic basement unit observed by Green and Garlick (2011) from the KwaZulu-Natal shelf, ~400 km north of the study area, and by Flemming and Martin (2017) in the Agulhas Bank shelf, ~600 km south of the study area. Both of these studies document sequences that comprise upper Cretaceous sedimentary rocks and therefore it is conceivable that this unit is the same.

6.1.2. Sequence boundary 1: Subaerial Unconformity

The sequence boundary that truncates the Campanian Limestone basement below (Fig. 6.1) and separates it from younger, overlying TST and HST stratigraphies, is coincident with the subaerial unconformities documented by Salzmann et al. (2013) and Green et al. (2013b). This surface is regionally continuous from Durban to the Mozambique border, and is considered to have formed when the continental shelf was subaerially exposed during the Last Glacial Maximum (LGM). Coring of the deposits that fill in depressions within this surface reveal these to comprise early Holocene sediments (Pretorius et al., 2016). In addition, the inshore extension of these surfaces are marked by Holocene age incised valley fills in most of South Africa's contemporary estuaries (e.g. Cooper, 2001).

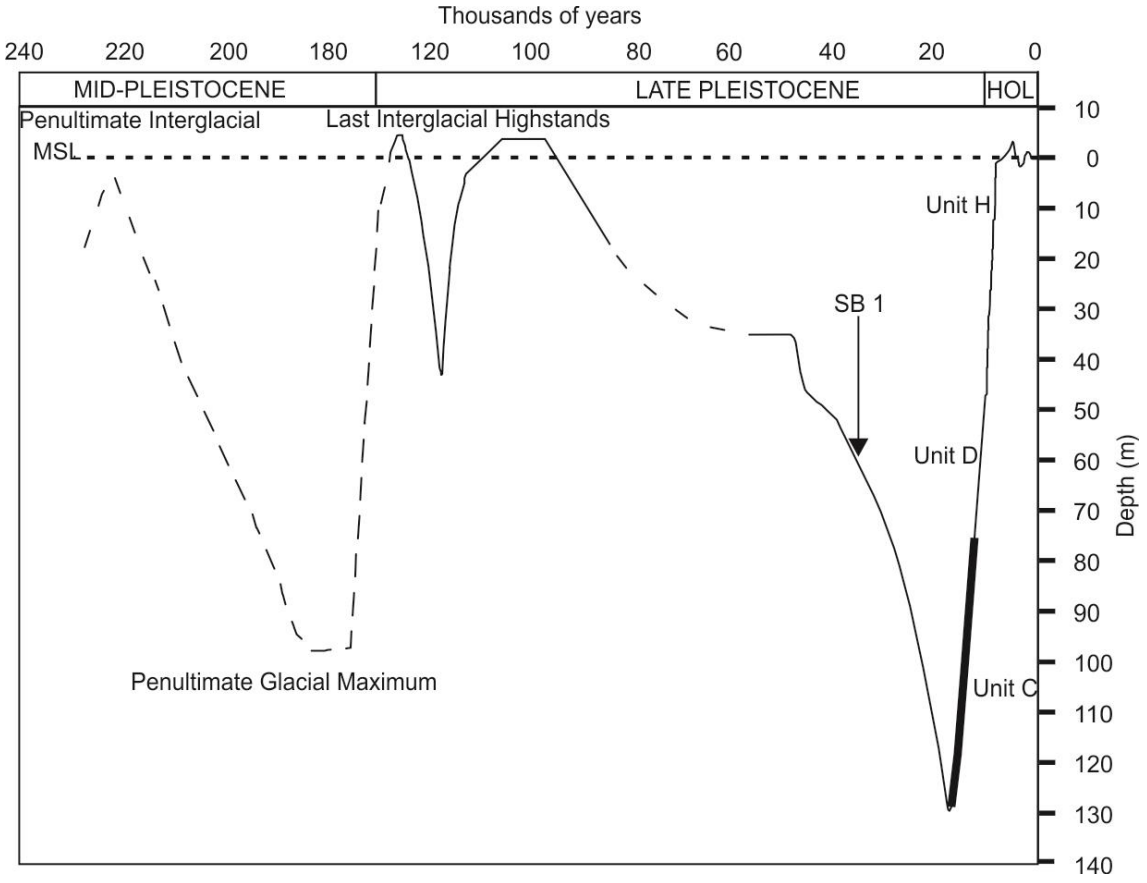

Fig. 6.1. Late Pleistocene sea level curve for the east coast of South Africa (modified from Ramsay and Cooper, 2002). The bold line indicates the time span of Unit C, the solid fine line indicates proven time frame and the dashed line indicated the estimated time frame.

6.1.3. Unit B: disaggregated shoreface deposits

Unit B displays variable amplitude, hummocky- aggrading to acoustically transparent, low continuity reflectors. These are almost identical to the shoreface deposits cored and described by Green et al. (2012) and Pretorius et al. (2016) for the shoreface of Durban. Pretorius et al. (2016) ascribe the evolution of these disaggregated deposits to the dislocation of the upper and lower shoreface as the wave base migrates over the palaeo-coastal plain during rapid sea-level rise. Similar features were found by Duncan et al. (2000) for the New Jersey mid-shelf. They consider the lower bounding surface to be a subaerial unconformity formed during forced regression and the overlying sporadic cover succession are marine sediments that were deposited prior to the period when the shoreline migrated out of the mid-shelf corridor.

6.1.4. Unit C: Incised valley fill

Unit C consists of Late Pleistocene to Holocene-aged incised valley fill sediments as described by Green et al. (2013a, 2013b). This unit was deposited during the transgression that followed the LGM regression (Fig.5.1). Unit C overlies SB1, onlaps the valley walls, and is capped by SB2. Its exact relationship with Unit B is not clear, so one either could pre-or post-date the other. Unit C displays similar features to the incised valley systems described by Green et al. (2013b) and Pretorius et al. (2016), the bulk of which are recognised as comprising a low energy (low reflector amplitude) central estuarine basin fill and overlying sandy flood-tide deltaic complex. Dabrio et al. (2000) recognised alternating sandy/muddy infill in the upper incised valley packages, which would account for the alternating high and low amplitude reflectors here. Where Unit C crops out on the seafloor offshore the Kei River, dredges reveal this to comprise very stiff organic muds, which date to 980-902 cal yr BP.

6.1.5. Unit D: Aeolianite barrier

Unit D rests on SB1 and in some places overlies Unit C (often associated with the circular seafloor depressions and ridges). Notwithstanding the acoustic opacity of the of the unit, its ridge-like morphology and architecture is synonymous with the calcareous cemented sandstone features found on shelves around the world (e.g., Carter et al.,1986; Locker et al., 1996; Jarrett et al., 2005; Brooke et al., 2014). These are equivalent to coastal dunes (barrier complexes) that have been calcified and later inundated (e.g., Ramsay, 1994). Dredge samples and the backscatter signature of this unit reveal a hard, cemented deposit. Inspection of the dredges show these ridges to comprise aeolianite/beachrock. These are laterally pervasive, and extend from Morgan Bay south to East London at relatively consistent depths (-64 m on the coast parallel profile). This was similarly recognised as a shelf pervasive feature of similar depth in KwaZulu-Natal, ~ 400 km north of the study area (e.g. Green et al., 2014; Cooper and Green, 2016). Where these crop out or subcrop, they mark an abrupt change in relief from the underlying platform formed in SB1.

6.1.6. Unit E: Back barrier fill

Unit E is a small-scale onlapping, low-amplitude reflector drape that rests within the depressions or saddles that occur to landward of the outcrops of Unit D. Unit E has similar back barrier drape features as those described by Green et al. (2013b). Based on the geometry of the deposit (onlapping drape behind the barriers of unit D) and its location relative to the barrier (Unit D), this unit is interpreted as a back-barrier lagoonal deposit transgressed during wave base translation up the profile (e.g., Green et al., 2013b and Pretorius et al., 2016). To achieve the formation of lagoonal deposits behind the aeolianite ridge (unit D) and its segmented plan (observed in bathymetry), sea level must have remained stable for some time. This scenario was discussed by Salzmann et al. (2013), who similarly considered that the cementation of the fronting barrier sands from the northern KwaZulu-Natal shelf, and barrier progradation from Durban (e.g. Green et al., 2013b) suggested a prolonged stillstand at the centennial scale. The lagoonal deposits together with the aeolianite barrier are capped by a wave ravinement surface formed during slowly rising sea level (e.g. Trenhaile, 2002). Unit D and Unit E are consistent with a sea level stillstand or slowstand at ~ -60 m.

6.1.7. Unit F: Disaggregated barrier accumulations

Unit F takes the form of small-scale acoustically transparent reflectors. Occasionally, low amplitude reflectors form high-angle prograding packages on the toe of the aeolianite barrier. This unit is similar to that recognised by Green et al. (2017) seaward of the Durban barrier/palaeo-shoreline complexes, considered to have been deposited after the formation and lithification of the dune/beach cordons (aeolianite barriers) which it rests against. The package comprises reworked clasts of aeolianite that stack and onlap against the preserved aeolianite core (Green et al., 2017). Therefore, this unit comprises reworked aeolianite barrier deposits. These deposits were deposited at the seaward face of the aeolianite barrier which was being undercut by wave action as the sea level rose; quarried, reworked and reorganised in a way that they were then stacked against the seaward face of the barrier to form an interlocked wedge (e.g. Green et al., 2017).

6.1.8. Sequence boundary 2: Wave Ravinement Surface (wRS)

This sequence boundary is a planar, gently seaward-dipping erosional surface that truncates much of the stratigraphy. This boundary coincides with the wave ravinement surface identified by many others for the South African coastline (e.g. Green, 2009; Cawthra et al., 2012; Green et al., 2014; Pretorius et al., 2016). The shelf shows both flatter and steeper ravinement profiles, and on the basis of the discussion of Davis and Clifton (1987) and Pretorius et al. (2016), signifies that the shelf was subjected to both fast and slow rates of relative sea-level rise. The flatter outer shelf ravinement surface formed during slowly rising sea level, which was associated with the development of the -100 m ridge, whereas the ravinement surface on the steeper inner shelf was subjected to rapid sea-level rise. Here the shoreline trajectory was much steeper (cf. Cattaneo and Steel, 2003), and points to an overstepping process.

6.1.9. Unit G: Unconsolidated Holocene Sediments

Unit G encompasses a shore attached Holocene sediment wedge as discussed by Flemming and Martin (2017). This unit displays hummocky bottomset reflectors that merge into tangential to sigmoidal topset seismic reflectors characteristics. Similar reflector configurations were described by Green et al. (2012) and Pretorius et al. (2016) for the shoreface of Durban, where they interpreted these seismic reflectors, together with core data, to represent storm-generated reworking of the lower shoreface. Dredge samples of this unit revealed that it is composed of terrestrial and marine bioclastic material comparable to that found by Flemming and Martin (2017).

6.1.10. Unit H: Rhodoliths

A dredge of unit H revealed this to comprise a series of rhodoliths. Rhodoliths preserve the record of the changing benthic associations through time or space (Basso and Tomaselli, 1994; Basso et al., 1998; Checconi and Monaco, 2008), occurring as extensive deposits of

biogenic calcium carbonate in shallow-marine waters usually away from sources of terrigenous sediment. Dates of the interior of the rhodoliths ranged from 7406 - 7225 cal yr BP, indicating the initial formation of these features. The surface dates to present day (150 - Post Bomb cal yr BP 0), indicating continuing accumulation. It stands to reason that the conditions necessary for their formation have been in existence since ~ 7400 years before present.

In the present-day oceans, rhodoliths and other skeletal grains produced in shallow-water carbonate factories are first moved across the platform under the action of strong currents (Kamp et al., 1988; Puga-Bernabeu et al., 2010; Brandano et al., 2012). Sediment is then accumulated on the slope-break and may move again as sediment gravity flow (Schlanger and Johnson, 1969; Halfar et al, 2001). These may also continue to grow by further coralline encrustation or by other constructive biostratinomic processes, which is indicated by sharp contrasts of bioturbation and macrofaunal assemblages between the rhodoliths nucleus and rhodolith surface (Checconi and Monaco, 2008; Checconi et al., 2010). The East London rhodoliths have been accumulating since the mid-Holocene to present day and suggest vigorous current sweeping of the mid-shelf and sea-level inundation since at least that time.

6.2. Seafloor morphology

6.2.1. Seafloor ridges

The ridges are the surface outcrop of Unit A and D, discussed above as a series of palaeo-shorelines that formed from nearshore environments and coastal dunes, which have subsequently been lithified before submergence by rising sea levels of the last deglaciation (Pretorius et al., 2016). Their presence is moreover demonstrative of early cementation of the dune/beach system and according to De Falco et al. (2015) and Green et al. (2017), they indicate a lengthy period of relative sea-level stability at that depth. The submerged shorelines observed in this study at -100 m and -60 m are laterally continuous, occurring intermittently on the South African shelf from the northernmost extents of the northern KwaZulu-Natal shelf, to as far south as the Agulhas Bank (Martin and Flemming, 1986, 1987; Ramsay, 1994; Green, 2009; Cawthra et al., 2012). De Lecea et al. (2017) recorded the presence of the same ridge at 60 m depth from the Limpopo River margin, thus implying a

significant amount of sediment supplied over an along-coast length of ~ 1300 km to form a near continuous barrier-dune system.

6.2.2. Segmented lagoonal waterbodies

The -100 m barriers take several interesting forms. Offshore the Morgan Bay area, the outer barrier forms what appears to be a barrier island system. To landwards of the barrier island, a series of recurved and segmented spits form in the flat back-barrier, separated by a small depression interpreted as a palaeo-inlet. The seafloor features look identical, albeit with a different orientation, to the contemporary barrier island systems of the SE Atlantic margin of the United States (Fig. 6.2).

The arcuate ridges and semi-circular seafloor depressions that occur further landward of the outer -100 m barrier between East London to Morgan Bay are particularly interesting. These are directly comparable in terms of morphology to features found offshore Durban by Green et al. (2013a), who interpreted them to represent a segmented lagoonal/coastal lake system. The presence of the inlet/barrier at -100 m, with lagoonal depressions, separated by features that appear to be cuspate spits, with small prograded ridges is remarkably similar to the coastal waterbodies of northern KwaZulu-Natal. Such features have achieved equilibrium form between sea-level rise, sediment supply and incipient coastal energy (c.f. Zenkovich, 1959) and as such provide further evidence for protracted sea-level stability at -100 m.

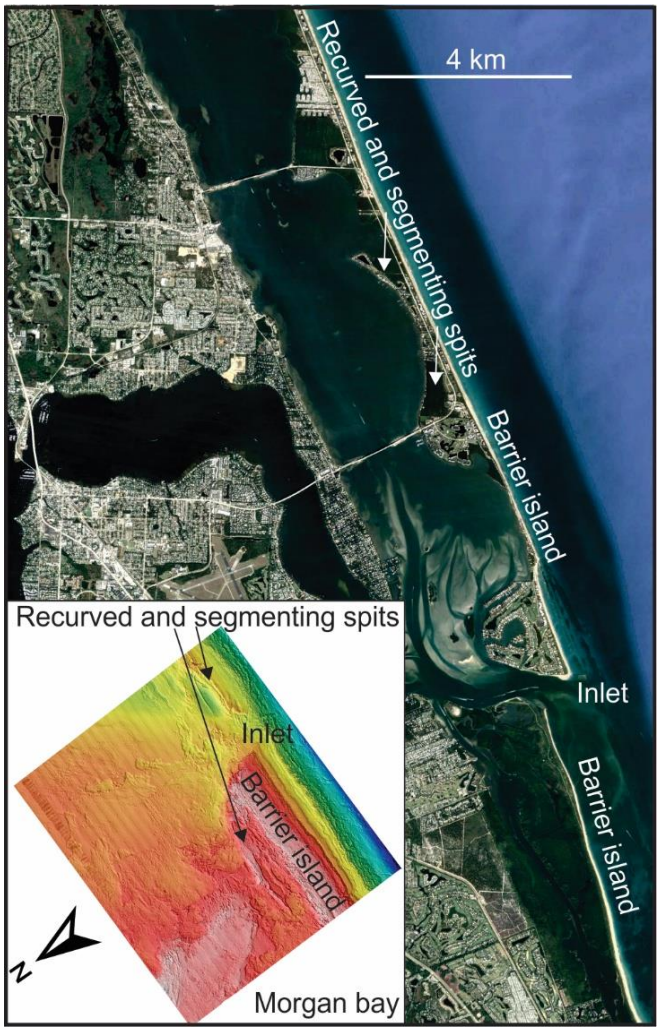

Fig. 6.2. Re-orientated multibeam bathymetry of the -100 m ridge offshore Morgan Bay, compared to the modern coastal morphology of West Palm Beach, Florida. Scales are approximately equal.

6.2.3. Parabolic dune forms

The localised pinnacles and ridges within the hardgrounds that lie adjacent to the palaeo-lagoonal depressions offshore the Kei River and continue south to Kidds beach (~ 50 km along coastal strike) form small, parabolic shapes. These aeolianite features are of similar shape and scale to the parabolic dune fields that are found along the coast of northern KwaZulu-Natal (Jackson et al., 2014; Green et al., 2017). By virtue of their cementation as aeolianite, and the preservation of such a form, they are consequently interpreted as relict parabolic dunes (see for example Brooke et al., 2017). In these dune systems, a bi-directional wind regime keeps up a ‘steady state’ dune position in which large quantities of

sand pulse backward and forward along/oblique to the shoreline (Jackson et al., 2014). Their orientations suggest a relatively vigorous wind regime blowing from NE to SW, similar to the conditions that prevail today (Jackson et al., 2014). Interestingly, there are no similar dunes from the adjacent contemporary East London coastline. The only comparable system, from both a size and form perspective, is the Alexandria dune field (Fig. 6.3), ~ 100 km to the south of East London. It thus appears that a dune field, similar to that of the Alexandria dune field, once occupied the palaeo-coastal plain when sea level occupied -100 m.

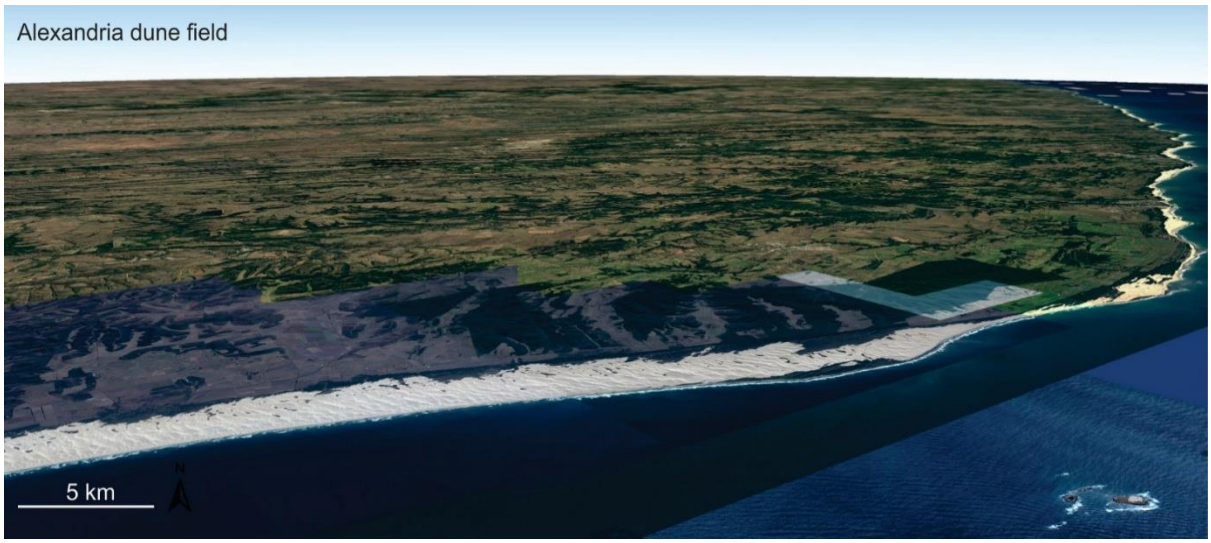

Fig. 6.3. Oblique view of the Alexandria dune field. Note the width of the dune field (~10 km) and an along coast length of ~ 40 km.

Using the available data, and interpolating outcrop between the data-rich zones, these dunes cover an along coast length of almost 80 km, with a width of ~ 12 km and a surface area of ~ 950 km^2 (Fig. 6.4).

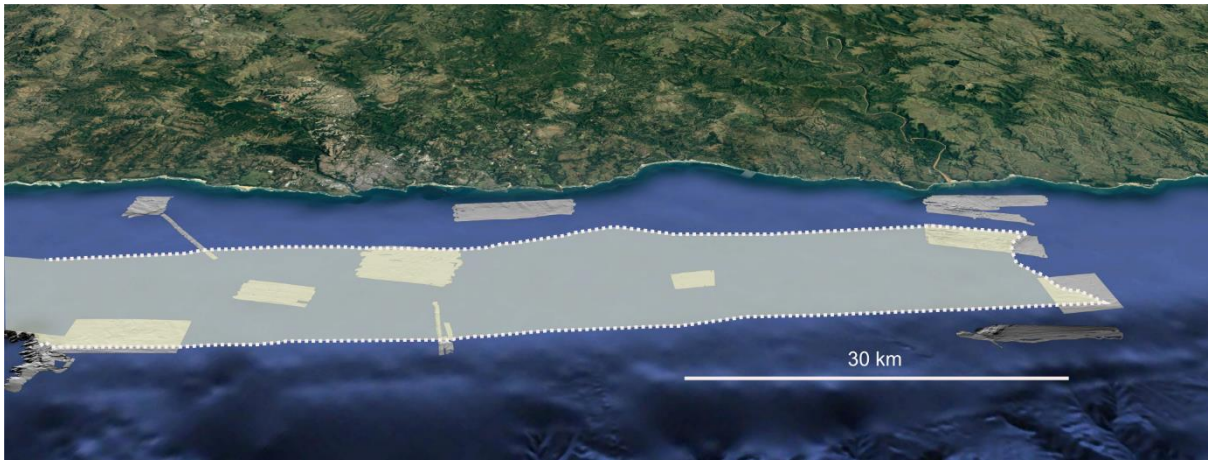

Fig. 6.4. Oblique view of the study area with the interpolated zone covered by the aeolian dunes of Unit D.

The steep slope of the shelf, together with the narrow palaeo-coastal plain acted to limit accommodation space and foster the development of a large dune complex (cf. Jackson et al., 2014). Pending more detailed bathymetric mapping, it remains unclear if this is a single phase of dune building, or the product of multiple phases. Furthermore, it is uncertain how the longshore sediment supply would have operated in light of the aeolian dune's close proximity to the shelf edge and Hamburg canyon system, which would have disrupted alongshore transport.

6.2.4. -60 m ridges and unusual morphologies

Seaward of the Gqunube Point area, a drumstick-shaped ridge occurs at a depth of 77 m. This feature forms an arcuate seafloor high that trends in a SW-NE direction, terminating in a series of small prograded ridges. The geomorphological features of this ridge correlates well with several palaeo-barrier islands such as those found along SW Florida platform margin (e.g. Jarrett et al., 2005) as well as modern barrier islands of the U.S. Southeast Embayment (coastline of South Carolina, Fig. 6.5 and Georgia; e.g. Hayes, 1994). The orientation of the drumstick implies that sediment supply via longshore drift was from the NE to SW, a reversal compared to today. Further dredge and Remotely Operated Vehicle work is planned to better understand this unusual feature.

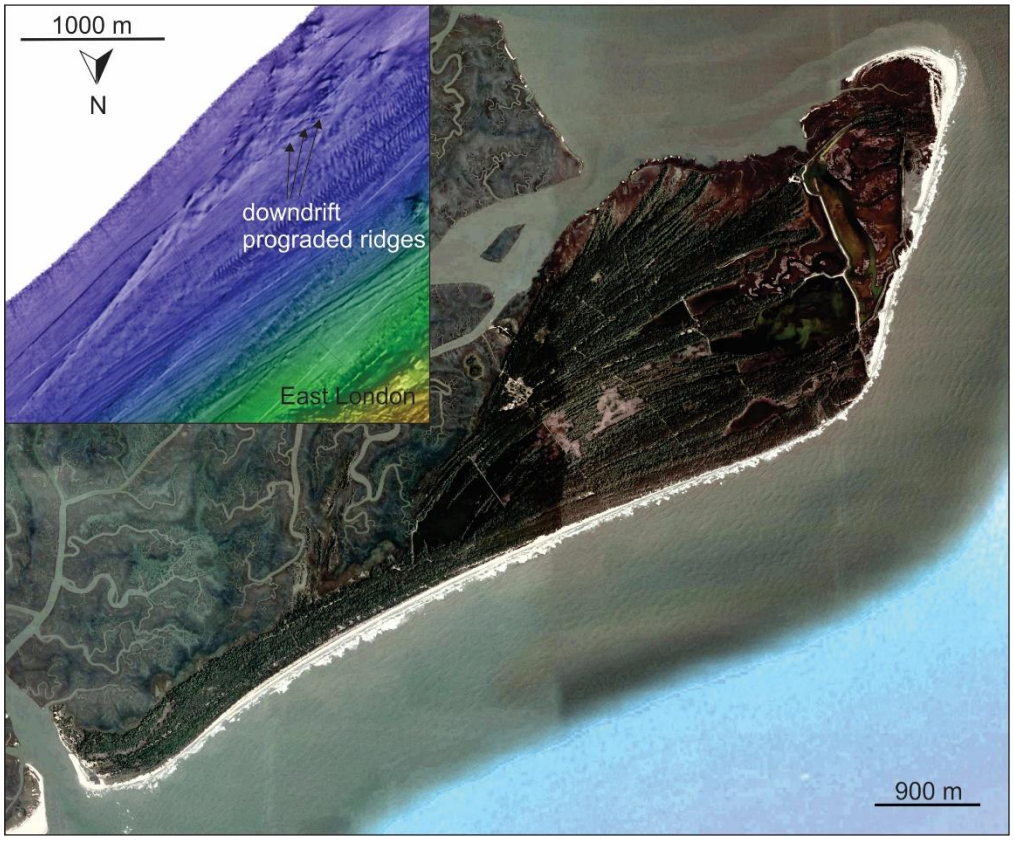

Fig. 6.5. Re-orientated multibeam bathymetry of the drumstick barrier offshore East London, compared to the modern drumstick barrier (Bull Island) from the coastline of South Carolina.

South of the Palaeo-Gqunube River, small crenulate bays with what appear to be cuspate-type spits at -60 m are superimposed on the outcrop of Karoo-aged rocks. These are similar in shape to modern crenulate bays that are found along much of southern Africa's coastline (e.g. the coastline of Port Elizabeth and Mossel Bay, Fig. 6.6). Crenulate bays are common on exposed sedimentary coasts (Hsu et al., 1989), with beaches that link two consecutive headlands subject to a predominant wave approach oblique to the alignment of the upcoast and downcoast headlands (Silvester, 1970). These unusual morphologies suggest planform equilibrium, having formed during a sea level stillstand/slowstand at -60 m.

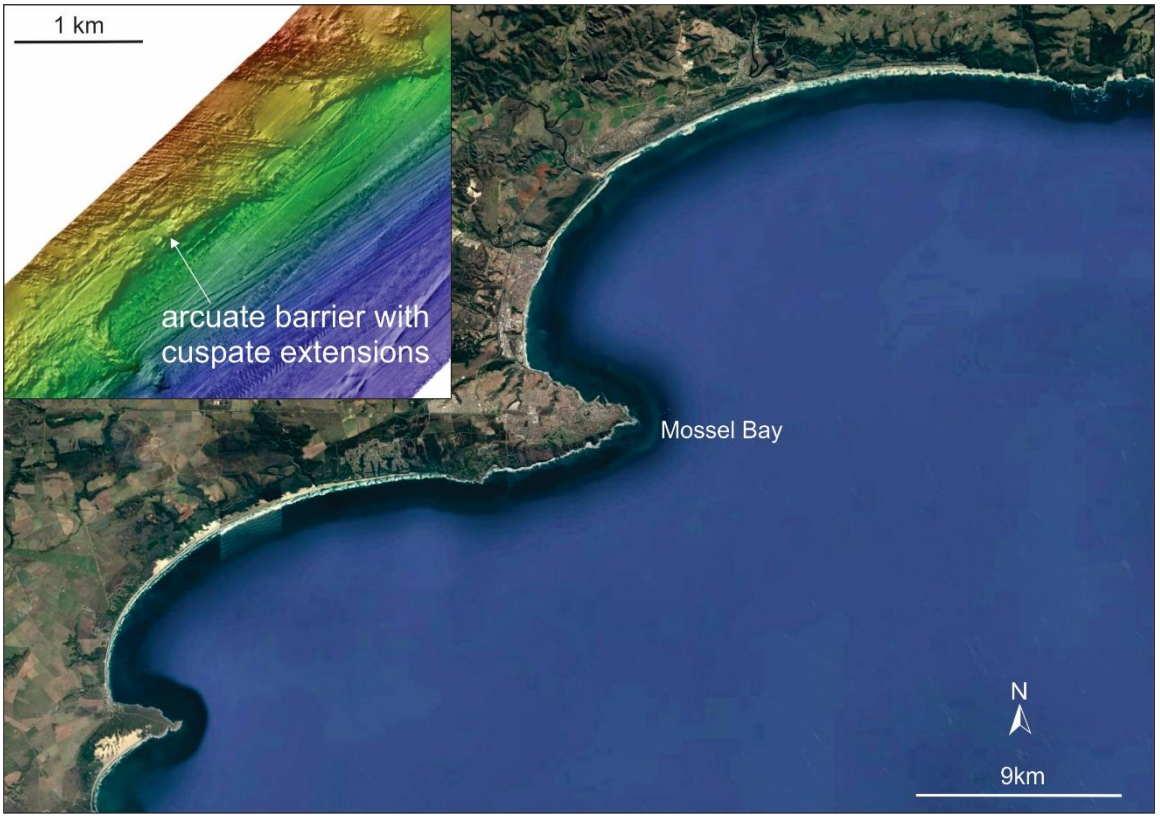

Fig. 6.6. Multibeam bathymetry revealing crenulated-shaped barriers offshore East London, compared to the modern crenulated coastline of (Mossel Bay) the Southern Cape.

6.2.5. Shoreline occupation and timing of barrier development

Based on the model of Salzmann et al. (2013), the barrier and cemented aeolian dune systems initially developed when sea level and the associated shoreline was at depths of 100 m and 60 m, fronting the outcrop of Unit D. Each shoreline developed during either stillstand or slowstand conditions, as emphasized by Green et al. (2017). Coring and dating of seismically identical back-barrier fills of Unit E, together with some of the underlying valley fill material, from Durban revealed these to be Holocene in age, thus having formed during periodic postglacial sea-level rise (Pretorius et al., 2016).

Salzmann et al. (2013) and Green et al. (2014) compared these depths with a number of global eustatic Holocene sea level curves. The depths matched major global changes in sea level that represented stable or slowly rising levels, interspersed with episodes of rapid sea-level rise. On this basis, this study considers the formation of the -100 m barrier at the

landward edge of the shelf break to correspond to the Bølling-Allerod Interstadial stillstand of ~14.5 ka age (Fig. 6.2). This ridge is comparable to the -100 m palaeo-shoreline described by Salzmann et al. (2013) in both height and width.

The genesis of the -60 m barrier is considered to be related to the Younger Dryas slowstand event of 12.7-11.6 ka BP (Camoin et al., 2004). The -60 m ridge is persistent in surface morphology and seismic character (Unit D) and from East London to Morgan Bay, a similar feature recognised by Green et al. (2013a) from Durban is evident (e.g. Green et al., 2014).

6.2.6. Preservation of the barrier shorelines

Preserved barrier complexes on the continental shelf are not well documented. This may reflect a paucity of data (cf. Swift and Moslow, 1982; Leatherman et al., 1983), as in recent years and with better mapping techniques, their prevalence in subtropical climates has become increasingly more evident (Green et al., 2017). A few factors will lower the preservation potential of a barrier shoreline as it is submerged by rising sea levels. These include:

1. A steep shelf gradient. Erosion by landward migration of a shoreline across a high gradient shelf is more intense than across their lower slope counterparts (Cattaneo and Steel, 2003). The steeper gradient causes the wave base to occupy the same place for longer periods of time during ravinement and effectively removes more material more effectively.
2. The sandy nature of the submerged East London barriers. Dredge samples show these to comprise medium sand. Sandy barriers have much shorter relaxation times compared to their gravel counterparts (cf. Orford et al., 2002), they are better able to survive the translation of the beach-shoreface over the barrier form (Long et al., 2006).
3. The high-energy wave regime, by which barrier dispersal during wave-ravinement would be aggravated (Swift et al., 1972).

The barrier shoreline and back-barrier stratigraphies have been exceptionally well-preserved, with spectacular evidence of planform coastal morphologies still evident. This is

in spite of the processes of ravinement, as evidenced by the erosion surface Sequence boundary 2 that has truncated these shorelines (Unit D).

The behaviour of barrier shorelines in the context of rising sea level is discussed by Carter (1988), who considered three main modes of barrier response, erosion, rollover, and overstepping. A fourth possible mechanism is partial overstepping, whereby remnants of the barrier are left after a portion of the barrier is eroded as the shoreface translates over the barrier form.

Overstepping has been considered the main mechanism responsible for the preservation of the palaeo-shorelines from SE Africa, associated with particularly abrupt phases of sea-level rise and in place drowning the shoreline (Green et al, 2014). A critical factor in preservation of the barrier form is the rate of relative sea-level rise (Storms et al., 2008). It is more likely that the shoreline, barrier, and back-barrier deposits will be overstepped with a more rapid rate of sea-level rise (Belknap and Kraft, 1981, Forbes et al., 1995, Storms et al., 2008), coupled with extensive and sandy back barrier sediment (e.g. Green et al., 2017). The back-barrier lagoonal deposits would be eroded and reworked to a large extent by bay ravinement processes, and fed back into the barrier-shoreface system as sea-level (Green et al., 2017). If the rate of sea-level rise was slow, these are heavily reworked and only sparse remnants, if any, of the postglacial back-barrier lagoon system are left behind. These deposits are best preserved if there is rapid creation of accommodation in the back-barrier and if there is no migration of the barrier landward (i.e., overstepping; Forbes et al., 1995; Mellett et al., 2012). This has the combined impact of dampening the impacts of both tidal and wave ravinement.

Early cementation of the barrier cannot be discounted as a preservative mechanism. Other authors show carbonate-cemented barriers from around the world's shelves, associated with conditions that favour subtropical diagenesis (e.g. Locker et al., 1996; Jarrett et al, 2005; De Falco et al., 2015; Green et al., 2017). There is evidence of carbonate diagenesis of the shoreline at Nahoon Point (see Roberts et al., 2006), currently preserving headlands and small embayments, together with the dredge samples of the cemented aeolianites. This undoubtedly played a role in the binding and protection of these sandy systems from wave ravinement. It is however most likely that these two independent factors of rapid sea-level

rise and cementation both influence how well the barriers are preserved. Rate of sea-level rise surely had an influence as it has been documented how quickly beachrock slabs can be reworked in shallow water environments with aggressive wave climates (Pretorius et al., 2016).

6.2.7. Rapid rise in RSL and meltwater episodes

The lagoonal deposits landward of both -100 m (Fig. 5.11 and 5.16) and -60 m (Fig. 5.2 and 5.3) barriers bears witness to the rapid creation of accommodation space in the back barrier and a reduction in the efficacy of the bay-ravinement process as the barrier was submerged (cf. Storms and Swift, 2003). The high gradient of the wRS, bounding the surface of the lagoonal/back barrier deposits (Fig. 5.2 and 5.3) indicates a steepened shoreline trajectory during overstepping. Salzmann et al. (2013) consider causes for steepened shoreline trajectories to include steep transgressed topographies, rapid rates of RSL rise and high rates of sediment supply (based on the work of Cattaneo and Steel, 2003). On this sediment-starved shelf, high sedimentation rates during infilling of the back barrier can be discounted (e.g. Green, 2009, 2011; Salzmann et al., 2013).

Therefore, the steepening of the wRS capping the lagoonal deposits of Unit E was probably the result of a rapid rate of RSL rise coupled with transgression over a cemented, high-relief barrier profile (Cattaneo and Steel, 2003).

These rapid pulses of RSL rise can be linked to meltwater pulses (MWP's) achieved that resulted from episodes of exceptionally rapid ice sheet melting. During MWP-1A, sea level rose from -96 m to -76 m, this was between 14.3 and 14.0 ka BP (Fairbanks, 1989, Bard et al., 1990, Bard et al., 1996; Camoin et al., 2004; Peltier and Fairbanks, 2006). MWP-1B is associated with RSL rises from -58 m to -45 m, between 11.5 and 11.2 ka BP (Liu and Milliman, 2004). Both these MWP's corresponds to the rapid acceleration in RSL rise after periods of either slowstand or stillstand at levels associated with shoreline development along palaeo-coastlines in East London. This is in keeping with the results of Pretorius et al. (2016), and the model of Green et al. (2014), and further adds evidence for the existence of these processes.

6.2.8. Shoreline occupation and barrier volume

The -100 m and -60 m ridges would have developed when the sea-level and associated shoreline was at those approximate depths, during either stillstand or slowstand conditions, though the timing is not clear as to how long they took to amalgamate. A 10^2 to 10^3-year time frame has been assigned for the development of large-scale equilibrium sandy shorelines by Cowell and Thom (1994). Similar time scales for gravel barrier development have been documented by Orford et al. (2002).

Given the mapped dimensions, the -100 m palaeo-barrier accumulated to a volume of 0.65 km^3 (65 X 10^7 m^3). In comparison, the contemporary northern KwaZulu-Natal (Kosi Bay) to southern Mozambique (Maputo) barrier system, has accumulated to a volume of 70 km^3 over the time frame of 1500 years (cf Botha and Porat, 2007). Over the course of ~ 200 years (the slowstand preceding MWP 1-A) and ignoring sediment losses due to erosion by ravinement, the Unit D barrier system accumulated at a minimum rate of ~ 325 X 10^4 m^3 per year. The contemporary barrier system consequently received much greater volumes of sediment with higher rates of sediment supply; the volume of sediment accumulated in the contemporary barriers to the north over two years is more than the volume of sediment accumulated over 200 years for the palaeo-barrier. This suggests either very limited sediment supply, or a large loss of materials during the ravinement of the palaeo-barrier. The large number of rivers and their high discharges means that there would have been a high likelihood of abundant sediment, especially on the palaeo-coastal plain, which would be almost fully exposed at a sea level of 100 m depth. It seems more likely that the volume discrepancies can be accounted for by incredibly effective ravinement processes, yet still not effective enough to remove these barriers wholesale.

6.2.9. Controls on unconsolidated sedimentary facies distribution

The narrow East London continental shelf continental shelf is dominated by the strong Agulhas Current, which now exerts a dominating influence on the distribution and zonation of the various sedimentary facies of the shelf. For example, maerle deposits require strong current sweeping to form. The quartz-rich shelf sands occur especially on the inner to mid

shelf of the mapped areas are comparable to areas mapped by Green (2009) for northern KwaZulu-Natal. These comprise the sediments of the modern transgressive sediment wedge. Morris et al. (2007) indicated that the southerly flowing Agulhas Current has denuded the mid-outer shelf of much of its sediment, by exceeding the critical bed shear velocity required to move medium sand (the dominant mean sand size). The carbonate gravels of Acoustic Facies F represent the relict gravel lag deposits identified by Flemming (1978; 1981). This is confirmed by the dredging work, which revealed beachrock and aeolianite pebbles mixed with shelly gravels along the outer shelf.

6.2.10. The transgression from MWP-1B

The Palaeo-Kei River and the Palaeo-Gqunube River systems are under-filled valley systems that incise the shelf (SB1), and truncate Karoo-age stratigraphy, together with the acoustic basement. Their under-filled nature is unusual, and is rarely reported from shelves worldwide. Simms et al. (2006) attribute underfilling to relatively low fluvial sediment supply conditions, though Cooper et al. (2012) show that underfilling can also be related to a lack of marine and fluvial inputs. In particular, a limited supply of marine sediment, coupled with rapid transgression can leave the incised valley as a relict feature post-transgression (e.g. Payenberg et al., 2006).

In examining the palaeo-Kei River, at ~ 60 m depth, a cuspate shoreline extends from the valley, which is associated with the -60 m stillstand. This area is also marked by rhodolith accumulations dated to ~ 7400 cal yr BP. Their presence indicates a lack of marine sediment and predominant current sweeping. The palaeo-Gqunube River is marked by a valley that crosscuts Karoo-age rocks, with superimposed barrier shorelines at -60 m. These are flanked on either side by a sediment-denuded shelf with upper flow regime bedforms such as gravel ribbons. These further suggest strong current sweeping in this zone.

It is proposed that sea level occupied the -60 m (as discussed previously), followed by MWP -1B which rapidly overstepped the palaeo-coastal plain and shelf up to a depth of ~ 48 m. This rapid step in sea-level rise, coupled with the current sweeping and sediment starvation, left this portion of the valley under-filled from marine influence. The fluvial supply may not

have been sufficient to supply enough material to fill the valley as bayhead deltas (e.g. Simms et al., 2006; Mattheus and Rodriguez, 2011), however it is unlikely given the large load of sediment currently carried by the Kei River for example. Instead, like Green et al. (2013b) proposed, the shelf gradient coupled with the large step in accommodation, refocused fluvial sediment deposition in the proximal areas. Deposition of rhodoliths at ~ 7400 cal yr BP indicate post-MWP sea levels that approximate the levels of today (cf. Ramsay and Cooper, 2002; Fig. 6.1).

At ~ 48 m, in the incised valley offshore the Kei River, organic muds, with large, seaward directed bedforms are encountered (see backscatter and unconsolidated sediments sections). These are almost certainly of terrestrial origin as they do not comprise any type of biogenic ooze. This marks the most distal point of the submerged Kei-River prodelta. Dates of this material point to deposition ~ 900 cal yr BP, when sea level was within the contemporary framework. These are quite likely to represent a palaeoflood that delivered a high quantity of suspended material to the shelf as a dense hyperpycnal plume that was entrained in the valley and then sheltered from later current erosion.

6.2.11. Sediment bypassing and loss from the shelf

Holocene sediments are focused mainly on the inner to middle shelf where they adjoin late Pleistocene palaeo-dune cordons. A sediment reservoir effect occurs behind these palaeo-shorelines. A similar effect of the -60 m submerged shoreline has been recognised along the northern (Green, 2009) and south coast of KwaZulu-Natal (Flemming, 1981; Flemming and Hay, 1988). There is widespread, along-shelf sediment transport, evidenced by the thin veneers of Unit H which cover the mid shelf, the prevalence of rocky outcrop mixed with maerle from the mid- to outer-shelf, and the very high flow regime bedforms preserved as ribbon marks and sediment streamers on the outer-shelf and upper slope. Sediment dispersal via entrainment into submarine canyons has been considered a major factor in the export of sediment to the adjacent abyssal areas (Ramsay, 1994; Cunningham et al., 2005; Covault et al., 2010). Given the strong sediment mobility associated with the prevailing shelf-sweeping of the Agulhas Current, the adjoining Hamburg canyon series may thus

capture appreciable amounts of shelf sediment and transport this to the distal deepwater environments.

In the inner to mid shelf, the presence of large dunes and sediment ribbons and furrows lined with gravel also indicate aggressive current sweeping. Here, the sediment is moved between topographic obstacles in the form of the palaeo-embayments and shorelines, essentially trapping some of the sediment in the active inner shelf wedge (cf. Flemming, 1978).

CHAPTER 7

Conclusions

Eight seismic units and two major erosion surfaces are evident. The oldest rocks imaged are correlated with limestones of the Algoa Formation associated with a Campanian-aged normal regression. This unit is truncated by the LGM-age subaerial unconformity SB 1. This is overlain by Unit B and C. Their time relationships are unclear. Disaggregated shoreface deposits of Unit B formed with rapid sea-level rise as the wave base migrated rapidly over the palaeo-coastal plain. Unit C marks the inshore extension of SB 1, where Holocene-aged incised valley fills began to form in areas of suitable accommodation. These incised valleys comprise low-energy central basin fills and overlying sandy flood-tide deltas. Stiff organic mud crops out in the most proximal areas of the underfilled incised valley and dates to 980-902 cal yr BP.

Unit D represents coastal dunes (aeolianite/beachrock) which were calcified and later inundated and overstepped. Behind the aeolianite/beachrock are back-barrier lagoonal deposits of Unit E, which were similarly transgressed during wave base translation up the palaeo-coastal plain. These two units formed during a sea level stillstand or slowstand. Unit F is made up of reworked aeolianite barrier deposits, deposited seaward on the toe of the aeolianite barrier.

The wave ravinement surface (SB 2) truncates much of the stratigraphy and merges with the subaerial unconformity (SB 1) seaward in the absence of disaggregated shoreface deposits. This wRS was formed by both slowly and rapid rising sea level, where the slowly rising sea level was associated with the flatter outer shelf and the development of a -100 m palaeo-shoreline. Rapid sea-level rise was associated with the steeper inner shelf and overstepping processes of the -60 m shoreline. Above the wRS, storm-generated reworking of the lower shoreface resulted in the deposition of the terrestrial and marine bioclastic material of the shoreface Unit G. Rhodoliths (Unit H) were formed post MWP's in shallow marine waters, from 7407-7225 cal yr BP to present day. Since then, current sweeping of the mid-shelf by the Agulhas Current has occurred.

The seafloor ridges of Unit D crop out to form extraordinarily well-preserved palaeo-shorelines which were lithified and reflect planform equilibria. The -100 m and -60 m submerged shorelines of this study area form near continuous barrier-dune systems, and reflect significant amounts of sediment supply over an along-coast of ~1300 km. A barrier island system is evident at -100 m offshore Morgan Bay, landwards of which segmented lagoonal/coastal lake systems formed. Parabolic dune fields adjacent to the segmented lagoonal/coastal lake systems are evident. These reflect vigorous wind regimes blowing from NE to SW, similar to present day conditions. These large dune fields developed due to a narrow palaeo-coastal plain that limited accommodation space. A drumstick barrier and crenulate bays with cuspate spits at -70 to -60 m, are also evident to landwards of the main shoreline that is preserved.

Each palaeo-shoreline formed during stillstand/slowstand conditions, the -100 m palaeo-shoreline corresponding to the Bølling-Allerod interstadial stillstand of ~14.5 ka age (preceding MWP-1A), and the -60 m palaeo-shoreline corresponding to the Younger Dryas slowstand of ~12.7—11.6 ka BP (preceding MWP-1B). Preservation of the palaeo-shorelines was a result of overstepping, in association with abrupt phases of sea-level. Early cementation also played a role in the preservation of these palaeo-shorelines, independent of rapid rise in sea level. The lagoonal/coastal lake systems point to rapid creation of accommodation space in the back barrier and a reduction in the effects of the bay-ravinement processes as the barrier was submerged. A steepened shoreline trajectory during overstepping is reflected by the high gradient of the wRS bounding the surface of the lagoonal/coastal lake systems, caused by the steep transgressed barrier topographies and rapid rates of RSL rise. These rapid pulses of sea level rise correspond to both MWP-1A and MWP-1B for the -100 and -60 m shorelines respectively.

The under-filled incised valleys systems of the study area relate to a lack of marine sediment and strong current sweeping during the rapid rise in sea level of MWP-1B. Fluvial sediment deposition was refocused in the proximal areas due to the gentle shelf gradient in combination with the large step-up in accommodation. The upper muddy infill of unit C relates to the muddy prodelta of the Kei River, infilling the relict valley topography

The contemporary shelf-sweeping by the strong Agulhas Current is reflected by the rocky outcrop mixed with maerle (rhodolith) from the mid- to outer-shelf and ribbon marks and

sediment streamers on the outer-shelf and upper slope. The inner shelf also appears to have strong flows, associated with large dune trains, sediment ribbons and furrows lined with gravel. Offshelf-transport of sediment occurs where large submarine canyons indent the shelf and interrupt transport by the Agulhas Current.

References

Allen, G.P., 1991. Sedimentary processes and facies in the Gironde estuary: A recent model of macrotidal estuarine systems, in Smith, G.D., Reinson, G.E., Zaitlin, B.A., and Rahmani, R.A., (eds.), Clastic Tidal Sedimentology: Canadian Society of Petroleum Geologists Memoir 16, p. 29--40.

Allen, G.P., Posamentier, H.W., 1993. Sequence stratigraphy and facies model of an incised valley fill: The Gironde estuary, France. Journal of Sedimentary Petrology 63, 378– 391.

Anderson, F.P., 1965. Some recent measurements in the Agulhas Current region. 12th Steering Committee Meeting. Marine Disposal Effluents p. 6 (Unpublished).

Anderson, A.M., 1974. Arthropod trackways and other trace fossils from early Permian lower Karoo beds of South Africa. Ph.D. Thesis (unpublished), University of Witwatersrand, Johannesburg.

Bang, H.D., Pearce, A.F., 1978. Physical oceanography. In: A.E.F. Heydorn (ed), Ecology of the Agulhas Current Region. Transactions of the Royal Society of South Arica 43, 156-162.

Bard, E., Hamelin, B., Fairbanks, R.G., 1990. U-Th ages obtained by mass spectrometry in corals from Barbados: sea level during the past 130 000 years. Nature 346, 456–458.

Bard, E., Hamelin, B., Arnold, M., Montaggioni, L., Cabioch, G., Faure, G., Rougerie, F., 1996. Deglacial sea-level record from Tahiti corals and the timing of global meltwater discharge. Nature 382, 241–244.

Basso, D., Tomaselli, V., 1994. Paleoecological potentiality of rhodoliths: A Mediterranean case history. Bollettino Bella Societa Paleontologica Italiana., Atti del V Simposio di Ecologia Paleoecologia delle Communita Bentoniche, Roma 28-3-/9/1992: 17-27.

Basso, D., Fravega, P., Piazza, M., Vannucci, C., 1998. Biostratigraphic, paleobiogeographic and paleoecological implications in the taxonomic review of Corallinaceae, Rendiconti Lincei 9, 201-211.

Bates, R.L., Jackson, J.A., 1980. Glossary of geology, 2nd ed.: American Geology Institute, Falls Church, Va. p. 749.

Baxter, A.E., Meadows, M.E., 1999. Evidence for Holocene sea-level change at Verlorenvlei, Western Cape, South Africa. Quaternary International 56, 65-79.

Belknap, D.F., Kraft, J.C., 1981. Preservation potential of transgressive coastal lithosomes on the US Atlantic shelf. Marine Geology 42, 429–442.

Bierman, P.R., Caffee, M.W., 2001. Slow rates of rock surface erosion and sediment production across the Namib Desert and escarpment, Southern Africa. American Journal of Science 301, 326-358.

Bird, E. C. F., 1967. Depositional features in estuaries and lagoons on the south coast of New South Wales: Australian Geographical Studies, v. 5, p. 113-125.

Bosman, C., 2012. The Marine Geology of the Aliwal Shoal, Scottburg, South Africa (unpublished).

Botha, G.A., Porat, N., 2007. Soil chronosequence development in dunes on the southeast African coastal plain, Maputaland, South Africa. Quaternary International 162–163, 111–132.

Bradley, B.S., 1999. Palaeoclimatology: Reconstructing the climates of the Quaternary, 2nd Ed. Academic Press, San Diego p. 612.

Brandano, M., Lipparini, L., Campagnoni, V. Tomassetti, L., 2012. Downslope-migrating large dunes in the Chattian carbonate ramp of the Majella Mountains (Central Apennines, Italy). Sedimentary Geology 225-256: 29-41.

Bremner, J.M., 1978. Surficial sediments in Algoa Bay, Joint Geological Survey/University of Cape Town. Marine Geology Programme 10, 66-74.

Brooke, B.P., Olley, J.M., Pietsch, T., Playford, P.E., Haines, P.W., Murray-Wallace, C.V., Woodroffe, C.D., 2014. Chronology of Quaternary coastal aeolianite deposition and the

drowned shorelines of southwestern Western Australia- A reappraisal: Quaternary Science Reviews, v. 93, p. 106-124.

Brooke, B.P., Nichol, S., Huang, Z., Beaman, R.J., 2017. Palaeoshorelines on the Australian continental shelf: morphology, sea-level relationship and applications to environmental management and archaeology. Continental Shelf Research 134, 26–38

Camoin, G.F., Montaggioni, L.F., Braithwaite, C.J.R., 2004. Late glacial to post glacial sea levels in the Western Indian Ocean. Marine Geology 206, 119–146.

Carr, A.S., Bateman, M.D., Roberts, D.L., Murray-Wallace, C.V., Jacobs, Z., Holmes, P.J., 2010. The Last interglacial sea-level high stand on the southern Cape coastline of South Africa. Quaternary Research 73, 351-363.

Carter, R.W.G., 1988. Coastal environments: an introduction to the physical, ecological and cultural systems of coastlines. Elsevier, London p. 617.

Carter, R.M., Cater, L., Johnson, D.P., 1986. Submergent shorelines in the SW Pacific: Evolution for an episodic post-glacial transgression: Sedimentology v. 33, p. 629-649.

Cattaneo, A., Steel, R.J., 2003. Transgressive deposits: a review of their variability. Earth-Science Reviews 62, 187–228.

Cawthra, H.C., Neumann, F.H., Uken, R., Smith, A.M., Guastella, L.A., Yates, A., 2012. Sedimentation on the narrow (8 km wide), oceanic current-influenced continental shelf off Durban, Kwazulu-Natal, South Africa. Marine Geology 323-325, 107–122.

Cawthra, H.C., Bateman, M.D., Carr, AS., Compton, J.S., Holmes, P.J., 2014. Understanding Late Quaternary change at the evolution of the Wilderness coastlines, South Africa. Quaternary Science Reviews v 99, p. 210-223.

Checconi, A., Monaco, P., 2008. Trace fossil assemblages in rhodolith from the Middle Miocene of Mt. Camposauro (Longano Formation, Southern Appenines, Italy). Studi Trentini di Scienza Naturali. Acta Geologica 83, 165-176.

Checconi, A., Bassi, D., Carannante, G., Monaco, P., 2010. Re-deposited rhodoliths in the Middle Miocene hemipelagic deposits of Vitulano (Southern Appenines, Italy): Coralline assemblage characterization and related trace fossils. Sedimentary Geology 225, 50-66.

Compton, J.S., 2001. Holocene sea-level fluctuations inferred from the evolution of depositional environments of the southern Langebaan Lagoon salt marsh, South Africa. The Holocene 11 (4), 395-405.

Compton, J.S., 2006. The mid-Holocene sea-level highstand at Bogenfels Pan on the southwest coast of Namibia. Quaternary Research 66, 303-310.

Compton, J.S., 2011. Pleistocene sea-level fluctuations and human evolution on the southern coastal plain of South Africa. Quaternary Science Reviews 30, 506-527.

Compton, J.S., Wiltshire, J.G., 2009. Terrigenous sediment export from the western margin of South Africa on the glacial to the interglacial cycles. Marine Geology 266, 212-222.

Cooper, J.A.G., 2001. Geomorphological variability among microtidal estuaries from the wave dominated South African coast. Geomorphology, Elsevier v.40, p. 99-122.

Cooper, J.A.G., 2002. The role of extreme floods in estuary-coastal behaviour: contrasts between river- and tide-dominated microtidal estuaries. Sedimentary Geology 150, 123–157.

Cooper, J.A.G., Green, A.N., 2016. Geomorphology and preservation potential of coastal and submerged aeolianite: example from KwaZulu-Natal, South Africa. Geomorphology 271, 1-12.

Cooper, J.A.G., Green, A.N, Wright, C.I., 2012. Evolution of an incised valley plain estuary under low sediment supply: a “give-up” estuary. Sedimentology 59, 899-916.

Cooper, J.A.G., Meireles, R.P., Green, A.N., Klein, A.H.F., Toldo, E.E., 2018. Late Quaternary stratigraphic evolution of the inner continental shelf in response to sea-level change, Santa Catarina, Brazil. Marine Geology 397, 1-14.

Covault, J.A., Romans, B.W., Fildani, A., McGann, M., Graham, S.A., 2010. Rapid climate signal progradation from source to sink in a Southern California sediment-routing system. The Journal of Geology v. 118 p. 247–259.

Curray, J. R., 1964. Transgressions and regressions. In: Miller, R. L. (Ed.), Papers in marine geology -Shepard commemorative volume: New York, Macmillan p. 175-203.

Cutler, K.B., Edwards, R.L., Taylor, F.W., Cheng, H., Adkins, J., Gallup, C.D., Cutler, P.M., Burr, G.S., Bloom, A.L., 2003. Rapid sea-level fall and deep-ocean temperature change since the last interglacial period. Earth and Planetary Science Letters 206, 253-271.

Cowell, P.J., Thom, B.J., 1994. Morphodynamics of coastal evolution. In: Carter, R.W.G., Woodroffe, C.D. (Eds.), Coastal evolution, late Quaternary shoreline morphodynamics. Cambridge University Press, Cambridge p. 33–86.

Cunningham, M.J., Hodgson, S., Masson, D.G., Parson, L.M., 2005. An evaluation of along- and downslope sediment transport processes between Goban Spur and Benot Spur on the Celtic Margin of the Bay of Biscay. Sedimentary Geology 179, 99-116.

Dabrio, C.J., Zazo, C., Goy, J.L., Sierro, F.L., Borja, F., Lario, J., Gonzales, J.A., Flores, J.A., 2000. Depositional history of estuarine infill during the last post glacial transgression (Gulf of Cadiz, southern Spain): Marine Geology v. 162, p. 381-404.

Dalrymple, R.W., Zaitlin, B.A., Boyd, R., 1992. Estuarine facies models: conceptual basis and stratigraphic implications. Journal of Sedimentary Petrology 62, 1130– 1146.

Darbyshire, J., 1972. The effect of bottom topography on the Agulhas Current. Pure and Applied Geophysics 101, 208-220.

Davies, J.L., 1972. Geographical Variation in Coastal Development. Oliver and Boyd, Edinburgh p. 204.

Davis, R.A., Clifton, H.E., 1987. Sea-level change and the preservation potential of wave dominated and tide dominated coastal sequences, in Nummedal, D., Pilkey, OH., Howard, J.D., (eds.), Sea-level fluctuation and Coastal Evolution: Society of Economic Palaeontologists and Mineralogists Special Publication 41 p. 167-178.

Dawson, A. G., 1992. Ice Age Earth. London: Routledge, p. 93.

De Falco, G., Antonioli, F., Fontolan, G., Presti, V.L., Simeone, S., Tonielli, R., 2015. Early cementation and accommodation space dictate the evolution of an overstepping barrier system during the Holocene. Marine Geology 369,52–66

De Lecea, A.M., Green, A.N., Strachan, K.L., Cooper, J.A.G., Wiles, E.A., 2017. Stepped Holocene sea-level rise and its influence on sedimentation in a large marine embayment: Maputo Bay, Mozambique. Estuarine, Coastal and Shelf Science. Elsevier v.193, p.25-36.

Dingle, R.V., Robson, S., 1985. Slumps, canyons and related features on the continental margin off East London, SE Africa (SW Indian Ocean). Marine Geology 67, 37-54.

Dingle, R.V., Siesser, W.G., Newton, A.R., 1983. Mesozoic and Tertiary Geology of Southern Africa. Balkema, Rotterdam p. 375.

Duncan, C.P., 1970. The Agulhas Current. Thesis, University of Hawaii, Honolulu (unpublished).

Duncan, C.S., Goff, J.A., Austin, J.A.Jr., Olson, H.C., 2000. Very high-resolution seismic stratigraphic investigation of the last sea level cycle: latest Quaternary stratigraphy of the New jersey inner shelf (abstr.). American Association of Petroleum Geologists, Annual Convention, official program 9, A44.

Eitner, V., 1996. Geomorphological response of the East Frisian barrier islands to sea-level rise: an investigation of past and future. Geomorphology 15, 57–65.

Fairbanks, R.G., 1989. A 17,000 year glacio-eustatic sea level record: Influence of glacial melting rates on the Younger Dryas event and deep ocean circulation. Nature 342, 637–642.

Flemming, B.W., 1978. Underwater sand dunes along the southeast African continental shelf- observations and implications. Marine Geology 26, 177–198.

Flemming, B.W., 1980. Sand transport and bedform patterns on the continental shelf between Durban and Port Elizabeth (southeast African continental margin). Sedimentary Geology 26, 179-205.

Flemming, B.W., 1981. Factors controlling shelf sediment dispersal along the south-east African continental margin. Marine Geology 42, 259–277.

Flemming, B.W., Hay, E.R., 1988. Sediment distribution and dynamics on the Natal continental shelf. In: Schumann, E.H. (Ed.), Coastal Ocean Studies off Natal, South Africa. Lecture Notes on Coastal and Estuarine Studies 26, 47–80.

Flemming, B.W., Kudrass, H.R., 2017. Large dunes on the outer shelf off the Zambezi Delta, Mozambique: Evidence for the existence of a Mozambique Current. Geo-Marine Letters, In Press, 1-12.

Flemming, B.W., Martin, A.K., 2017. The Tsitsikamma coastal shelf, Agulhas Bank, South Africa: example of an isolated Holocene sediment trap. Geo-Marine Letters.

Forbes, D.L. 1995. Differential preservation of coastal structures on paraglacial shelves: Holocene deposits of southeastern Canada. Marine Geology 124, 187-201.

Forbes, D.L., Taylor, R.B., Shaw, J., Carter R.W.G., Orford, J.D., 1990. Development and stability of barrier beaches on the Atlantic coast of Nova Scotia. Proceeding of the Canadian Coastal Conference, Kingston, Ontario p. 83–98.

Forbes, D.L., Taylor, R.B., Orford, J.D., Carter, R.W.G., Shaw, J., 1991. Gravel-barrier migration and overstepping. Marine Geology 97(3-4), 305–313.

Forbes, D.L., Orford, J.D., Carter, R.W.G., Shaw, J., Jennings, S.C., 1995. Morphodynamic evolution, self-organisation, and instability of coarse-clastic barriers on paraglacial coasts. Marine Geology 126, 63–85.

Gardner, J.V., Dartnell, P., Mayer, L.A., Hughes-Clarke, J.E., Calder, B.R., Duffy, G., 2005. Shelf-edged deltas and drowned barrier-island complexes on the northwest Florida outer continental shelf. Geomorphology 64, 133-166.

Gardner, J.V., Calder, B.R., Hughes-Clark, J.E., Mayer, L.A., Elston, G., Rzhanov, Y., 2007. Drowned shelf-edge deltas, barrier island and related features along the outer continental shelf north of the head of De Soto Canyon, NE Gulf of Mexico. Geomorphology 89, 370-390.

Gill, A.E., Schumann, E.H., 1979. Topographically induced changes in the structure of an inertial coastal jet: application to the Agulhas Current. Journal of Physical Oceanography 9, 975-991.

Green, A.N., 2009. Palaeo-drainage, incised valley fills and transgressive systems tract sedimentation of the northern KwaZulu-Natal continental shelf, South Africa, SW Indian Ocean. Marine Geology 263, 46-63.

Green, A.N., 2011. The late Cretaceous to Holocene sequence stratigraphy of a sheared passive upper continental margin, northern KwaZulu-Natal, South Africa. Marine Geology 289, 17–28.

Green, A.N., Uken, R., 2005. First observations of sea level indicators related to glacial maximum at Sodwana Bay, KwaZulu-Natal: South African Journal of Science v. 101, p. 236–238.

Green, A., Garlick, G.L., 2011. A sequence stratigraphic framework for a narrow, current-swept continental shelf: The Durban Bight, central KwaZulu-Natal, South Africa. Journal of African Earth Sciences 60, 303-314.

Green, A.N., Ovechkina, M.N., Mostovski, M.B., 2012. Late Holocene shoreface evolution of the wave-dominated Durban Bight, KwaZulu-Natal, South Africa: A mixed storm and current driven system: Continental Shelf Research v. 49, p. 56-64.

Green, A.N., Cooper, J.A.G., Leuci, R., Thackeray, Z., 2013a. Formation and preservation of an overstepped segmented lagoon complex on a high-energy continental shelf: Sedimentology v. 60, p. 1755-1768.

Green, A.N., Dladla, N.N., Garlick, L., 2013b. The evolution of incised valley systems from the Durban continental shelf, KwaZulu-Natal, South Africa: Marine Geology v. 335, p. 148-161.

Green, A.N., Cooper, J.A.G., Salzmann, L., 2014. Geomorphic and stratigraphic signals of postglacial meltwater pulses on continental shelves. Geology v. 42, p. 151-154.

Green, A.N., Cooper, J.A.C., Salzmann, L., 2017. The role of shelf morphology and antecedent setting in the preservation of palaeo-shoreline (beachrock and aeolianite) sequences: the SE African shelf. Geo-Marine Letters. DOI 10.1007/s00367-017-0512-8.

Halfar, J., Godinez-Orta, L., Goodfriend, G.A., Mucciarone, D.A., Ingle, J.C. Jr., Holen, P., 2001. Holocene-late Pleistocene non-tropical carbonate sediments and tectonic history of the western rift basin margin of the southern Gulf of California. Sedimentary Geology 144, 149-178.

Harris, T.F.W., 1978. Review of coastal currents in Southern African waters. South African National Science Programme 30 p. 103.

Hayes, M.O., 1994. The Georgia Bight barrier system. In: Davis, R.A. (Ed.), Geology of Holocene barrier island systems. Springer-Verlag, Berlin p. 233– 304.

Helland-Hansen, W., Gjelberg, J.G., 1994. Conceptual basis and variability in sequence stratigraphy: a different perspective. Sedimentary Geology 92, 31–52.

Hijma, M.P., Cohen, K.M., 2010. Timing and magnitude of sea-level jump precluding the 8200 yr event. Geology 38, 275–278.

Howell, J.A., Flint, S.S. 2003. Tectonic setting, stratigraphy and sedimentology of the Book Cliffs. In Coe A.L.(ed.), The Sedimentary Record of sea-level change p. 135-157.

Hsu, J.R.C., Silvester, R., Xia, Y.M., 1989. Static equilibrium bays: new relationships. Journal of Waterways, Port, Coastal and Ocean Engineering 115, 285-311.

Illenberger, W.K., 1992. Lihostratigraphy of the Schelm Hoek Formation (Algoa Group). Lithostratigraphic Series. South African Committee for Stratigraphy 21 p. 7.

Jackson, D.W.T., Cooper, J.A.G., Green, A.N., 2014. Preliminary classification of coastal dunes of KwaZulu-Natal. Journal of Coastal Research SI 74, 718-722.

Jarrett, B.D., Hine, A.C., Halley, R.B., Naar, D.F., Locker, S.D., Neumann, A.C., Twichell, D., Hu, C., Donahue, B.T., Jaap, W.C., Palandro, D., Ciembronowicz, K., 2005. Strange bedfellows- A

deep-water hermatypic coral reef superimposed on a drowned barrier island; southern Pulley Ridge, SW Florida platform margin: Marine Geology v. 214, p. 295-307.

Johnson, M.R., Kingsley, C.S., 1993. Lithostratigraphy of the Ripon Formation (Ecca Group), Including Pluto's Vale, Wonderfontein and Trumpeters Members. Lithostratigrsphic Series of South African Committee for stratigraphy 26 p. 8.

Johnson, M.R., Van Vuuren, C.J., Visser, J.N.J., Cole, D.I., Wickens, H. de V., Christie, A.D.M., Roberts, D.L., 1997. The foreland Karoo Basin, South Africa. In: Selley, R.C. (ed.), Sedimentary Basins of Africa. Elsevier, Amsterdam 269-317.

Johnson, M.R., Van Vuuren, C.J., Visser, J.N.J., Cole, D.I., Wickens, H. de V., Christie, D.L., Brandl, G., 2006. Sedimentary rocks of the Karoo Supergroup. The Geology of Southern Africa 461-500.

Kamp, P.J.J., Harmsen. F., Nelson. C.S., Boyle, S.F., 1988. Barnacle-dominated limestone with giant cross-beds in a non-tropical, tide swept, Pliocene forearc seaway, Hawke's Bay, New Zealand. Sedimentary Geology 60, 173-195.

Kelley, J.T., Belknap, D.F., Kelley, A.R., Claesson, S.H., 2010. Drowned coastal deposits with associated archaeological remains from a sea-level —slowstand : Northwestern Gulf of Maine, USA. Geology 38, 695–698, doi:10.1130/G31002.1

Kingsley, C.S., 1977. Stratigraphy and Sedimentology of the Ecca Group in the Eastern Cape Province, South Africa. Ph.D. thesis (unpublished), University of Port Elizabeth p. 286.

Kingsley, C.S., 1981. A composite submarine fan-delta-fluvial model for the Ecca and Lower Beaufort Groups of Permian age in the Eastern Cape Province, South Africa. Transactions Geological Society of South Africa 84, 27-40.

Klinger, H.C., Lock, B.E., 1979. Upper Cretaceous from the Igoda River mouth, East London, South Africa. Annals of the South African Museum 77, 71-83.

Kounov, A., Niedermann, S., De Wit, M.J., Viola, G., Andreoli, M., Erzinger, J., 2007. Present day denudation rates bearing on erosion processes along selected west- and south-facing

sections of the South African Great Escarpment and its interior derived from in situ produced cosmogenic ^{3}He and ^{21}Ne. South African Journal of Geology 110, 235-248.

Lambeck, K., Yokoyama, Y., Purcell, T., 2002a. Into and out of the Last Glacial Maximum: sea-level change during Oxygen Isotope Stages 3 and 2. Quaternary Science Reviews 21, 343–360. Lambeck, K., Esat, T.M., Potter, E.K., 2002b. Links between climate and sea-levels for the past three million years. Nature 419, 199–206.

Leatherman, S.P., Rampino, M.R., Sanders, J.E., 1983. Barrier island evolution in response to sea level rise; discussion and reply. Journal of Sedimentary Research 53(3), 1026–1033.

Le Roux, F.G., 1987a. Lithostrtigraphy of the Alexandra Formation. Lithostratigraphic Series. South African Committee for Stratigraphy 1 p. 18.

Le Roux, F.G., 1987b. Note on the fluvial deposits overlying the Tertiary Alexandra Formation in the Algoa Basin. Annals of the Geological Survey of South Africa 21, 77-88.

Le Roux, F.G., 1989. Lithostratigraphy of the Nashoon Formation (Algoa Group). Lithostratigraphic series. South African Committee for Stratigraphy 9 p. 14.

Le Roux, F.G., 1990a. Algoa Group. In: Johnson, M.R. (Ed.), Catalogue of South African Lithostratigraphic Units. South African.

Le Roux, F.G., 1990b. Palaeontological correlation of Cenozoic marine deposits of the southeastern, southern and western coasts, Cape Provinces. South African journal of Geology 93, 514-5-8.

Le Roux, F.G., 1991. Lithostratigraphy of the Salnova Formation (Algoa Group). Lithostratigraphic Series. South African Committee for Stratigraphy 15, p. 9.

Le Roux, F.G., 1992. Lithostratigraphy of the Nanaga Formation (Algoa Group). Lithostratigraphic Series. South African Committee for stratigraphy 15, p. 9.

Liu, J.P., Milliman, J.D., 2004. Reconsidering melt-water pulses 1-A and 1-B: Global impacts of rapid sea-level rise. Journal of Ocean University of China (Oceanic and Coastal Sea Research) 3, 183–190.

Liu, J., Saito, Y., Wang, H., Yang, Z., Nakashima, R., 2007. Sedimentary evolution of the Holocene subaqueous clinoforms off the Shadong Peninsula in the Yellow Sea. Marine Geology 236, 165–187.

Lock, B.E., 1973. Tertiary limestones at needs camp, near East London, Transactions Geological Society of South Africa 76, 1-5.

Locker, S.D., Hine, A.C., Tedesco, L.P., Shinn, E.A., 1996. Magnitude and timing of episodic sea-level rise during the last deglaciation. Geology v. 24, p. 827-830.

Long, A.J., Waller, M.P., Plater, A.J., 2006. Coastal resilience and late Holocene tidal inlet history: The evolution of Dungeness Foreland and the Romney Marsh depositional complex (U.K.). Geomorphology 82, 309–330.

Luft, F.F., Luft, J.L.Jr., Chemale, F,Jr., Lelarge, M.L.M.V., Avila, J.N., 2005. Post-Gondwana break-up record constrains from apatite fission track thermochronology in NW Namibia. Radiation Measurements 39, 675-679.

Mallory, J.K., 1974. Abnormal waves on the south-east coast of South Africa. International Reviews of Hydrology 51, 99-129.

Martin, A.K., Flemming, B.W., 1986. The Holocene shelf sediment wedge off the south and east coast of South Africa. In: Knight, R.J., McLean, J.R. (Eds.), Shelf Sands and Sandstones. Canadian Society of Petroleum Geologists Memoir II 27–44.

Martin, A.K., Flemming, B.W., 1987. Aeolianite of the South African coastal zone and continental shelf as sea-level indicators. South African Journal of Science 83, 597–598.

Mattheus, C.R., Rodriguez, A.B., 2011. Controls on late Quaternary incised-valley dimension along passive margins evaluated using empirical data. Sedimentology v. 58 (5), p. 1113-1137.

Maud, R.R., Partridge, T.C., 1990. Bathurst Formation. In: Johnson, M.R. (Ed.), Catalogue of South African Lithostratigraphic Units. South African committee for stratigraphy 2-7,2-8.

Maud, R.R., Partridge, T.C., Siesser, W.G., 1987. An early Tertiary marine deposit at Pato's Kop, Ciskei. Transactions Geological Society of South Africa 90, 231-238.

Mellett, C.L., Hodgson, D.M., Lang, A., Mauz, B., Selby, I., Plater, A.J., 2012. Preservation of a drowned gravel barrier complex: a landscape evolution study from the north-eastern English Channel. Marine Geology 315-318, 115–131.

Miller, D.E., Yates, R.J., Parkington, J.E., Vogel, J.C., 1993. Radiocarbon-date evidence relating to a mid-Holocene relative high sea level on the south-western Cape coast, South Africa. South African Journal of Science 89, 35-44.

Morris, T., Roberts, M.J., Schleyer, M.H., 2007. The current on the Sodwana Bay shelf (South Arica): characteristics, driving forces and implications. In: Symposium Guide and Book of Abstracts 5th Western Indian Ocean Marine Science Association Science Symposium, Elangeni Hotel, Durban 77.

Nichol, S.L., 1991. Zonation and sedimentology of estuarine facies in an incised valley, wave-dominated, microtidal setting, in Smith, D.G., Reinson, G.E., Zaitlin, B.A., and Rahmani, R.A., eds., Clastic Tidal Sedimentology: Canadian Society of Petroleum Geologists Memoir 16, p. 41-58.

Nichols, M.M., Johnson, G.H., Peebles, P.C., 1991. Modern sediments and facies model for a microtidal coastal plain estuary, the James estuary, Virginia: Journal of Sedimentary Petrology v. 61, p. 883-899.

Nordfjord, S., Goff, J.A., Duncan, L.S., Austin Jr., J.A., 2009. Shallow stratigraphy and transgressive ravinement on the New Jersey shelf: Implications for sedimentary lobe deposition and latest Pleistocene–Holocene sea level history. Marine Geology 266, 232–243.

Norström. E., Risberg, J., Gröndahl, H., Holmgren, K., Snowball, I., Mugabe, J.A., Sitoe, S.R., 2012. Coastal palaeo-environment and sea-level change at Macassa Bay, southern Mozambique, since c 6600 cal BP. Quaternary International 260, 153-163.

Okuno, J., Nakada, M., 1999. Total volume and temporal variation of meltwater from last glacial maximum inferred from sea-level observations at Barbados and Tahiti. Palaeogeography, Palaeoclimatology, Palaeoecology 146, 283-293.

Orford, J.D, Forbes, D.L., Jennings, S.C., 2002. Organisational controls, typologies and time scales of paraglacial gravel-dominated coastal systems. Geomorphology 48, 51–85.

Partridge, T.C., Maud, R.R., 1987. Geomorphic evolution of southern Africa since the Mesozoic. Transactions Geological Society of South Africa 90, 179-208.

Pattison, S. A. J., 1992. Recognition and interpretation of estuarine mudstones (central basin mudstones) in the tripartite valley-fill deposits of the Viking Formation, central Alberta, in Pemberton, S. G., (ed.), Applications of Ichnology to Petroleum Exploration: SEPM (Society for Sedimentary Geology), Core Workshop 17, p. 223-250.

Payenberg, T.H.D., Boyd, R., Beaudoin, J., Ruming, K., Davies, S., Roberts, J., Lang, S.C., 2006.The filling of an incised valley by shelf dunes - an example from Hervey Bay, East Coast of Australia. Dalrymple, R.W., Leckie, D.A., Tillman R.W., (Eds.), Incised Valleys in Time and Space, SEPM Special Publication 85 p. 87-98

Pearce, A.F., 1977. The shelf circulation off the east coast of South Africa. National Research Instutute for Oceanology (South Africa) 1 p.220.

Pearce, A.F., Schumann, E.H., Lundie, G.S.H., 1978. Features of the shelf circulation off the Natal coast. South African Journal of Science 74, 328-331.

Peltier, W.R., 2005. On the hemispheric origins of meltwater pulses 1a. Quaternary Science Reviews 21, 377-396.

Peltier, A.F., Fairbanks, R.G., 2006. Global glacial ice volume and Last Glacial Maximum duration from the extended Barbados sea level record. Quaternary Science Reviews 25, 3322- 3337.

Pillans, B., Naish, T., 2004. Defining the Quaternary. Quaternary Science Reviews 23, 2271–2282.

Pretorius, L., Green, A., Cooper, A., 2016. Submerged shoreline preservation and ravinement during rapid postglacial sea-level rise and subsequent slowstand. Geological Society of America Bulletin 128, 1059-1069.

Puga-Bernabeu, A., Martin, J.M., Braga, J.C., Sanchez-Almazo, I.M., 2010. Downslope platform-margin clinoforms in a current-dominated, distally steepened temperate-carbonate ramp (Guadix Basin, Southern Spain). Sedimentology 57, 293-311.

Rampino, M.R., Sanders, J.E., 1980. Holocene transgression in south-central Long Island, New York. Journal of Sedimentary Research 50, 1063–1079.

Rampino, M.R., Sanders, J.E., 1982. Holocene transgression in South0central Long Island, New York; reply. Journal of Sedimentary Research 52 (3), 1020-1025.

Ramsay, P.J., 1994. Marine Geology of the Sodwana Bay shelf, southeast Africa: Marine Geology, v. 120, p. 225-247.

Ramsay, P.J. 1995. 9000 years of sea-level change along the southern African Coastline. Quaternary International 31, 71-75.

Ramsay, P.J., 1997. Holocene sea-level changes. In: Botha, G.A. (Ed.), Maputaland focus on the Quaternary evolution of the south-east African coastal plain. International Union for Quaternary Research, Workshop Abstracts. Council for Geoscience, Private Bag X112, Pretoria, South Africa 56–57.

Ramsay, P.J., Cooper, J.A.G., 2002. Late Quaternary sea level change in South Africa. Quaternary Research 57, 82-90.

Ramsay, P.J., Smith, A.M., Lee-Thorp, J.C., Vogel, J.C., Tyldsley, M., Kidwell, W., 1993. 130 000 year-old fossil elephant found near Durban: preliminary report. South African Journal of Science 89, 165.

Reinson, G.E., 1977. Tidal current control of submarine morphology at the mouth of the Miramichi estuary, New Brunswick, Canada: Canadian Journal of Earth Science v. 14, p. 2524-2532.

Reinson, G.E., 1992. Transgressive barrier island and estuarine systems, in Walker, R.G., James, N.P. (eds.), Facies models: Response to sea-level change, 179-194, Geological Association of Canada.

Reinson, G.E., Clark, J.E., Foscolos, A.E., 1988. Reservoir geology of Crystal Viking field, Lower Cretaceous estuarine tidal channel-bay complex, south-central Alberta: American Association of Petroleum Geologists Bulletin v. 72, p. 1270-1294.

Riek, E.F., 1973. Fossil insects from the Upper Permian of Natal, South Africa. Annals of the Natal Museum 21, 513-532.

Riek, E.F., 1976. New Upper Permian insects from Natal, South Africa. Annals of the Natal Museum 22, 755-789.

Roberts, D.L., Botha, G.A., Maud, R.R., Pether, J., 2006. Coastal Cenozoic deposits. In: Johnson MR, Annhauser CR, Thomas RJ, editors. The geology of South Africa. Johannesburg/Pretoria: Geological Society of South Africa/ Council for Geoscience p. 605-628.

Roy, P. S., 1984. New South Wales estuaries: their origin and evolution, in Thom, B. G., (ed.), Coastal Geomorphology in Australia: Sydney, Academic Press, p. 99-122.

Salzmann, L., Green, A.N, Cooper, J.A.G., 2013. Submerged barrier shoreline sequences on a high energy, steep and narrow shelf. Marine Geology 346, 366-374.

Schlanger, S.O., Johnson, C.J., 1969. Algal banks near La Paz, Baja California- Modern Analogues of source areas of transported shallow water fossils in Pre-Alpine flysch deposits. Palaeogeography, Palaeoclimatology, Palaeoecol 6, 141-157.

Schumann, E.H., 1976. High waves in the Agulhas Current. Journal for Marine Weather Log 20, 1-5.

Scrutton, R.A., Du Plessis, A., 1973. Possible marginal fracture ridge south of South Africa. Nature, Physical Science 242, 180-182.

Shone, R.W., 2006. Onshore Post-Karoo Mesozoic Deposits. In: Johnson, M.R., Anhaeusser, C.R., Thomas, R.J., (eds.), The Geology of South Africa. Geological Society of South Africa, Johannesburg/Council for Geoscience, Pretoria 514-552.

Siegert, M.J., 2001. Ice sheets and late Quaternary environmental change. John Wiley and Sons Ltd., Chichester, UK p. 231.

Siesser, W.G., Dingle, R.V., 1981. Tertiary sea level movements around southern African Journal for Geology 89, 523-536.

Silvester, R., 1970. Growth of crenulate shaped bays to equilibrium. Journal of Waterways Harbors and Coastal Engineering, American Society of Civil Engineering, Proceedings 96, 275-287.

Simms, A. R**.,** Anderson, J. B., Taha, Z. P., Rodriguez, A. B., 2006. Overfilled versus underfilled incised valleys: Lessons from the Quaternary Gulf of Mexico. in Dalrymple, R., Leckie, D., and Tillman, R. (Eds.), Incised Valleys in Time and Space, SEPM Special Publication 85 p. 117-139.

Sink, K. Samaai, T., 2009. Identifying Offshore Vulnerable Marine Ecosystems in South Africa, Unpublished Report for South African National Biodiversity Institute p. 29

Smith, A.J., 1961. Meteorological aspects, especially surface winds and associated weather along the Natal coast. Marine Studies off the Natal Coast, Council for Sciencific and Industrial Research Symposium (Durban, 16 March, 1961) 52, 10-17.

Smith, R., 1976. Grant waves. Journal of Fluid Mechanics 11, 417-431.

Solano-Fernandez, S., Attwood, C.G., Chalmers, R., Clark, B.M., Cowley, P.D., Fairweather, T., et al. Assessment of the effectiveness of South Africa's marine protected areas at representing ichthyofaunal communities. Environmental Conservation 39, 259-27.

Stanford, J.D., Rohling, E.J., Hunter, S.E., Roberts, A.P., Rasmussen, S.O., Bard, E., McManus, J., Fairbanks, R.G., 2006. Timing and meltwater pulse 1a and climate responses to meltwater injections. Paleoceanography 21, PA4103 p. 9.

Stanford, J.D., Hemingway, R., Rohling, E.J., Challenor, P.G., Medina-Elizalde, M., Lester, A.J., 2011. Sea-level probability for the last deglaciation: A statistical analysis of far-field records. Global and Planetary Change 79, 193–203.

Storms, J.E.A., Swift, D.J.P., 2003. Shallow-marine sequences as the building blocks of stratigraphy: insights from numerical modelling. Basin Research 15, 287–303.

Storms, J.E.A., Weltjie, G.J., Terra, G.J., Cattaneo, A., Trincardi, F., 2008. Coastal dynamics under conditions of rapid sea-level rise: Late Pleistocene to early Holocene evolution of barrier-lagoon systems on the northern Adriatic shelf (Italy). Quaternary Science Reviews 27, 1107-1123.

Swift, D.J.P., 1968. Coastal erosion and transgressive stratigraphy. Journal of Geology 76, 444–456.

Swift, D.J.P., 1975. Tidal sand ridges and shoal retreat massifs. Marine Geology 18, 105–134.

Swift, D.J.P., Moslow, T.F., 1982. Holocene transgression in South-central Long Island, New York; discussion. Journal of Sedimentary Research 52(3), 1014–1019.

Swift, D.J.P., Kofoed, J.W., Saulsbury, F.P., Sears, P., 1972. Holocene evolution of the shelf surface, central and southern Atlantic Shelf of America. In: Swift, D.J.P., Duane, D.B, Pilkey, O.H. (Eds.), Shelf Sediment Transport: Process and Pattern, Hutchinson & Ross, Stroudsberg, PA p. 499–574.

Swift, D.J.P., Phillips, S., Thorne, J.A., 1991. Sedimentation on continental margins, V: Parasequences. In: Swift, D.J.P., Oertel, G.F., Tillman, R.W., Thorne, J.A. (Eds.), Shelf Sand and Sandstone Bodies—Geometry, Facies and Sequence Stratigraphy. International Association of Sedimentologists Special Publication 14, 153–187.

Taljaard, J.J., 1972. Synoptic meteorology of the Southern Hemisphere. Meteorological Monographs 13, 129-213.

Tankard, A.J., Jackson, M.P.A., Eriksson, K.A., Hobday, D.K., Hunter, D.R., Minter, W.E.L., 1982. Crustal evolution of southern Africa. Springer-Verlag, New York, p. 523.

Thomas, M.A., Anderson, J.B., 1994. Sea-level controls on the facies architecture of the Trinity/Sabine incised-valley system: Origin and Sedimentary Sequences. Society for Sedimentary Geology. Special Publication 51. SEPM p. 63-83.

Tinker, J., De Wit, M., Brown, R., 2008a. Mesozoic exhumation of the southern Cape, South Africa, quantified using apatite fission track thermochronology. Tectonophysics 455, 77-93.

Tinker, J., De Wit, M., Brown, R., 2008b. Linking source and sink: evaluating the balance between onshore erosion and offshore sediment accumulation since Gondwana break-up, South Africa. Tectonophysics 455, 94-103.

Trenhaile, A.S., 2002. Rocky coasts, with particular emphasis on shore platforms: Geomorphology v. 48, p. 7-22.

Trincardi, F., Correggiari, A., Roveri, M., 1994. Late Quaternary transgressive erosion and deposition in a modern epicontinental shelf: The Adriatic semi-enclosed Basin. Geo-Marine Letters 14, 41–51.

Voelker, A.H.L., 2002. Global distribution of centennial-scale records for Marine Isotope Stage (MIS) 3: a database. Quaternary Science Reviews21, 1185–1212.

Waelbroeck, C., Labeyriea, L., Michaela, E., Duplessya, J.C., McManus, J.C., Lambreck, K., Balbona, E., Labracherie, M. 2002. Sea-level and deep water temperature changes derived from benthic foraminifera isotopic records. Quaternary Science Reviews 21, 295-305.

Watkeys, M.K., 2006. Gondwana break-up: South African perspective. In: Johnson, M.R., Anhaeusser, C.R., Thomas, R.J., (eds.), The Geology of South Africa. Geological Society of South Africa, Johannesburg/Council for Geoscience, Pretoria 531-539.

Winker, H., Kerwath, S.E., Attwood, C.G., 2014. Report on age-structured stock assessments and the simulation of the impact of various fisheries management options for the South African linefishery. Report No. LSWG/1. Department of Agriculture, Forestry and Fisheries, Cape Town.

Zaitlin, B.A., Dalrymple, R.W., Boyd, R., 1994. The stratigraphic organization of incised-valley systems associated with relative sea-level change. In: Dalrymple, R.W., Zaitlin, B.A., Scholle,

P.A. (Eds.), Incised-Valley Systems: Origin and Sedimentary Sequences. SEPM Special Publication 51 p. 45–60.

Zaitlin, B.A., Shultz, B.C., 1990. Wave-influenced estuarine sand body, Senlac heavy oil pool, Saskatchewan, Canada, in Barwis, J.H., McPherson, J.G., and Studlick, J.R.J., (eds.), Sandstone Petroleum Reservoirs: New York, Springer-Verlag p. 363-387.

Zenkovich, V.P., 1959. On the genesis of cuspate spits along lagoon shores. Journal of Geology 67, 269–277.

Professor Sven Kerwath, personal communications